EFFECT OF CATALASE/SUPEROXIDE DISMUTASE MIMETIC EUK-134 ON DAMAGE, INFLAMMATION, AND FORCE GENERATION OF THE DIAPHRAGM MUSCLE IN *MDX* MICE

A Dissertation

by

JONG HEE KIM

Submitted to the Office of Graduate Studies of
Texas A&M University
in partial fulfillment of the requirements for the degree of

DOCTOR OF PHILOSOPHY

August 2009

Major Subject: Kinesiology

EFFECT OF CATALASE/SUPEROXIDE DISMUTASE MIMETIC EUK-134 ON DAMAGE, INFLAMMATION, AND FORCE GENERATION OF THE DIAPHRAGM MUSCLE IN *MDX* MICE

A Dissertation

by

JONG HEE KIM

Submitted to the Office of Graduate Studies of
Texas A&M University
in partial fulfillment of the requirements for the degree of

DOCTOR OF PHILOSOPHY

Approved by:

Chair of Committee,	John M. Lawler
Committee Members,	James D. Fluckey
	Steven E. Riechman
	David M. Hood
Head of Department,	Richard B. Kreider

August 2009

Major Subject: Kinesiology

ABSTRACT

Effect of Catalase/Superoxide Dismutase Mimetic EUK-134 on Damage, Inflammation, and Force Generation of the Diaphragm Muscle in *mdx* Mice. (August 2009)

Jong Hee Kim, B.Ed., Seoul National University;

M.Ed., Seoul National University

Chair of Advisory Committee: Dr. John M. Lawler

Duchenne muscular dystrophy (DMD) is the most devastating form of muscular dystrophy caused by a mutation in the dystrophin gene. Defects in the dystrophin gene in DMD, are homologous to that found in *mdx* mice, and result in profound muscle damage, inflammation and weakness in diaphragm and limb muscles. Dystrophin, a scaffolding protein located in the sarcolemmal cytoskeleton, helps cells to maintain their structural integrity and associates with critical cell signaling molecules that regulate cell growth and repair (e.g., nNOS).

While the contributing mechanisms leading to DMD-induced degenerative muscle function and damage are multi-factorial, elevated oxidative stress has been proposed as a central mechanism. In contrast, antioxidants can attenuate muscle damage as well as improve contractile function in dystrophin-deficient muscles. However, it is unknown if oxidative stress is a causal factor in dystrophin-deficient diaphragm muscle pathology and specifically targeted antioxidant (e.g., EUK-134) treated early in the

course of the disease (3-4 weeks) can modulate oxidative stress, functional damage and weakness in *mdx* diaphragm.

Therefore, the purpose of this study was to determine the effects of catalase/superoxide dismutase mimetic EUK-134 on damage, inflammation, and contractile function of the diaphragm muscle in *mdx* mice. We hypothesized that (a) EUK-134 would attenuate muscle damage and oxidative stress in *mdx* diaphragm, (b) EUK-134 would reduce inflammatory cells and an important transcription factor including nuclear factor-kappaB (NF-κB) in *mdx* diaphragm and (c) EUK-134 would restore proteins that attach to dystrophin such as nNOS and cytoskeletal proteins back to sarcolemmal region and improve muscle contractility in *mdx* diaphragm.

C57BL/10ScSn wild type and *mdx* mice were given EUK-134 (30mg/kg, i.p., injection) beginning at 20 days of age for 8 days. The mice were euthanized and the diaphragm muscle was harvested at 4 weeks of age, the time of peak inflammation, and analyzed to measure myofiber inflammation, NF-κB activation, cytoskeletal proteins and oxidative stress markers using Western immunoblotting, ELISA, immunofluoresence, and immunohistochemistry. We found that EUK-134 ameliorated muscle damage and oxidative stress in *mdx* diaphragm. EUK-134 protected against inflammation by decreasing NF-κB activation in the nucleosome fraction of *mdx* diaphragm. Further, EUK-134 partially rescued nNOS and α-1 syntrophin back to sarcolemmal membranes and recovered force generation even in acute application in vitro in *mdx* diaphragm.

These results are the first to demonstrate a causal relationship between oxidative stress and pathology caused by dystrophin-deficient diaphragm muscle. Moreover, the

data indicate that EUK-134 has a protective effect against muscle damage, inflammation, and contractility in *mdx* diaphragm. We believe that the results from our investigation will provide clinical significance, as we expect to elucidate mechanisms by which oxidative stress contribute to tissue damage and weakness in dystrophic diaphragm.

DEDICATION

To Youngsin, Jungwoo and Jungmin

ACKNOWLEDGEMENTS

I would like to thank my committee chair Dr. Lawler for his guidance, support, and feedback throughout my graduate study. It was pleasure to have had the opportunity to work with him. The success of this project and the vision of my future are in large part of a function of his good mentorship.

I would like to give my deep gratitude to committee members Dr. Fluckey, Dr. Riechman, and Dr. Hood for their valuable advice, suggestions and encouragement throughout the course of this research project.

I would like to acknowledge all our lab members, Sean, Brandon, and Claire for their support and encouragement during the time spent on this research.

I would like to thank my mother for her dedication and support throughout my many years of school. Most of all, I am mostly indebted to my wife, Youngsin Kim, for her love, patience and prayer. Without her help, I could not have worked so hard for so long.

TABLE OF CONTENTS

CHAPTER Page

LIST OF FIGURES

FIGURE Page

FIGURE Page

LIST OF TABLES

CHAPTER I

INTRODUCTION

Duchenne muscular dystrophy (DMD) is a severe genetically determined muscle-wasting disorder characterized by gene mutations or deletions of the structural protein, dystrophin. Genetic defect in DMD, which is homologous to that found in *mdx* mice, has been related to tissue damage, weakness, inflammation, apoptosis, necrosis, and fibrosis in respiratory and locomotor muscles. Mounting evidence indicates that oxidative stress, inflammation, cytoskeletal disruption, mitochondrial dysfunction, and impaired stress response are important contributors to degenerative tissue function and damage in *mdx* mice.

Elevated oxidative stress has been proposed as a central mechanism to DMD-induced muscle damage and dysfunction (Appendix 1). In contrast, antioxidants can attenuate muscle damage as well as improve contractile function in dystrophin-deficient muscles. However, it is unknown if oxidative stress is a causal factor in dystrophin-deficient diaphragm muscle pathology and specifically targeted antioxidant (e.g., EUK-134) treated early in the course of the disease (3-4 weeks) can modulate oxidative stress, functional damage and weakness in *mdx* diaphragm.

Therefore, we examine our hypothesis by pursuing the following specific aims. (i) identify the role of oxidative stress on functional and morphological properties in *mdx* diaphragm (ii) identify the role of oxidative stress on inflammatory signaling pathways

---

This dissertation follows the style of *Journal of Applied Physiology*.

in *mdx* diaphragm (iii) identify the role of oxidative stress on dislocation of nNOS, dystrophin-associated scaffolding proteins and contractile properties in *mdx* diaphragm.

To accomplish the above specific aims, we hypothesized that (i) EUK-134 will reduce oxidative stress and muscle damage in *mdx* diaphragm (ii) EUK-134 will reduce inflammatory cells and NF-κB activation in *mdx* diaphragm (iii) EUK-134 will restore nNOS and α-1 syntrophin back to sarcolemmal region and improve contractile function in *mdx* diaphragm.

DMD and dystrophin

Duchenne muscular dystrophy (DMD) is the most common and devastating type of human muscular dystrophy, first described in the mid-1800s by Meryon and Duchenne. DMD is an intrinsic X-linked recessive disorder in dystrophin gene and affects approximately 1 in every 3500 males. Two-thirds of genetic mutations in the dystrophin gene are caused by deletions and duplications, and remaining one-third has point mutations or insertions (30, 97, 132). Genetic defects in DMD result in profound muscle damage, inflammation, weakness and fibrosis in both respiratory and locomotor muscles. The symptoms of DMD appear by 3 years causing walking difficulties and balance problems and by 12 years are typically no longer able to breathe or walk on their own (48). The progressive, rapid, and severe deterioration in muscles eventually leads to premature death in their late teens to early twenties mainly due to respiratory and cardiovascular failure (48, 170).

One of the hallmarks of the muscular dystrophies initiated by a mutation of single gene, dystrophin is that the severity and progress of pathology differ that range from the most mild and slow to the most severe and fast. In human, dystrophin deficiency leads to the most severe and fast muscle disease, Duchenne muscular dystrophy (DMD), whereas reductions or truncations of dystrophin causes a milder and slow muscle disease, Becker muscular dystrophy (BMD).

The *mdx* mouse is most widely used animal model for DMD in human that carries a naturally occurring point mutation at position 3185 of dystrophin gene (132). Although dystrophin is absent in both *mdx* mice and DMD patients the phenotype of *mdx* mice is much less severe than that seen with DMD in humans. Moreover, the hindlimb muscles in *mdx* mice are different histologically from diaphragm muscle, which more closely resembles DMD muscles. The dystrophin-deficient limb muscles in *mdx* mice undergo a series of degeneration, necrosis and inflammation starting at 2-3 postnatal weeks and persisting throughout the lifespan of animals. Then most of the locomotor muscles are efficiently regenerated and only undergo mild weakness in adult mice (111). However, the diaphragm muscle in dystrophin-deficient *mdx* mice initially display a regeneration process that does not compensate for massive degeneration and fails to restore muscle structure and function which are similarly seen in DMD patients (140). Therefore, diaphragm in *mdx* mice can be more valuable for studying the human DMD than other muscles.

Another different characteristic between DMD humans and *mdx* mice is the average lifespan. Dystrophin-deficient *mdx* mice live a relatively longer period of time

than DMD patients whose average lifespan is shortened by 60 to 70%. However, the lifespan in *mdx* mice is reduced moderately in both male and female compared with wild-type mice. The *mdx* mice rarely live past two years, while wild-type mice live two and a half to three years. Recently, Chamberlain *et al* (27) demonstrated that lifespan reduction for male (-19%) and female (-17%) occur in *mdx* mice compared with wild type mice.

Dystrophin is a large (427kD) protein and a central component of the sarcolemmal dystrophin-associated protein complex (DAPC). Genetic mutations in dystrophin or DAPC proteins results in a variety of muscular dystrophy, which are often associated with defects in sarcolemmal membrane. Dystrophin consists of an amino(N)-terminal actin-binding domain, a central rod-like domain, and cystein-rich carboxy(C)-terminal domain that allows assembly of the DAPC (47). Dystrophin binds to cytoplasmic γ-actin at its amino terminus and regions along the spectrin-repeated rod domain and to transmembrane protein β-dystroglycan at its carboxyl terminus. The N-terminal and extracellular portion of β-dystroglycan associate with α-dystroglycan and basement membrane (114).

In muscles, dystrophin plays an important role in maintaining sarcolemmal integrity by bridging the subsarcolemmal cytoskeleton, the sarcolemma, and the extracellular matrix (ECM), and transmiting force laterally across the sarcolemma to the ECM (89). DMD compromises the mechanical resilience of the cytoskeleton and cellular membrane to repeated mechanical strain (116). The muscles in DMD patients display a lower threshold for material fatigue injury with repeated stretch or eccentric contractions

(32, 161). The limb muscle of DMD that is absent in dystrophin is abnormally susceptible to contraction-induced cytoskeletal disruption, immune cell invasion and muscle wasting (42, 96, 116, 128), resulting in massive inflammation, apoptosis, necrosis, damage and atrophy (136, 146), along with an increase in connective tissue, and thus stiffness and internal work (59). Muscle wasting with DMD is primarily a function of muscle protein breakdown and cell loss, and not a result of impaired protein production (8).

In addition to its mechanical and structural role, dystrophin also regulates signaling molecules, such as neuronal nitric oxide (nNOS), Grb2, and others to the sarcolemma, which are involved in protein turnover, growth, blood flow and adhesion proteins (79, 116).

DMD and dystrophin-associated protein complex (DAPC)

Dystrophin deficiency in DMD humans and *mdx* mice leads to a marked reduction of other dystrophin-associated protein sarcolemmal and subsarcolemmal proteins, called dystrophin-associated protein complex (DAPC). The DAPC plays a major role in linking the actin cytoskeleton to the extracellular matrix, stabilizing the sarcolemma during contraction and relaxation, transmitting force generated in the muscle sarcomeres to extracellular matrix, and integrating cell signaling in response to mechanical strain (79).

Based on their biochemical properties, the DAPC can be subdivided into three subcomplexes as follows: the dystroglycan complex (DGC), the sarcoglycan-sarcospan

complex (the sarcoglycan complex associated with sarcospan), and the cytoplasmic complex (e.g., dystrophin, syntrophin, and dystrobrevin) (34, 147).

Dystroglycan complex (DGC) constitutes an essential core of the DAPC as it establishes a transmembrane link between laminins and dystrophin (34). DGC consists of an α-dystroglycan binding to lamin-2 and a β-dystroglycan binding to α-dystroglycan as well as the C-terminal of dystrophin and so complete the connection from the inside to the outside of the cell. Targeted deletion of dystroglycan in mice results in embryonic death than progressive muscle damage, indicating that dystroglycan is indispensable for early embryonic development (168).

Sarcoglycan proteins are integral membrane glycoproteins which associate with β-dystroglycan (89). There are five sarcoglycan proteins: α-sarcoglycan(50kDa, also called adhalin), β-sarcoglycan(43kDa), γ-sarcoglycan(35kDa), δ-sarcoglycan(35kDa), and ε-sarcoglycan(50kDa) (47). α-dystrobrevin and γ-sarcoglycan can interact directly and genetic mutation or deletion for α-, β-, γ-, and δ-sarcoglycan results in various types of limb-girdle muscular dystrophy (LGMD) types 2D, 2E, 2C, and 2F, indicating that sarcoglycan loss is the major mediator of membrane frailty and muscle disease (23, 33, 43, 55, 140). Sarcoglycan proteins participate in protein interaction between the membrane and the matrix (160).

Each α-sarcoglycan and β-sarcoglycan binds to a small biglycan in their extracellular portions. Biglycans are proteoglycan aggregates that play an important role in organizing the intracellular components of the DAPC, including the syntrophins, dystrobrevins by way of its interaction with sarcoglycan-sarcospan complex (160).

Sarcospan is a 25kD membrane protein predominantly seen in skeletal and cardiac muscle sarcolemmal membrane. Although the amount of sarcospan is reduced in DMD muscle, lack of sarcospan does not develop muscular dystrophy (47).

The cytoplasmic complex of DAPC includes the syntrophins, dystrobrevins, nNOS, and dystrophin. Syntrophins are a family of scaffolding proteins that contain multiple protein interaction motifs. In human and mouse, five highly conserved but distinct syntrophin isoforms, α1-, β1-, β2-, γ1-, and γ2-syntrophin, have been described (167). Each syntrophin isoform consists of two pleckstrin homology domains (PH1 and PH2), an N-terminal PSD/Discs-large/ZO-1 homologous (PDZ) domin, and a short syntrophin unique (SU) COOH-terminal domain (80). Syntrophins bind directly to dystrophin, utrophin, and dystrobrevin and its interaction is mediated by the PH2 domain and SU COOH-terminal domain together (2). The PDZ domain of α1-syntrophin binds to voltage-gated sodium channels and neuronal nitric oxide synthase (nNOS). Thus, α1-syntrophin is of major importance for recruiting and anchoring nNOS to the sarcolemma via dystrophin. α1-Syntrophin, localized on the sarcolemma and neuromuscular junction with dystrophin, is predominantly expressed in skeletal and cardiac muscle whereas β1 and β2-syntrophin, primarily restricted to the neuromuscular junction, are expressed in wide variety of tissues (73, 112). It has been demonstrated that lack of syntrophin leads selective loss of nNOS but not develop muscular dystrophy (102).

Dystrobrevins are components of DAPC and form an intracellular peripheral subcomplex thought to serve as a scaffold for signaling proteins (52). The two dystrobrevin isoforms α and β, are encoded by different genes. α-Dystrobrevin, localized

to the sarcolemma and neuromuscular junction, is the predominant isoform in skeletal muscle (71). β-Dystrobrevin is expressed in brain, liver, lung and kidney, but not in skeletal muscle (66). α-Dystrobrevin binds both dystrophin and syntrophin. Lack of dystrobrevins exhibits milder muscle pathology than humans with DMD (52, 71).

Nitric oxide (NO), generated from L-arginine by nitric oxide synthase (NOS), is an important and highly versatile signaling modulator involved in regulation of numerous cellular functions including tissue injury, repair and disease (31, 74). In mammals, three isoforms of NOS, neuronal (nNOS, NOS1), inducible (iNOS, NOS2), endothelial (eNOS, NOS3), have been reported to be expressed under normal conditions. Neuronal nitric oxide synthase (nNOS) is a predominant isoform expressed in muscle, where it is co-localized at the sarcolemma within the DAPC (19, 158). nNOS interacts directly with α1-Syntrophin, which is associated with dystrophin (158). In the absence of dystrophin of DMD humans and *mdx* mice, nNOS is absent from sarcolemma and partially accumulates in the cytosol where it maintains some of its enzymatic activity (20, 28). Dislocation of nNOS from the dystroglycan complex could (a) increase NAD(P)H oxidase activity, (b) increase inflammation, (c) increase protein degradation via activation of ubiquitin ligases, and (d) impair satellite cell activation (107, 153). Reduction in nNOS coupled with increase susceptibility to material fatigue injury could exacerbate damage and inflammation (153). However, the loss of nNOS from the sarcolemma is not sufficient to make a dystrophic phenotype but plays a contributory role in boosting tissue damage in response to dystrophic loss (118).

DMD and inflammation

Inflammation in muscle damage and repair

Inflammation is one of the first responses of the immune system which is initiated when tissues are damaged through a variety of mechanisms, including trauma, hypoxia, infections, toxins, heat or other causes (149). Various types of tissue damage results in the initiation of regeneration and repair response which is a coordinate process accompanied by the proliferation and differentiation of muscle progenitor cells also referred to as satellite cells. The process of muscle regeneration and repair is completed by a series of degeneration, inflammation, regeneration, and fibrosis (68, 70, 148).

Inflammation can be divided into two phases: acute and chronic. Acute inflammation is regarded as a transient, beneficial response to tissue injury. Hallmarks of acute inflammation is increased blood flow with vasodilation and vascular permeability changes along with the accumulation of fluid, leukocytes, and inflammatory mediators such as neutrophils, monocytes and macrophages (50, 148). Inflammatory response is apparent in the muscle within 1 to 24 hour of damage. However, in various types of acute muscle damage, the high concentration of inflammatory cells persists for several days following damage, after which they gradually return to normal concentration over a period of several days to weeks (151).

Chronic inflammation, a persistent phenomenon that progress from acute inflammation if the injurious agent exists, is characterized by infiltration of inflammatory cells such as macrophages, lymphocytes and plasma cells, leading to tissue damage (94). A rapid and sequential invasion of inflammatory cell populations can

persist for days to weeks until tissue repair, regeneration, and growth occur (149). It has been also demonstrated that dystrophin-deficient pathology is related to chronic inflammation (63).

Inflammatory response is a compelling candidate and plays an important role in mediating myofiber damage after ischemia-reperfusion, trauma, exposure to toxins, or inheritable muscle pathologies including muscular dystrophy (144, 150). Inflammation also has a beneficial effect promoting muscle repair and regeneration after injury as well as detrimental effect disrupting muscle homeostasis. The dual role of inflammation is overall influenced by the magnitude of the response, the previous history of muscle use, and injury-specific interactions between muscle and the inflammatory cells (149). However, the interactions between muscle and inflammation are highly complex and not seem to be wholly beneficial for muscle (149).

A dominant inflammatory response against modified muscle use and damage includes massive infiltration by neutrophils (6, 21, 144, 149, 151, 156). Neutrophils are rapid and early respondent inflammatory cells to appear in the damaged site since they migrate into the muscle from the vasculature (151). The main function of neutrophils is to destroy damaged tissue via phagocytosis and degrade damaged area by proteases either intrinsic to muscle or proteolytic systems introduced by phagocytic cell infiltrations (156). Phagocytic and proteolytic activation of neutrophils in response to tissue damage is dominated by the respiratory burst and degranulation, in which neutrophils rapidly release free radicals such as superoxide ($O2^{\bullet -}$), are potentially cytotoxic and may cause muscle damage (156).

Several observations have provided that neutrophil-mediated damage to muscle is related to defects in muscle contractility as well as oxidative stress production. This has been most convincingly demonstrated in muscle using ischemia reperfusion (I/R) model. Neutrophil depletion prior to I/R showed significant less decrease in peak isometric tension than occurred in non-depleted animals (159) and neutrophil-mediated muscle damage has been largely prevented by administration of superoxide dismutase (SOD) (106, 134). Another important finding that neutrophils cause muscle damage through an $O_2^{\bullet-}$ and hypochlorous acid-mediated mechanisms includes the rodent hindlimb muscle unloading/reloading models (107).

Macrophages are involved in muscle damage and repair. Macrophages are more predominant during the later stages of inflammation after damage. However, the roles in influencing the course of muscle injury and repair are more complicate than the role of neutrophils, since macrophages are activated by diverse growth factors (e.g., fibroblast growth factor [bFGF], VEGF), chemokines (e.g., MCPs), cytokines (e.g., tumor necrosis factor-α[TNF-α], interleukins[ILs], interferons[IFNs]) as well as free radicals (149). Macrophages in muscle can be divided into two distinct populations: Classically activated macrophages (also called type I^+, EDI^+, Ia macrophages) and alternatively activated macrophages (also called type II^+, $EDII^+$, dMHC macrophages) (11, 21, 65). Type I^+ macrophages are associated with necrosis in muscle injury, whereas type II^+ macrophages are associated with muscle regeneration (139). Therefore, the localization of type I^+ macrophages inside necrotic myofibers indicates that these cells function as phagocytes, whereas type II^+ macrophages function as non-phagocytic regenerative role

in muscle. St. Pierre *et al* (139) demonstrated that type I^+ macrophages invaded necrotic fiber in 2-day reloaded muscles and type II^+ macrophages were increased significantly and not infiltrated to necrotic muscle fiber in 4- and 7-days of reloading muscle.

Nguyen and Tidball (106) demonstrated cytotolytic capacity of macrophages has been increased in muscle cells by nitric oxide-dependant mechanisms in which increased NO-medicated toxicity by macrophages promotes muscle damage. Several observations indicate that macrophages play an important role in promoting muscle repair and remodeling after injury and modified use. Part of the contribution of macrophages in repair process is due to the removal of debris via phagocytosis although it is not known if removal of debris is required for repair after injury (149).

Inflammation in dystrophin-deficient muscles

Muscle degeneration, necrosis, inflammation, and fibrosis are prominent pathological features of muscular dystrophy in DMD humans and *mdx* mice (84). Mounting evidence indicate that inflammatory processes are highly integrated into the pathologies of dystrophin-deficient muscle (63, 136). It has been suggested that the complex pathology of human DMD and *mdx* mice due to the disruption of structural protein, dystrophin leads to the immune cell infiltrations in response to the damage and degeneration (64, 135).

Inflammation of dystrophic-deficient muscle involves a specific invasion of autoreactive immune cells into damaged sites (136). The major constituents of the inflammatory cell population of dystrophin-deficient muscle are macrophages, T-cells,

and eosinophils (135). Macrophages, $CD4^+$ cells (helper lymphocytes) and $CD8^+$ cells (cytotoxic lymphocytes), commonly existing in perimysial and endomysial sites of muscles, are involved in muscle degeneration, necrosis, apopotosis, and fibrosis in *mdx* mice (104, 137). The depletion of macrophages, $CD4^+$ and $CD8^+$ cells or impairment of cytotoxicity by the removal of perforin ameliorated muscle histopathology and increased muscle repair and regeneration in 3-4 week old *mdx* mice (135, 137, 164). Moreover, depletion of T-cells in *mdx* mice reduces other inflammatory cells such as eosinophils, which have the capacity to promote cell membrane lysis and cell deaths by surrounding the degenerative muscle fibers (24, 163) . Morrison *et al* (104) suggest that T-cells play a role in the onset of the fibrosis which deteriorates the ability of dystrophic muscle to regenerate.

Inflammation is an early event in the pathological feature in dystrophin-deficient mdx mice and DMD humans. Inflammation and muscle cell death is first apparent at 3-4 weeks of age, with regenerative muscle replacing pathological muscle by 14 weeks of age in *mdx* mice (136). In human DMD, inflammation display mild, histotologically discernible at birth but remain no symptomatic until 3-4 years of age (110, 136). The mechanisms by which inflammatory cells promote the dystrophic pathology remain unknown. However, NF-κB activation, oxidative stress and cytokines appear to have an integrative effect in the progression of muscular dystrophy (83, 113).

NF-κB in dystrophin-deficient muscles

NF-κB is a major transcription factor which regulates a variety of gene expression involved in cell survival, proliferation, inflammation and apoptosis (76, 113). In mammals, NF-κB family consists of 5 subunit proteins: p65 (Rel-A), Rel-B, c-Rel, p50, and p52 (1). In normal condition, NF-κB is maintained in an inactive form in the cytosol through binding of the I-kappaB (IκB). Typical IκB family members consist of IκBα, IκBβ, and IκBε. IκB family contains a nuclear export sequence (NES) which retains NF-κB heterodimer (p65 and p50) in the cytosol as an inactive complex. NF-κB transcriptional activity is inhibited by function of IκB which masks one of the subunit's nuclear localization sequence (NLS) and inhibits DNA binding (62). NF-κB activation and IκB degradation are tightly regulated through inhibitory kinase complex known as IκB kinase (IKK). IKK consists of two catalytic subunits (IKKα, IKKβ) and a regulatory subunit (IKKγ/NEMO) (1). NF-κB can be activated in response to different stimuli such as proinflammatory cytokines (e.g., TNF-α, IL1-β) (56) and oxidative stress (93, 157). Such stimulatory signals result in IKK-mediated phosphorylation and proteolytic degradation of IκB, leading its dissociation from NF-κB complex with translocation heterodimer p50/p65 to nucleus Translocated NF-κB p50/p65 subunit binds to target DNA and activates transcription, which include a variety of cellular gene involved in inflammatory, immune, and proliferative response (145).

Skeletal muscle specific NF-κB activation is not an inherent consequence in dystrophin-deficient muscles. Recent evidence suggested that NF-κB activity has been diminished during first 1.5 weeks of postnatal muscle development of *mdx* mice (1). However,

NF-κB activity in *mdx* mice subsequently become reactivated and persisted at 3 weeks of age (1). Mounting evidence indicates that elevated nuclear NF-κB activation is a key feature and plays an important role in the process of muscle pathology in both DMD in humans (103) and *mdx* mice (1, 82, 103).

Monici *et al* (103) have reported that NF-κB immunoreactivity was increased in the cytoplasm of all regenerating fibers and 20-40% of necrotic fibers in DMD patients. Kumar *et al* (82) have demonstrated that NF-κB DNA binding activity and the expression of NF-κB-regulated inflammatory cytokines such as TNF-α and IL-1β was significantly higher in *mdx* diaphragm, even in 15-day-old compared with controls and IκBα protein levels were also lower in *mdx* diaphragm. Acharyya *et al* (1) also have reported that NF-κB DNA binding activity was found to be higher in *mdx* diaphragm, tibialis anterior (TA) and gastrocnemius muscle. Specifically, immunohistochemical analysis of dystrophin-deficient DMD and *mdx* mice muscle have showed that NF-κB p65 subunit has been localized to infiltrating immune cells (113). The protein levels of NF-κB p65 in nuclear fraction were much greater for *mdx* skeletal muscle than for wild-type muscle (165). The supershift analysis of NF-κB/DNA complex and genetic manipulation have revealed that NF-κB subunit p50 and p65 proteins are activated in immune cells and myofibers of *mdx* mice and p65 is transcriptionally more active subunit contributing to dystrophin-deficient pathology (1, 82).

Involvement of dysregulated NF-κB in dystrophin deficient muscle makes NF-κB an attractive target to explore for the potential to approach pathological treatment in a comprehensive manner. It has been demonstrated that genetic manipulation (1) or

pharmacological blockade (25, 100, 109) of NF-κB can alleviate the severity of the pathological phenotype in *mdx* mice. Acharyya *et al* (1) have reported that genetic deletion of NF-κB subunit p65 and IKKβ promote muscle regeneration and reduce pathologic phenotype including inflammation in *mdx* muscle. Carlson *et al* (25) have suggested that treatment with pyrrolidine dithiocarbamate (PDTC), an agent which inhibits NF-κB nuclear activation by cytosolic stabilization of IκB-α, significantly improve the survival of muscle fibers and resting potentials (RPs) in passively stretched dystrophic skeletal muscle. Messina *et al* (100) also showed the beneficial effects of PDTC on biochemical, functional and morphological parameters in *mdx* muscle, resulting in decreased necrosis, and enhanced muscle regeneration and contractile function. The administration of curcumin, a plant-based NF-κB inhibitor derived from the spice turmeric used in curry, has been reported to attenuate NF-κB activation and dystrophic pathology in *mdx* skeletal muscle (109). However, Durham *et al* (46) have failed to reduce NF-κB activation and improve contractile function with curcumin in diaphragm and skeletal muscle. Methodological discrepancy can account for the inconsistent outcome. Recently, the use of NBD (NEMO-binding domain) peptide, a more specific non-toxic IKK inhibitor has shown to be a promising candidate for treatment of *mdx* pathology, resulting in improved muscle contractile function and reduced macrophage accumulation and myofiber necrosis in dystrophin-deficient muscle (1).

DMD and oxidative stress

Muscle damage and weakness with DMD are proposed to result from repetitive, material fatigue injury and inflammation (32, 117, 136, 161). Mounting evidence suggests that inflammatory signaling, including nuclear factor-kappaB (NF-κB), cytokine (TNF-α, IL-1β) pathways, may be linked to increased oxidative stress (54, 153). A potential primary mechanism that may link material fatigue injury and inflammation with clinical symptoms of diaphragm dysfunction in DMD patients is proposed to be oxidative stress (49, 119, 125, 153).

Oxidative stress is the result of (a) increased reactive oxygen species (ROS) and reactive nitrogen species (RNS) (b) decreased, insufficient, or imbalanced antioxidant enzymes and stress proteins (e.g., heat shock proteins, IGF-1). An imbalance between ROS/RNS production and antioxidant defense mechanisms lead to increased ROS/RNS-induced cellular dysfunction, damage and tissue degeneration (117).

The possibility that oxidative stress contributes to muscle pathology in DMD has been proposed first by Binder *et al* (14) who noted the similarities to muscle pathology that occurred in tocopherol (e.g., vitamin E) deficiency, which directly increase in free radicals and oxidative damage. Subsequently, Mendell *et al* (98) have suggested that ischemia-reperfusion injury to muscle produces oxidative lesions and damage with pathological characteristics which is very similar to those of the muscular dystrophy.

The markers of oxidative stress have been extensively investigated in DMD humans and *mdx* mice. Byproducts of lipid peroxidation (e.g., TBARS, expired pentane), DNA and protein oxidation are elevated with DMD in humans and *mdx* mice (60, 61, 72,

115, 125). Nakae *et al* (105) have suggested that lipofuscin, a biomarker of oxidative injury, formed by the oxidative degradation of celluar macromolecules by oxygen-derived free radicals and redox-active metal ions has been accumulated early phases in dystrophin-deficient DMD humans (~2 years) and *mdx* mice (~4 weeks).

In addition, the dystrophin-deficient muscle is also more susceptible to oxidative damage than normal muscle (40, 41, 119). Rando *et al* (119) showed that dystrophin-deficient myotubes are more susceptible to oxidative stress-induced damage compared with normal cells. Disatnik *et al* (40) reported that the susceptibility of the cell populations to oxidative stress is increased with severity of the phenotype in the respective *mdx* and *mdx*-transgenic strain. Rando (118) has proposed a "two-hit" hypothesis where the combination of oxidative stress with disturbances in the dystrophin-glycoprotein complex (DCG) leads to pathology with DMD. However, only more recently has the tie between oxidative stress and pathology in muscles with DMD moved beyond association (138, 153, 165, 166).

Various sources of ROS in respiratory and locomotor muscles with DMD include the inflammatory cells (e.g., myeloperoxidase), NAD(P)H oxidase (NOX), xanthine-xanthine oxidase, mitochondria, and decoupling of inducible nitric oxide synthase (iNOS) (3, 10, 138, 165, 166). Furthermore, oxidative stress may also be exacerbated in muscle wasting disease by insufficient stress response including heat shock proteins and IGF-1 (17).

In addition, downregulation and dislocation of nNOS from the DAPC may also elevate oxidative stress and lead to muscle damage (107, 131, 152, 164). nNOS known

as μNOS in skeletal muscle appears to be attached to DAPC scaffolding proteins dystrophin and dystrobrevin via a- and ß-syntrophin (116). DMD-induced impairment of mitochondrial function can lead to oxidative stress, apoptosis, and necrosis (12).

DMD and therapeutics

Muscle necrosis, inflammation, and fibrosis are prominent pathological features of dystrophin-deficient DMD humans and *mdx* mice. These pathological changes lead to progressive muscle damage and weakness in dystrophin-deficient muscles. One of important therapeutic approaches to improve muscle function and dystrophin-deficient phenotype therefore is to ameliorate these pathological changes. Many therapeutic trials have been treated with the purpose of ameliorating and curing the muscular dystrophy. However, there has been no successful treatment for the diseases.

Gene therapy or cell therapy to replace the absence of dystrophin are promising but not yet applicable. The treatment of corticosteroids such as prednisone and deflazacort offers partial benefit by reducing oxidative damage and inflammation, but has some side effect profile including impaired growth and maturation, weight gain, osteopenia, immunosuppression, and susceptibility to infection (26, 133). NF-κB inhibitor curcumin (109) and pyrrolidine dithiocabamate (PDTC) (100) might attenuate muscle degeneration and enhances muscle regeneration and function in *mdx* mice, suggesting a beneficial effect of NF-κB blockade on muscle repair. Imatinib, an anti-inflammatory and anti-fibrotic agent, markedly ameliorated muscle necrosis,

inflammation and fibrosis via downregulating platelet-derived growth factor (PDGF) and c-abl signaling pathways and significantly improved muscle function in *mdx* mice (67).

Prevention of oxidative damage by providing different antioxidant in dystrophin-deficient muscles has positive effect. Antioxidant green tea extract (22), low-iron diet (16) resulted in a significant reduction of necrosis in dystrophin-deficient *mdx* mice, but no similar benefits were not demonstrated in DMD humans (7, 51, 126, 141). These studies were performed on some patients already undergoing muscle pathologies, which may have limited their effectiveness. In addition, depending on the types of ROS produced by dystrophic muscles, some antioxidants may be more effective than others in preventing oxidative stress-induced muscle damage and weakness in dystrophin-deficient muscles. Therefore, even if oxidative stress is in indeed the primary pathological mechanism leading to muscle damage and weakness, effective treatment will need to be targeted to the specific deficit in antioxidant defense and initiated early in the course of the disease (117).

NAD(P)H oxidase is a source of oxidative stress localized in cell membrane and inflammatory cells (107). Importantly, elevations of NAD(P)H oxidase have been identified in the heart and muscles of *mdx* mice that indeed may play a significant role in muscle damage, weakness, and wasting (138, 166). Recently, a 6 week treatment of N-acetylcysteine (NAC), a NAD(P)H oxidase inhibitor, was found to protect against damage, incidence of internal nuclei, and weakness in the EDL muscle of 8 week old *mdx* mice (165). In addition, NAC also increased protein levels of the ß-dystroglycan and utrophin while decreased caveolin-3 proteins. NAC also reduced dihydroethidine

oxidation (DHE, a marker of superoxide generation) and protein expression of the p65 subunit of NF-κB (165), an inflammatory transcription factor that also stimulates proteolysis via the ubiquitin pathway. NAC treatment also reduced macrophage invasion and collagen accumulation in the hearts of *mdx* mice (166).

Given the emerging promise of oxidative damage preceding pathological changes and antioxidant therapy attenuating muscle pathology and weakness with DMD, increasing data implicate the importance of hydrogen peroxide and superoxide in muscle wasting models (5, 87, 165). In dystrophin-deficient muscle, xanthine-xanthine oxidase system and NAD(P)H oxidase may contribute to the generation of superoxide, which, in turn, is dismutated to hydrogen peroxide by superoxide dismutase (10, 165). EUK-134 is a part of salen-manganese family compounds, which quench superoxide anion and hydrogen peroxide, developed by Eukaryon (Appendix 2). It has been demonstrated that EUK compounds protect against oxidative damage, radiation, and may increase lifespan (9, 18, 39, 88, 127). Therefore, administration of EUK-134 on dystrophin-deficient *mdx* muscles can be a potential target for therapeutics. However, the efficacy to modulate oxidative stress, functional damage and weakness in the *mdx* diaphragm is unknown.

The diaphragm muscle suffers from significant fibrosis, damage, and weakness with DMD, and is also susceptible to oxidative stress (13, 154). Oxidant production may be higher in the *mdx* diaphragm than limb muscles, which could contribute to more profound fibrosis, weakness, and fatigue in that muscle (59, 142). In addition, the diaphragm muscle in *mdx* genetic mouse model experiences muscle damage, disease progression, and gene expression profiles that are more similar to human DMD

pathology than observed in limb muscles, which tend to recover or adapt (153, 154). Therefore, the study of the mechanisms by which oxidative stress causes pathology in *mdx* diaphragm, and development and testing of targeted, antioxidant therapeutics is vital in translation to human health and pathology with DMD.

CHAPTER II

METHODS

Animals

We used C57BL/10ScSn-*mdx*/J dystrophic (*mdx*) mice and wild-type C57BL/10ScSn mice as controls. C57BL mice are one of the most widely used inbred strains and used as a human DMD in rodents (155). Mice were purchased from Jackson Laboratory and cared for at the Comparative Biology Laboratory facility at Texas A&M University complied with the code of conduct for University Laboratory Animal Care Committee (ULACC) standards. Mice were housed in a temperature-controlled (20ºC±2 ºC) environment with a 12-h light-dark cycle, and free access to water and mouse chow (4% standard powder) provided *ad libitum* after weaning at 18 days of age.

Experimental design

Twenty-day old *mdx* mice and C57BL wild type controls were assigned to the following groups: wild-type controls + saline (WS, n=7), wild-type controls + EUK-134 (WE, n=7), *md*x mice + saline (MS, n=7), *mdx* mice + EUK-134 (ME, n=7). EUK-134 (30mg/kg, 0.05cc-0.2cc, i.p) were injected daily beginning at 20 days of age for 8 days. At 28 days of age, mice were euthanized by Na pentobarbital (120mg/kg). To avoid last treatment effect, mice were sacrificed 24 h after the last treatment of EUK-134. Diaphragm was then quickly extracted, weighted and snap frozen in isopentane cooled in liquid nitrogen and stored at -80°C until analyses.

Homogenization procedure

Diaphragm was minced into fine pieces, weighted and suspended (26:1 v/w) in ice-cold complete lysis buffer A (pH=7.4) comprised of the following: 10 mM HEPES, 350 mM NaCl, 20 % glycerol, 1% Igepal-CA630, 1 mM $MgCl_2$, 0.1 mM DTT, 0.1 mM EGTA, and protease inhibitor cocktail (Roche Applied Science). Each diaphragm was homogenized in a Dounce ground glass homogenizer (Bellco Biotechnology; Vineland, NJ) at 4°C. The homogenates were first centrifuged (4°C) for 10 min at 3,000g, and supernatant was separated from the pellet. The supernatant was centrifuged (4°C) for 10 min at 10,000g to get soluble fraction. Nucleosome fraction was isolated using this pellet resuspended by complete lysis buffer B containing the following: 20 mM HEPES, 350 mM NaCl, 10 % glycerol, 1 mM $MgCl_2$, 0.1 mM DTT, and protease inhibitor cocktail (Roche Applied Science) and centrifuged again for 30 min at 12,000g. The supernatant of this fraction contains nuclei. Protein concentration was measured using BCA protein assay reagent kit (Pierce) at 562 nm absorbance with spectrophotometer.

Measurement of citrate synthase activity

Citrate synthase activity in the diaphragm was measured as a marker of oxidative capacity and indicative of mitochondrial density and function as described previously (78). Briefly, citrate synthase cocktail including DTNB (dithio-bis 2-nitrobenzoic acid; 0.1 mM), Triton X-100 (0.07%), and Acetyl CoA (0.1 mM) was mixed with 20 µl samples of 1:26 homogenates in a cuvette and incubated for 5 min. Then oxaloacetate

(12.2 mM) was added and citrate synthase activity that catalyzes reaction of carbon acetyl CoA with carbon oxaloacetate was measured from 1 to 4 min at 412 nm. Enzyme activity was expressed as μmol/g/min.

Measurement of total hydroperoxides

The levels of total hydroperoxides as a marker of lipid peroxidation were measured as described previously (78). Briefly, lipid hydroperoxides were with $FeSO_4$ in H_2SO_4 and a reactive dye (xylenol orange). The principle depends on the oxidation Fe^{2+} to Fe^{3+} when hydroperoxides are reduced. Ionized sulfuric acid assists the reduction and prevents spontaneous reaction of Fe^{2+} with xylenol orange, unless oxidized by hydroperoxides first. The Fe^{3+} reacted with the xylenol orange to form a Fe^{3+}-xylenol complex purple in color. Diaphragm homogenates was mixed with 1mM $FeSO_4$, 0.25M H_2SO_4, and 1mM Xylenol orange by twice inversion with parafilm. The mixture was then incubated at room temperature for 1 hour. Absorbance was then read at 580nm. Concentration of hydroperoxides was quantified against a tert-butyl hydroperoxide standard curve.

Nuclear binding activity of NF-κB

The nuclear binding activity of the p65 subunit of NF-κB in diaphragm muscle tissue homogenates was quantified using an ELISA-based method, TransAM NF-κB kit, according to the manufacturer's instructions (Active motif: Carlsbad, CA). In brief, 20 μg nuclear extract diluted in complete lysis buffer was loaded in the 96-well microplate

on which has been coated with oligonucleotide containing the NF-κB consensus binding site (5'-GGGACTTTCC-3'). Then the wells were incubated with a 100ul diluted anti-p65 antiobody for 1 hour at room temperature without agitation. After three times washing with 200ul 1X washing buffer, 100 µl diluted HRP-conjugated secondary antibody were added to each well and incubated for an hour at room temperature. Sensitive colorimetric absorbance was quantified at 450nm with a reference wavelength of 655nm.

Western immunoblot analysis

Protein levels were measured by Western immunoblot analysis. Separating gel (375 mM Tris-HCl; pH=8.8; 0.4% sodium dodecyl sulfate (SDS); 10% acrylamide) and stacking gel (125 mM Tris-HCl; pH=6.8; 0.4% SDS; 10% acrylamide monomer) solutions were made, and polymerization then was initiated by N,N,N',N' - tetramethylethylene diamine (TEMED) and ammonium persulfate (APS). Separating and stacking gels were then quickly poured into a Bio-Rad Protein III gel-box (Bio-Rad, Hercules, CA). Twenty µg of protein from diaphragm homogenates in sample buffer (100 mM Tris-HCl, pH=6.8, 2% SDS, 30 mM dithiothreitol, 25% glycerol) were then loaded into the wells of the 10% SDS-PAGE gels, and electrophoresed at 150V for 60 min. The gels were then transferred at 30V overnight onto a nitrocellulose membrane (Bio-Rad, Hercules, CA). Membranes were blocked in 5% nonfat milk in PBS with 0.1% Tween-20 for 7 hours. After blocking, membranes were incubated in phosphate-buffered saline (PBS) at room temperature overnight with the appropriate primary antibodies: p65 (1:1,000). Following three washings in PBS with 0.4% Tween-20,

membranes were incubated with horseradish peroxidase–conjugated secondary antibodies in PBS at room temperature for 90 min. Following three washings in PBS with 0.4% Tween-20, an enhanced chemiluminescence (ECL) detection system (Amersham, Piscataway, NJ) were used for visualization. Densitometry and quantification were performed using a Kodak film cartridge, a scanner interfaced with a microcomputer, and the NIH Image J Analysis software program. To ensure equal loading of protein, Ponceau-S-staining were performed for each membrane. Membranes were stripped and reprobed for GAPDH (1:2000, Advanced Immunochemical) as "housekeeping" proteins to further confirm protein loading.

Histochemistry

Cross-sections (10 μm thick) were cut from the middle portion of diaphragm muscle strips in a cryostat (-15°C), placed on slides and air-dried for 30 min. To measure the fiber cross-sectional area (CSA), CSA variability and centralized nuclei, cross-sections were stained with two drops of hematoxylin, incubated for 1 min at room temperature. Hematoxylin stains a bluish-purple color for myocytes and mitochondria, while nuclei stain dark blue. Stained sections were then rinsed with tapped water and air dried for 20 min before mounting with Vectamount medium (Vector Laboratories). Diaphragm cross-sectional images were visualized and captured using a Zeiss Axioplot Vision-series microscope and software program at a magnitude of 40X. For measurement of muscle fiber cross-sectional area, muscle fiber membrane perimeters were traced and quantified using the NIH Image J Analysis software program. The total

average areas within the membrane outlines were used to determine the cross sectional area per unit and expressed in μm^2. Muscle cell area was calibrated against images taken using a stage micrometer.

Immunohistochemistry

Sample cross-sections were cut (10 μm thick) in a cryostat (-15°C) and fixed in cold acetone (-20°C) for 1 hour. After drying samples for 30 min, sections were blocked with 10% normal serum and 0.05% Tween 20 in TBS for 15 min. The desired primary antibodies: Macrophage (1:100), $CD4^+$ (1:100), $CD8^+$ (1:100), dystrophin (1:500), nNOS (1:500), α1-syntrophin (1:500), β-sarcoglycan (1:200) and α-dystrobrevin (1:500) were applied in blocking buffer and placed on the section for an hour. After washing, biotinylated secondary antibody were applied to the sections in PBS buffer for 30 min. Cross-sections were stained for 5 min with Vectastain elite ABC reagent and incubated in peroxidase substrate solution (Vector) at room temperature for approximately 10 min until desired stain intensity appears. Stained sections were then rinsed with PBS and air dried for 20 min before mounting with Vectamount medium.

Images were captured on a Zeiss Axio-Vision-series microscope and software at a magnitude of 10X to 20X, and quantified using the NIH Image J program. To measure the proportional area of inflammatory cells stained, NIH image J program was used as described previously (http://rsb.info.nih.gov/ij/). After opening the image, the image was separated into the red/green/blue (RGB) windows. Using an automatic threshold function calculated by formula (average background + average object)/2), the area

fraction of color image was determined. For immunofluorescence, Alexa Fluor 488 (green) IgG secondary antibody was used to detect the 4-hydroxynonenol (4-HNE) and DAPI (blue) was used to detect the all nuclei.

Metachromatic ATPase Staining

The diaphragm muscle was cut on a crystat and stained using a metachromatic ATPase protocol modified from Kanatous *et al* (75) and Ogilvie & Feeback (108). Serial sections were placed in acidic (pH=4.3) and alkali (pH=10.5) myosin ATPase preincubation medium for 8 min in room temperature. After washing the sample three times with Tris buffer (18mM $CaCl_2$, 45mM Trizma base, 55mM Tris HCl, pH=7.8) for 2 min, the sections were incubated in Guth's ATP solution (18mM $CaCl_2$, 0.15% ATP, 6.7% Sigma 221 buffer, pH=7.8) for 25 min. Then sections were washed 3 times in 1% calcium chloride solution for 2 min and counterstained in 0.1% toluidine blue solution for 90 sec. After brief washing with distilled water, samples were dehydrated with 95% ethanol, 100% ethanol (twice) for 5 min apiece, and then cleared twice in xylene for 5 min apiece.

In vitro muscle preparation and contractile measurements

The diaphragm muscle was studied to determine muscle contractile function. The isolated diaphragm muscle preparation used was similar to that described by Lawler *et al* (85) (Appendix 3). After the whole diaphragm was quickly removed (<30 sec without blood flow), muscle strips were placed in ice-cold (4°C) Krebs-Ringer solution

(118mM NaCl, 4.7mM KCl, 1.8mM $CaCl_2$, 1.18mM $MgSO_4$, 1.18mM KH_2PO_4, 25mM $NaHCO_3$, and 11mM glucose, pH=7.4) aerated with a 95% O_2, 5% CO_2 gas mixture. Fiber bundles were cut parallel to the fibers leaving the lateral portion of the costal diaphragm with the rib intact on one end and the central tendon intact on the other end. The rib end of each diaphragm was tied to a glass rod supporter using silk 4-0 sutures, with another suture tied to the central tendon which was attached to an isometric force transducer (Grass FT03). Each fiber bundle was positioned in a temperature-controlled (36°C) muscle bath (Harvard Apparatus) containing Krebs-Ringer solution (pH=7.4).

Tension was determined by a DC amplifier and displayed on a chart recorder (Allen Datagraph 2125E). Following a 10 minute thermo-equilibration period, diaphragm muscle was adjusted to optimal length (Lo) which coincides with the length at which isometric twitch forces are maximized. Fiber bundles were stimulated by field generation via two platinum foil electrodes driven by a Glass stimulator (S48). Stimulus trains were 250ms in duration and each pulse was 2.0trains/sec. Twitch, 20Hz (low-frequency) and 150Hz (maximal isometric tension: Po) were used as a pulse paradigm to measure the contractile function of diaphragm muscle (86). After determination of Lo, the force production in response to stimulation at 20Hz and Po was measured. One minute was allowed between contractions to eliminate hysteresis.

We also investigated the effect of a single exposure in vitro to EUK-134 on muscle contractility in diaphragm muscle fiber bundles. After baseline contractile properties (twitch, 20Hz, 150Hz) were measured in control Krebs solution (PRE), diaphragm fiber

bundles were placed in test media comprised of EUK-134 (50mM) in Krebs solution for 5 min and contractile properties were measured for each fiber bundle (POST).

At the completion of functional test, diaphragm muscle was removed from the bath, trimmed of tendon, and weighted on an analytical balance. Muscle mass and Lo were used to calculate muscle quality ($N \cdot cm^{-2}$) which is force normalized per total muscle cross-sectional area (muscle mass / [fiber length x 1.056]).

Statistical analysis

Data were analyzed with one-way ANOVA to determine the mean differences for each group. Student-Newman-Keuls test was performed for post hoc test. All values were presented as mean ± SEM. Statistical significance was set at $P < 0.05$ (Appendix 4).

CHAPTER III

RESULTS

Effect of EUK-134 treatment on body mass changes in wild type and *mdx* mice

The body mass changes as an index of animal growth from 20- to 28-days old wild type and *mdx* mice are illustrated in Figure1 and Table 1. There is significant difference between *mdx* and wild type animals. In 20 days old, *mdx* mice weighted 35.1% less than age-matched wild type mice ($P<0.001$). All mice treated with either saline or EUK-134 increased in body mass were observed following onset or during treatment periods. There was no difference in body mass change between saline-treated wild type mice and EUK-134 treated wild type mice. For saline-treated wild type mice, the body masses increased 74.2% from 20 days (9.086±0.458g) to 28 days (15.829±0.797g) of age. The body masses of EUK-134 treated wild type mice increased 67.4% from 20 days (9.329±0.749g) to 28 days (15.617±1.129g). For saline-treated *mdx* mice, the body masses increased in 76.8% from 20 days (5.900±0.145g) to 28 days (10.429±0.480g). 8 days of EUK-134 treatment in the *mdx* mice resulted in increased the mean body mass about 113.5% from 20days (5.817±0.339g) to 28 days (12.05±0.598g). However, following EUK-134 treatment, body masses of *mdx* mice were higher with 15.5 %, but not significantly different from the saline-treated *mdx* mice.

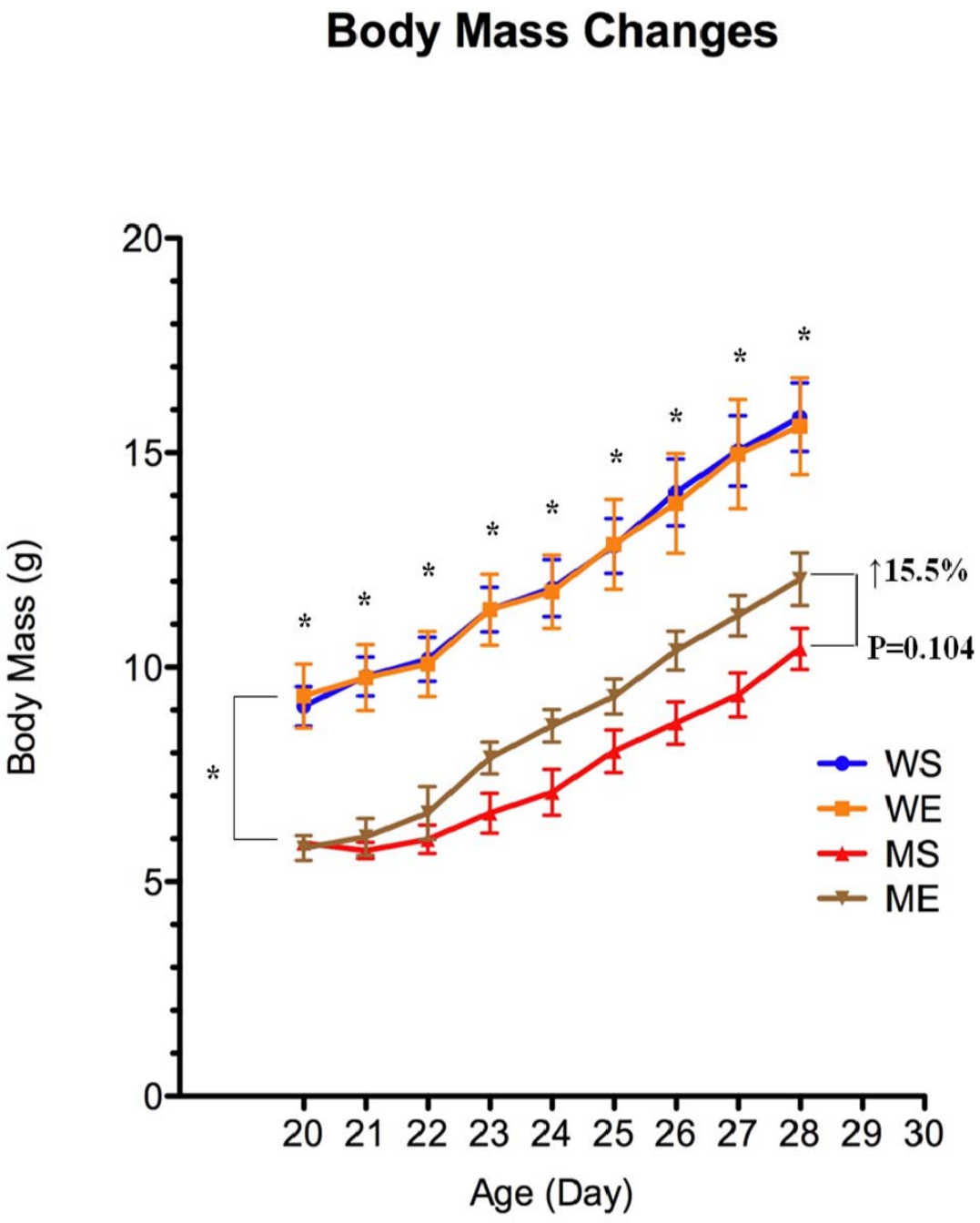

Figure 1. Effect of EUK-134 treatment on body mass changes in wild type and *mdx* mice. * indicates that saline-treated wild type mice (WS) is significantly different from saline-treated *mdx* mice (MS) ($P<0.001$).

Effect of EUK-134 treatment on diaphragm muscle mass and diaphragm muscle mass / body mass in wild type and *mdx* mice

Diaphragm muscle mass was significantly lower in *mdx* mice than age-matched wild type mice (-42.2%, $p<0.01$) (Table 1). EUK-134 had a significant, positive effect in protecting against reduced diaphragm muscle mass in *mdx* mice (+61.2%, $p<0.01$). Moreover, EUK-134 treatment resulted in higher diaphragm muscle mass in the wild-type mice (+57.3%, $p<0.001$). There was no difference in diaphragm muscle mass / body mass between *mdx* and wild type mice (Table 1). However, EUK-134 treatment increased diaphragm muscle mass/body mass in both *mdx* (+38.7%, $p<0.01$) and wild type mice (+60.0%, $p<0.001$).

Table 1. Effect of EUK-134 treatment on body mass, diaphragm mass and diaphragm muscle mass / body mass in wild type and *mdx* mice

Groups	Body mass (BM) (g)		Diaphragm muscle mass (DM) (g)	DM/BM (mg/g)
	Before (20 days)	After (28 days)		
WS	9.086 ± 0.458 [cd]	15.829 ± 0.797 [cd]	0.056 ± 0.003 [bc]	3.544 ± 0.146 [bd]
WE	9.329 ± 0.749 [ab]	15.617 ± 1.129 [cd]	0.088 ± 0.008 [acd]	5.669 ± 0.391 [acd]
MS	5.900 ± 0.145 [ab]	10.429 ± 0.480 [ab]	0.032 ± 0.002 [abd]	3.112 ± 0.170 [bd]
ME	5.817 ± 0.339 [ab]	12.050 ± 0.613 [ab]	0.052 ± 0.003 [bc]	4.316 ± 0.179 [abc]

Data are expressed as mean ± SEM. BM, body mass; DM, diaphragm muscle mass; WS, wild type with saline; WE, wild type with EUK-134; MS, *mdx* with saline; ME, *mdx* with EUK-134. Indicating significant change relative to a: WS ($P<0.05$), b: WE ($p<0.05$), c: MS ($p<0.05$), d: ME ($p<0.05$)

Effect of EUK-134 treatment on diaphragm muscle cross-sectional area (CSA), CSA variability and internal nuclei in wild type and *mdx* mice

Hematoxylin-stained histological characteristics of diaphragm muscle with *mdx* and wild type mice were illustrated in Figure 2. Diaphragm muscle cross-sectional area was significantly smaller in *mdx* mice than age-matched wild type mice (-23.3%, $p<0.001$) (Figure 3). There was no EUK-134 treatment effect on CSA changes in both *mdx* (696.39±12.29g vs. 694.78±18.77g) and wild type mice (858.45±11.20g vs. 874.78±17.37g). Variability of diaphragm muscle cross sectional area was elevated in *mdx* mice (+37.3%) compared with wild type mice, but significantly reduced by EUK-134 treatment in *mdx* mice ($p<0.01$) (Figure 4). Internal nuclei numbers per 100,000μm^2 were increased in *mdx* mice compared with wild type mice ($p<0.001$), and reduced by EUK-134 treatment in *mdx* mice ($p<0.001$) (Figure 5).

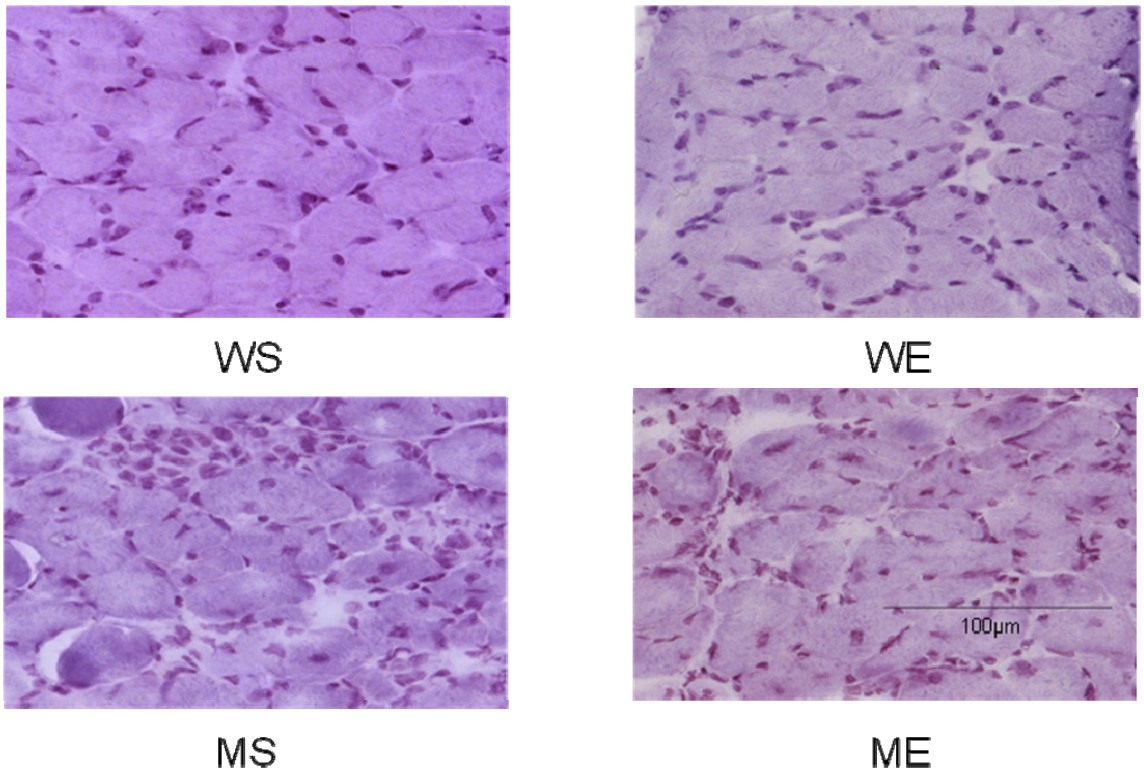

Figure 2. Hematoxylin-stained cross-sections of diaphragm in wild type and *mdx* mice. The diaphragm cross-sections (40X) were stained with hematoxylin from the following groups: wild type + saline (WS), wild type + EUK-134 (WE), *mdx* + saline (MS), and *mdx* + EUK-134 (ME).

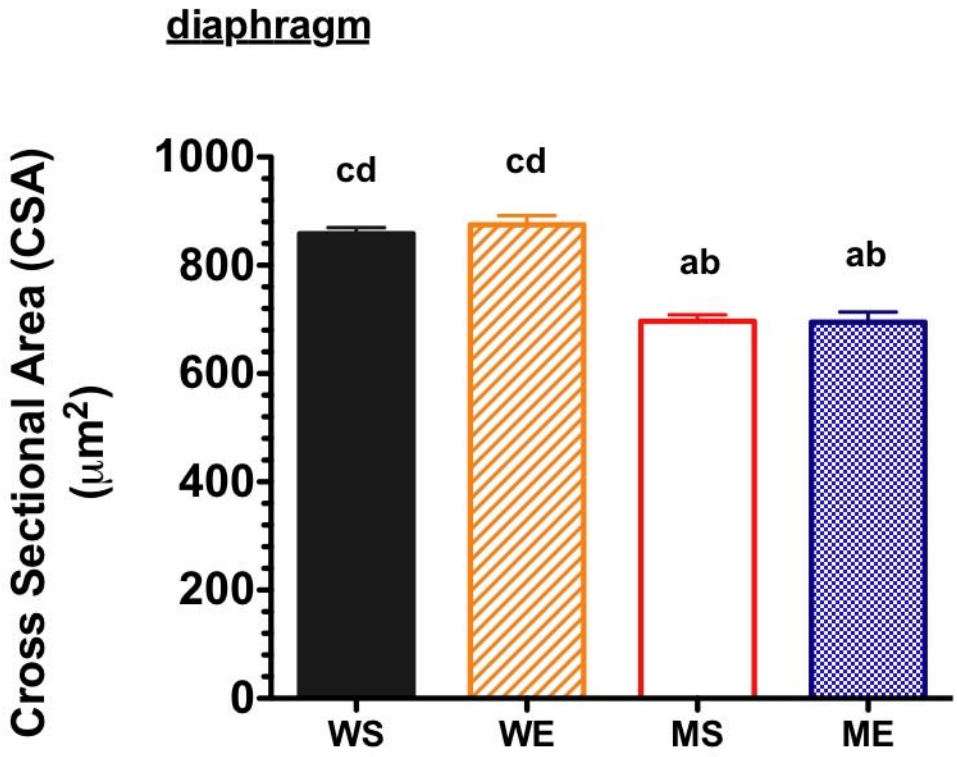

Figure 3. Effect of EUK-134 treatment on diaphragm muscle cross-sectional area (CSA) in wild type and *mdx* mice. Data are expressed as mean ± SEM. Indicating significant change relative to a: WS ($P<0.05$), b: WE ($p<0.05$), c: MS ($p<0.05$), d: ME ($p<0.05$).

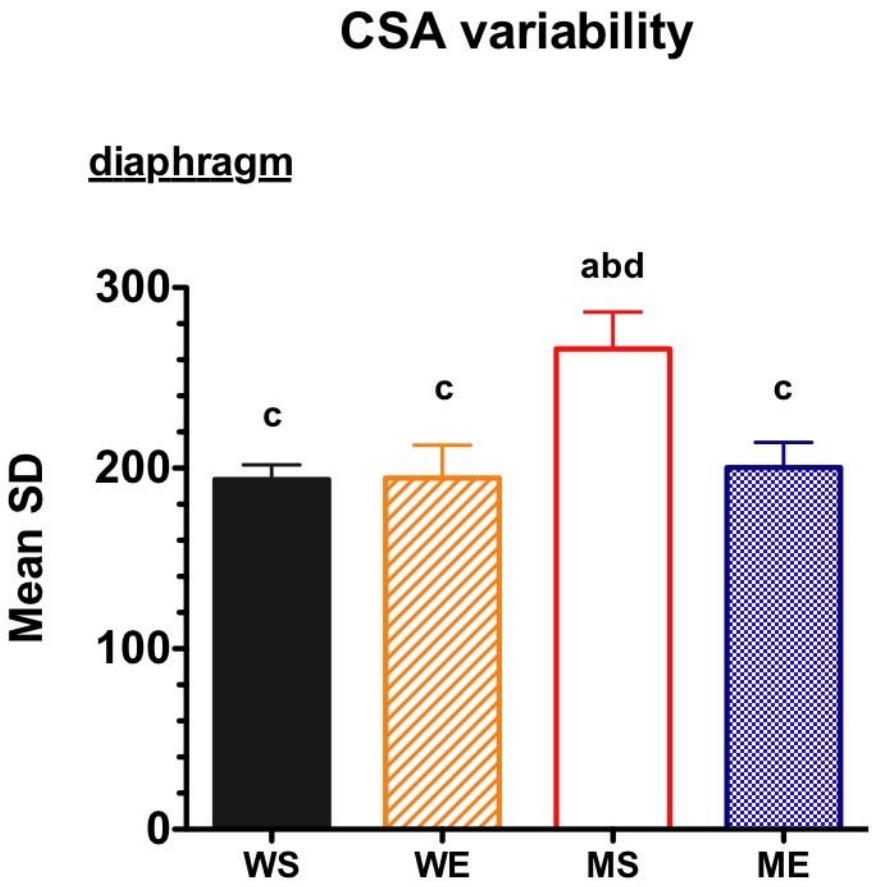

Figure 4. Effect of EUK-134 treatment on diaphragm muscle CSA variability in wild type and *mdx* mice. Data are expressed as mean ± SEM. Indicating significant change relative to a: WS ($P<0.05$), b: WE ($p<0.05$), c: MS ($p<0.05$), d: ME ($p<0.05$).

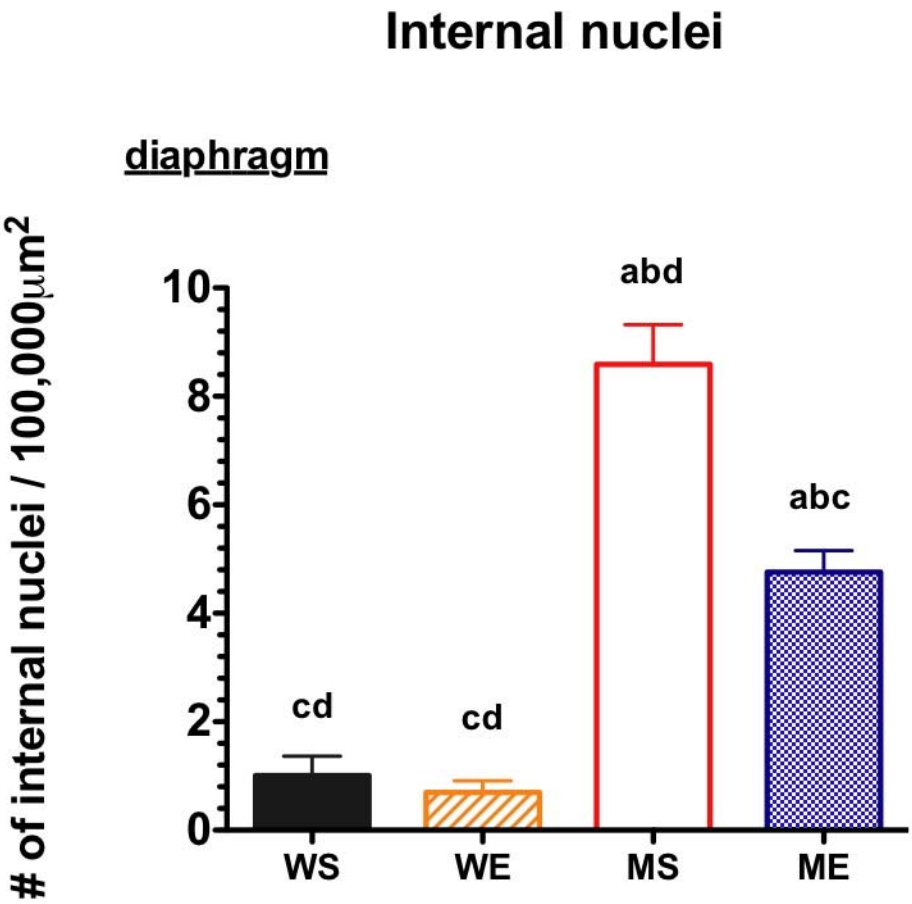

Figure 5. Effect of EUK-134 treatment on # of internal nuclei in wild type and *mdx* mice. Data are expressed as mean ± SEM. Indicating significant change relative to a: WS ($P<0.05$), b: WE ($p<0.05$), c: MS ($p<0.05$), d: ME ($p<0.05$).

Effect of EUK-134 treatment on diaphragm fiber type changes in wild type and *mdx* mice

Given that EUK-134 reversed diaphragm muscle damage, the depression of the mitochondrial oxidative enzyme citrate synthase and diaphragm muscle contractility in *mdx* mice, we sought to determine if EUK-134 also affect the fiber type proportion in diaphragm muscle. Type I fibers were darkly stained for acid ATPase, but lightly stained for alkaline ATPase. Adversely, type II fibers darkly are reactive for alkaline ATPase, lightly stained for acid ATPase. Type IIc fibers were moderately-to-darkly reactive for acid ATPase and moderately reactive for alkaline ATPase (Figure 6). The proportions of type I and type II fiber (%) were lower in saline-treated *mdx* mice than in saline-treated wild type mice (Table 2). There was no EUK-134 treatment effect in type I fiber composition changes both wild type and *mdx* mice (Table 2). Compared with saline-treated *mdx* mice, EUK-134 treated *mdx* mice showed increase in type II fiber. The proportion of type IIc fiber (%) were higher in *mdx* mice compared with wild type mice, but significantly reduced by EUK-134 treatment in *mdx* mice (Table 2).

Figure 6. Effect of EUK-134 treatment on fiber type changes in wild type and *mdx* mice. Staining for myofibrillar ATPase (A, C, E, G: acid preincubation, pH 4.3; B, D, F, H: alkaline preincubation, pH 10.5) of cross sections from diaphragm muscles. Indicate that I : Type I fiber, II: Type II fiber, C: Type IIc fiber.

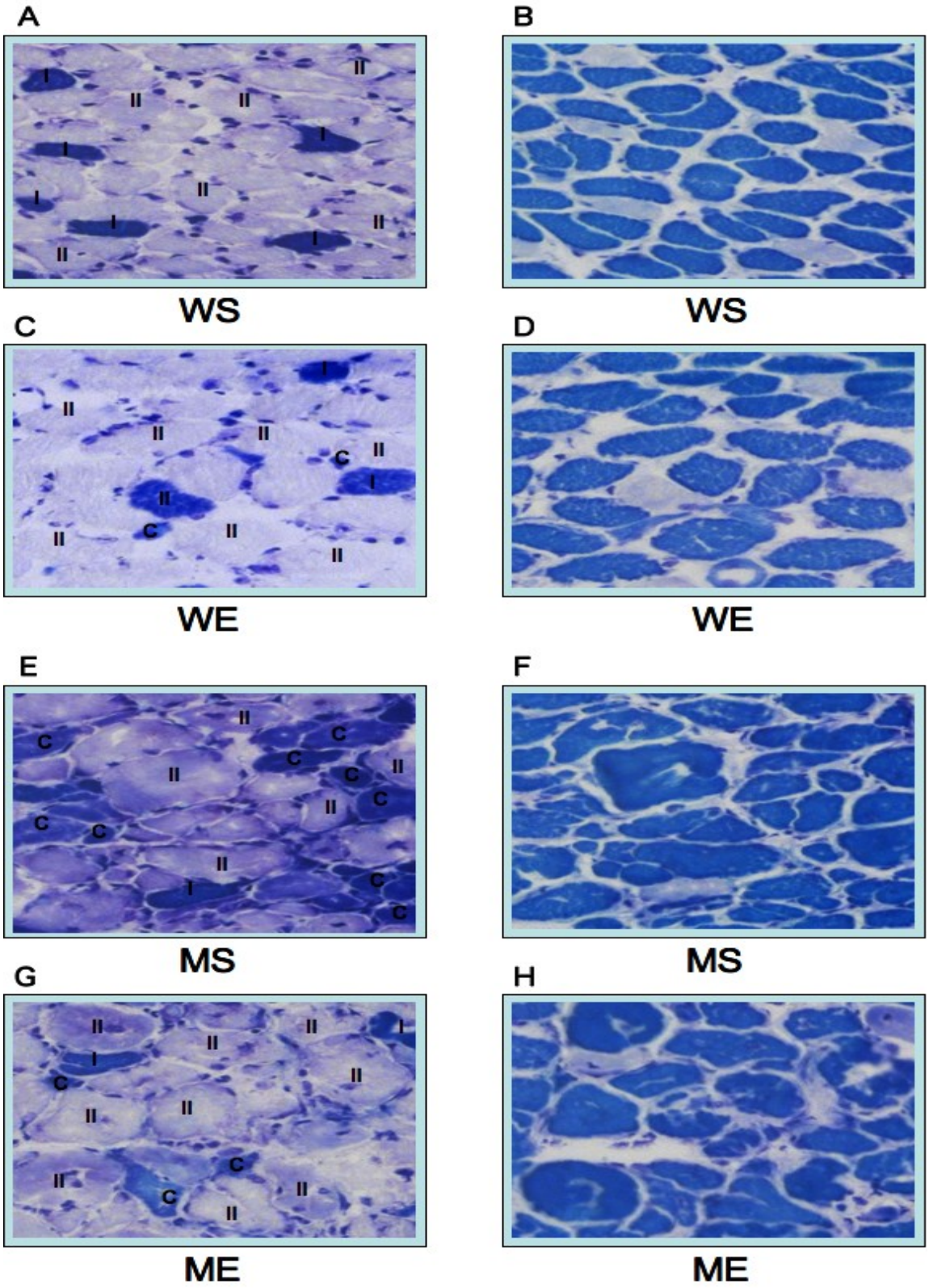
A
B
WS
WS
C
D
WE
WE
E
F
MS
MS
G
H
ME
ME

Table 2. Effect of EUK-134 treatment on changes in fiber type composition (%) in wild type and *mdx* mice

Groups	Type I	Type II (a/b)	Type IIc
WS	8.365 ± 0.390 [c]	89.598 ± 0.227 [c]	2.037 ± 0.390 [c]
WE	7.673 ± 0.200	90.633 ± 0.141 [c]	1.694 ± 0.165 [c]
MS	6.789 ± 0.439 [a]	84.774 ± 1.473 [abd]	8.437 ± 1.507 [abd]
ME	7.435 ± 0.400	87.964 ± 1.105 [c]	4.601 ± 1.167 [c]

Data are expressed as mean ± SEM. WS, wild type with saline; WE, wild type with EUK-134; MS, *mdx* with saline; ME, *mdx* with EUK-134. Indicating significant change relative to a: WS ($P<0.05$), b: WE ($p<0.05$), c: MS ($p<0.05$), d: ME ($p<0.05$)

Effect of EUK-134 treatment on diaphragm muscle protein concentration and citrate synthase activity in wild type and *mdx* mice

Figures 7 & 8 illustrate the soluble and nucleosome protein concentration of diaphragm muscle in *mdx* and wild type mice. There was significant decrease in soluble protein concentration in *mdx* mice compared with wild type mice ($p<0.01$) (Figure 7). However, EUK-134 treatment increased soluble protein concentration in *mdx* mice ($p<0.001$) (Figure 7). There was no difference in nucleosome protein concentration between saline-treated *mdx* and wild type mice (Figure 8). However, EUK-134 treatment increased nucleosome protein concentration in *mdx* mice ($p<0.001$) (Figure 8).

Citrate synthase activity, a marker of oxidative capacity and indicative of mitochondrial density and function, was significantly lower in *mdx* mice (- 27.1%) compared with wild type mice, but increased with EUK-134 treatment in *mdx* mice (+42.8%, $p<0.01$) (Figure 9).

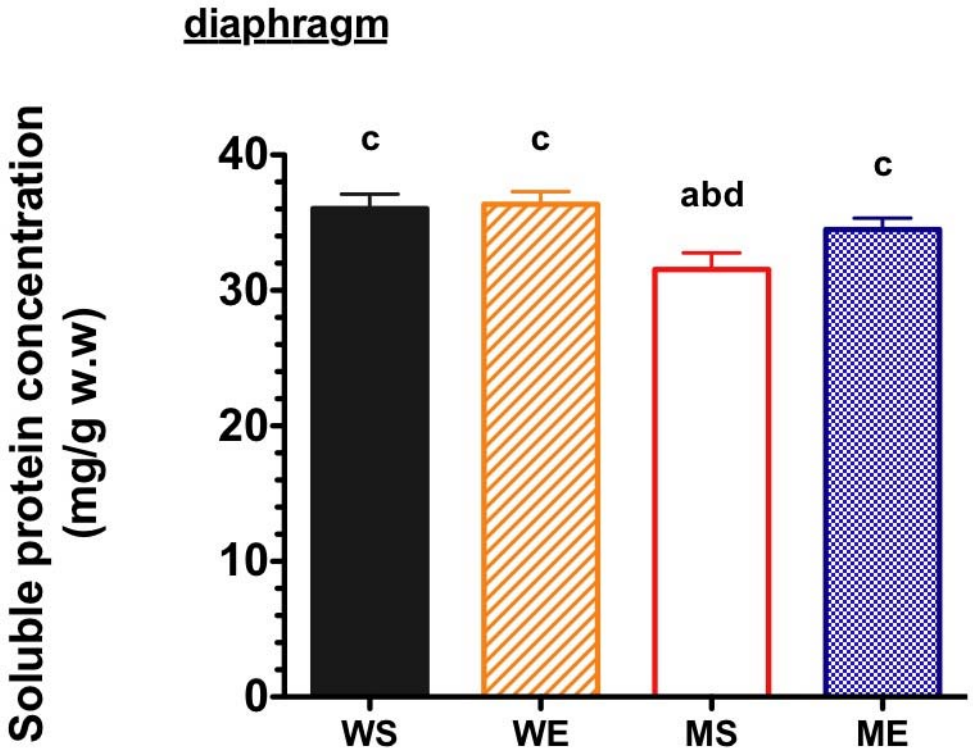

Figure 7. Effect of EUK-134 treatment on diaphragm muscle protein concentration (soluble) in wild type and *mdx* mice. Data are expressed as mean ± SEM. Indicating significant change relative to a: WS ($P<0.05$), b: WE ($p<0.05$), c: MS ($p<0.05$), d: ME ($p<0.05$).

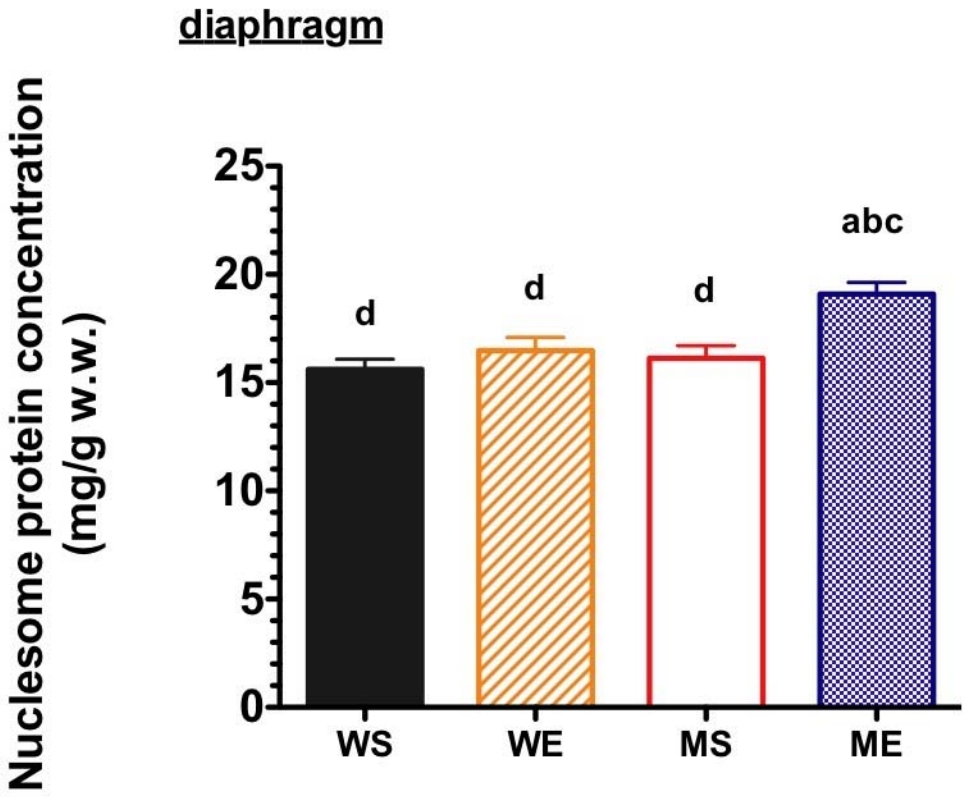

Figure 8. Effect of EUK-134 treatment on diaphragm muscle protein concentration (nucleosome) in wild type and *mdx* mice. Data are expressed as mean ± SEM. Indicating significant change relative to a: WS ($P<0.05$), b: WE ($p<0.05$), c: MS ($p<0.05$), d: ME ($p<0.05$).

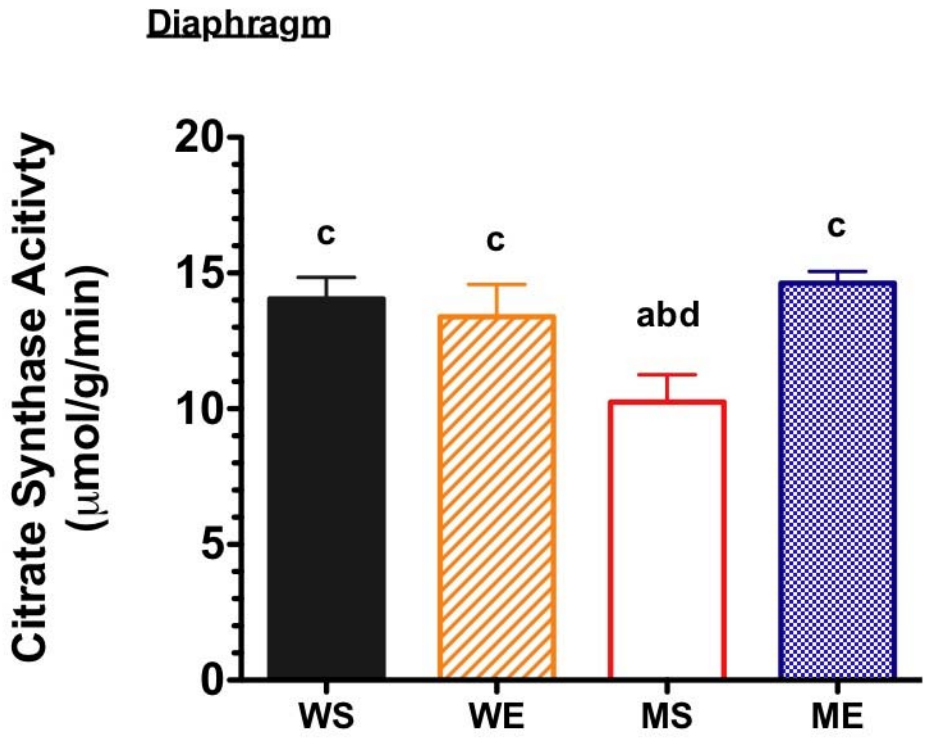

Figure 9. Effect of EUK-134 treatment on diaphragm muscle citrate synthase activity in wild type and *mdx* mice. Data are expressed as mean ± SEM. Indicating significant change relative to a: WS ($P<0.05$), b: WE ($p<0.05$), c: MS ($p<0.05$), d: ME ($p<0.05$).

Effect of EUK-134 treatment on oxidative stress in wild type and *mdx* mice

Total hydroperoxide levels were significantly higher in *mdx* mice compared with wild type mice (+12.0 %, $p<0.01$) (Figure 10). In diaphragm muscle, total hydroperoxides were not different between saline-treated wild type and EUK-134 treated wild type mice. However, EUK-134 treatment in *mdx* mice blunted oxidative stress compared with saline-treated *mdx* mice, with total hydroperoxides that were not different with saline-treated wild type mice. Localization of 4-HNE protein abducts in wild type and *mdx* mice were higher in both cytoplasms and nucleus (Figure 11). Compared with saline-treated wild type, labeling density of 4-HNE in cytoplasm and nucleus was higher in saline-treated *mdx* mice. However, EUK-134 decreased labeling density of 4-HNE in *mdx* mice.

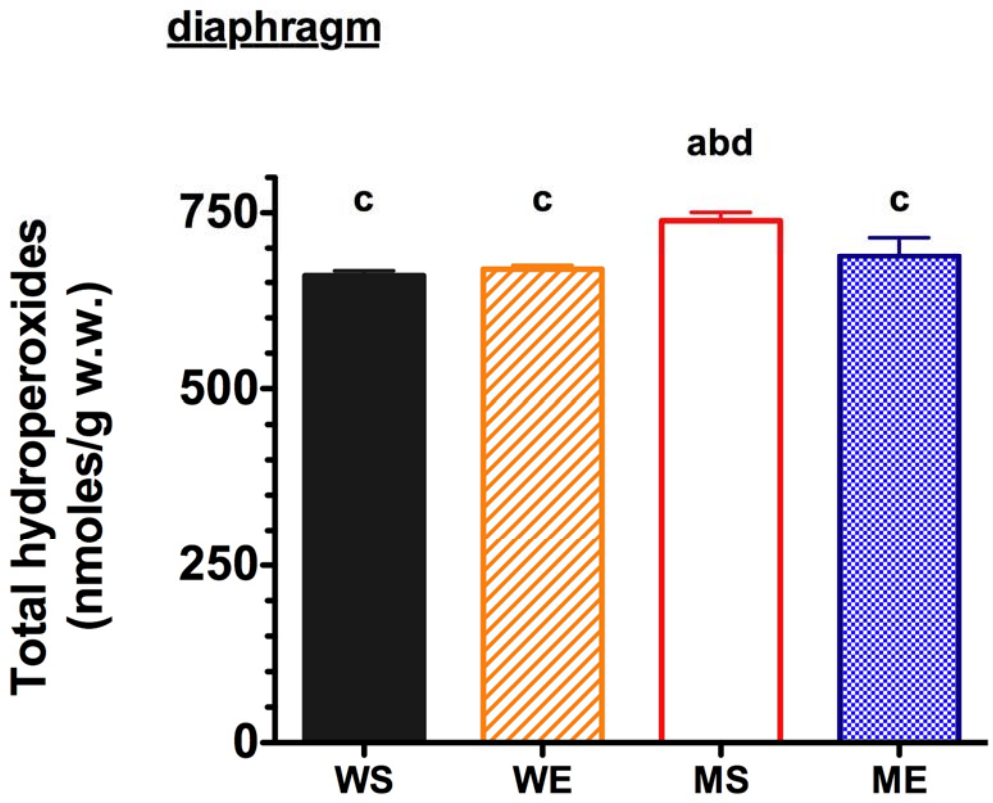

Figure 10. Effect of EUK-134 treatment on total hydroperoxides in wild type and *mdx* mice. Data are expressed as mean ± SEM. Indicating significant change relative to a: WS ($P<0.05$), b: WE ($p<0.05$), c: MS ($p<0.05$), d: ME ($p<0.05$).

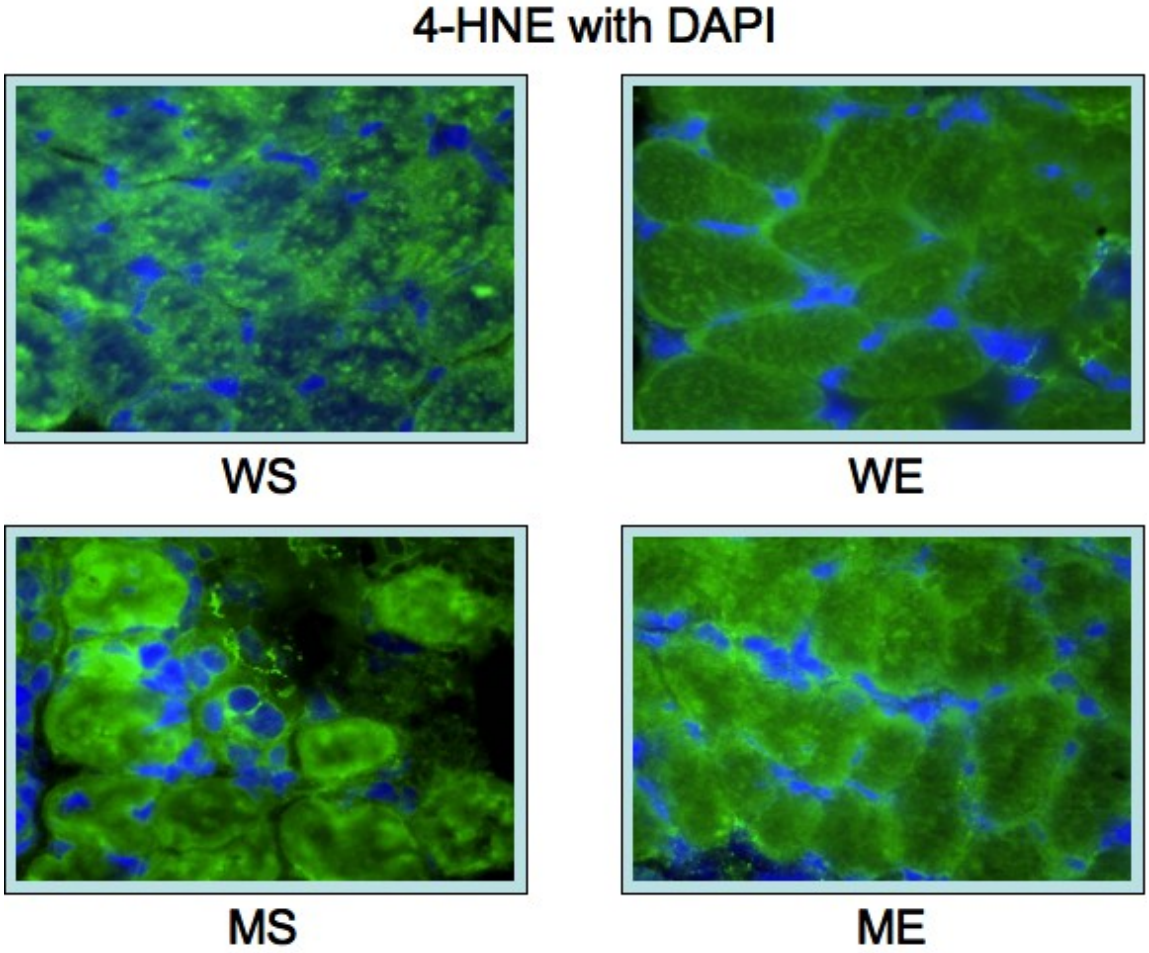

Figure 11. Effect of EUK-134 treatment on localization of 4-hydroxynonenal (4-HNE) in wild type and *mdx* mice.

Effect of EUK-134 treatment on T-cells ($CD4^+$ & $CD8^+$) and macrophages in wild type and *mdx* mice

To verify if EUK-134 treatment attenuated diaphragm muscle inflammation, we measured the immunoreactivity of T-cells ($CD4^+$ & $CD8^+$) and macrophages in the diaphragm muscles of 4 groups of mice at 28 days of age. Compared with saline-treated *mdx* mice, EUK-134 treated *mdx* mice showed substantial reduction of inflammation in the diaphragm highlighted by $CD4^+$ and $CD8^+$, macrophages (CD11b) immunostaining (Figures 12-17). $CD4^+$ immunoreactivity area (%) was higher in saline-treated *mdx* mice (+12.9% and +12.7%, respectively) than in saline-treated and EUK-134 treated wild type mice (Figures 13 & 14). EUK-134 treatment significantly reduced immunoreactivity of $CD4^+$ in *mdx* mice (-6.3%) (Figure 13). $CD8^+$ immunoreactivity area was higher in saline-treated *mdx* mice (+15.0% and +14.9%, respectively) than in saline-treated and EUK-134 treated wild type mice (Figures 14 & 15). Immunoreactive inflammation area of $CD8^+$ was reduced in EUK-134 treated *mdx* mice compared with saline-treated *mdx* mice (-13.1%, $p<0.001$) (Figure 15). Macrophages immunoreactive area (%) was significantly higher in saline-treated *mdx* mice (+15.0% and +14.9%, respectively) than in saline-treated ($p<0.001$) and EUK-134 treated wild type mice ($p<0.001$) (Figures 16 & 17). Likewise, immunoreactive inflammation area (%) of macrophages was significantly reduced in EUK-134 treated *mdx* mice as compared with saline-treated *mdx* mice (-13.1%, $p<0.01$) (Figure 17). These findings demonstrated that EUK-134 significantly attenuated diaphragm inflammation associated with dystrophin-deficient *mdx* mice.

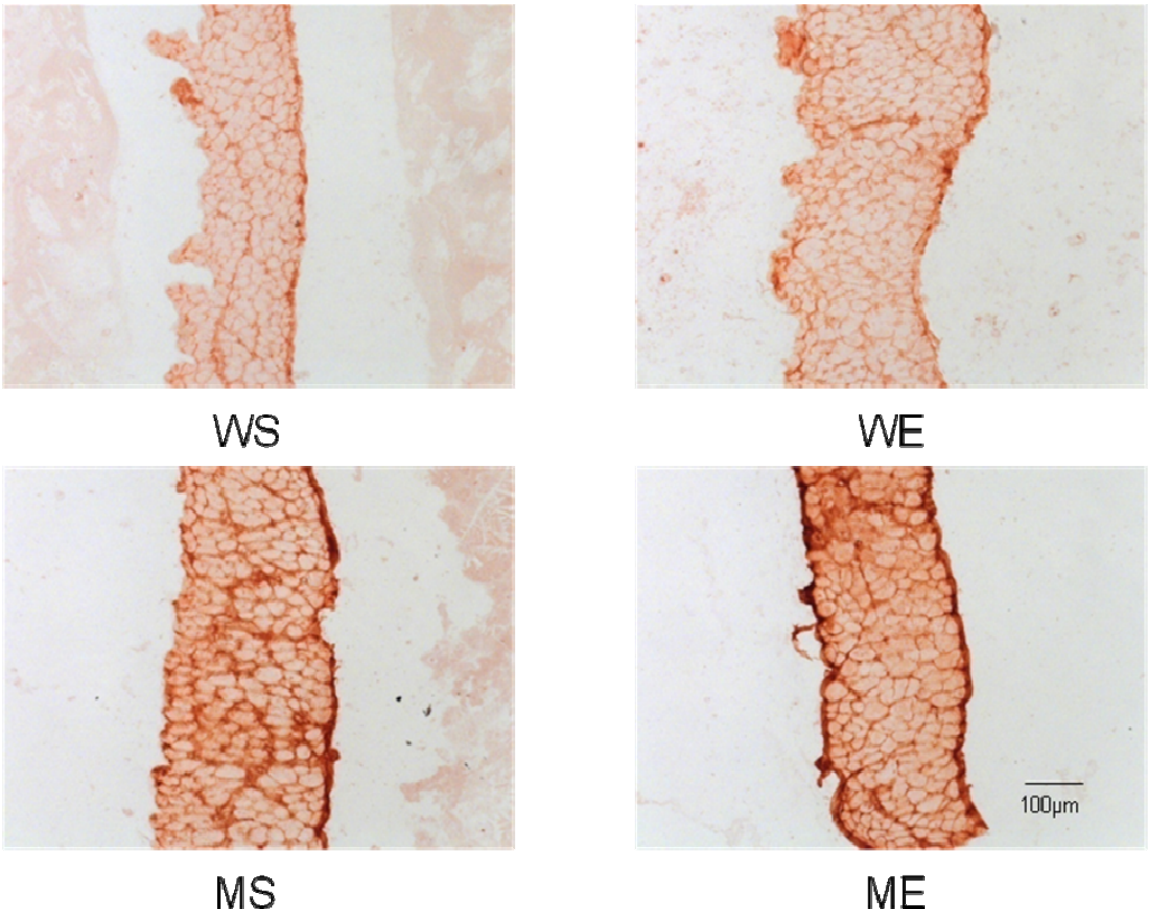

Figure 12. Effect of EUK-134 treatment on localization of $CD4^+$ in wild type and *mdx* mice. Data are expressed as mean ± SEM. Indicating significant change relative to a: WS ($P<0.05$), b: WE ($p<0.05$), c: MS ($p<0.05$), d: ME ($p<0.05$).

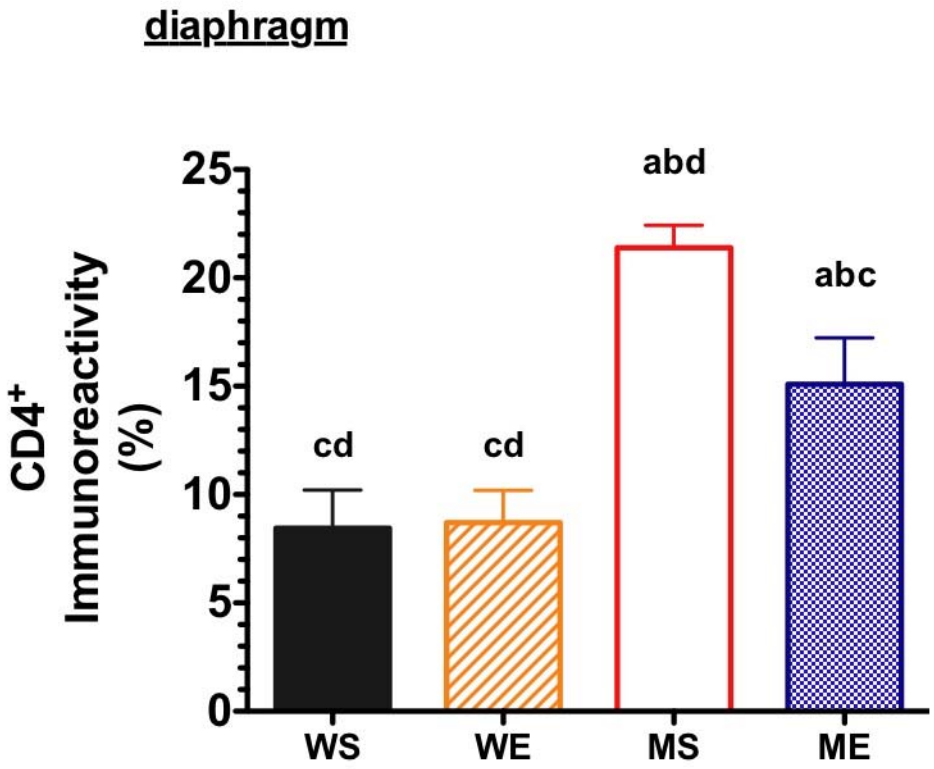

Figure 13. Effect of EUK-134 treatment on $CD4^+$ immunoreactivity in wild type and *mdx* mice. Data are expressed as mean ± SEM. Indicating significant change relative to a: WS ($P<0.05$), b: WE ($p<0.05$), c: MS ($p<0.05$), d: ME ($p<0.05$).

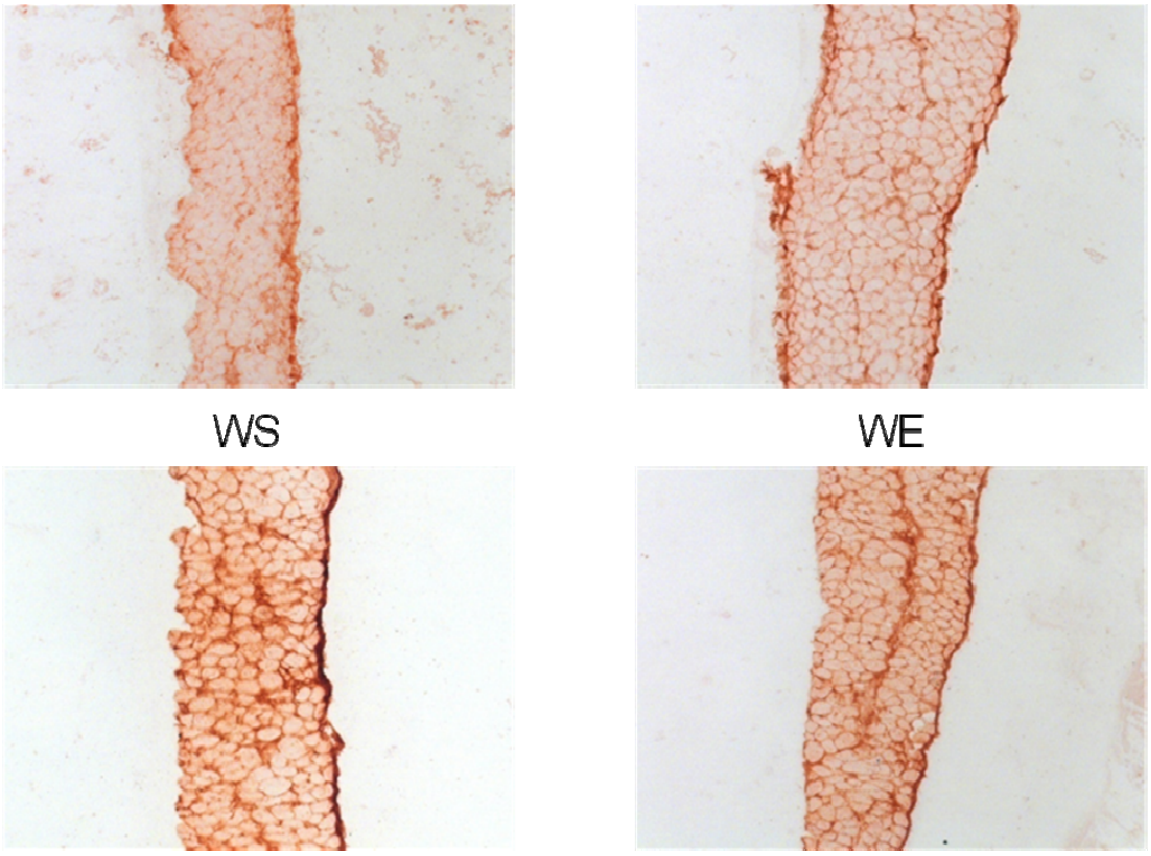

Figure 14. Effect of EUK-134 treatment on localization of $CD8^+$ in wild type and *mdx* mice. Data are expressed as mean ± SEM. Indicating significant change relative to a: WS ($P<0.05$), b: WE ($p<0.05$), c: MS ($p<0.05$), d: ME ($p<0.05$).

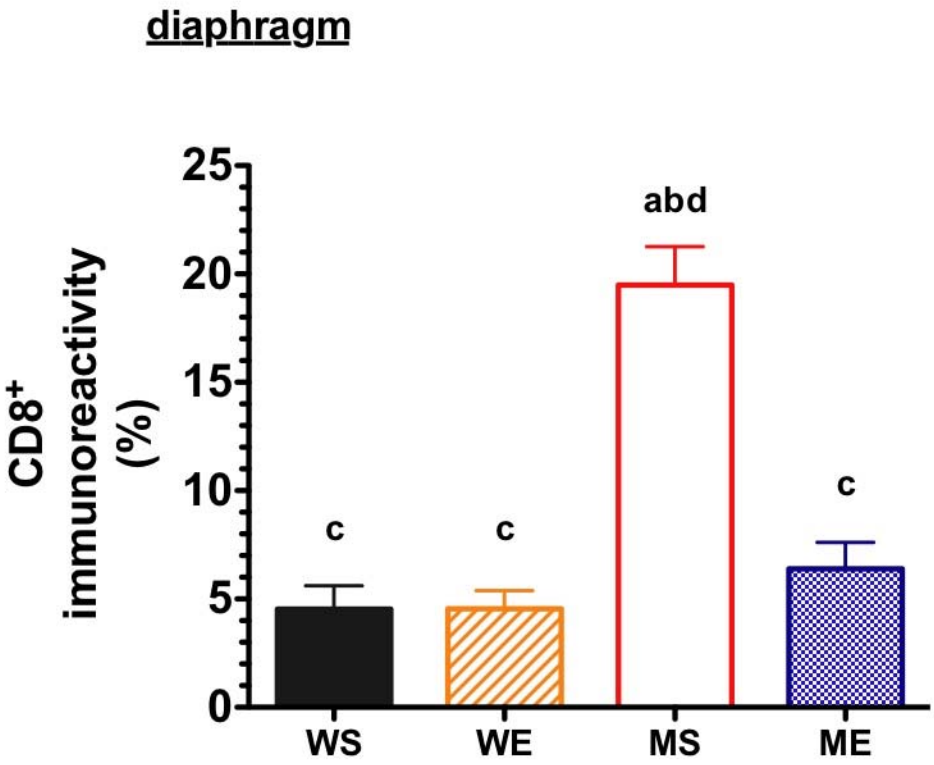

Figure 15. Effect of EUK-134 treatment on $CD8^+$ immunoreactivity in wild type and *mdx* mice. Data are expressed as mean ± SEM. Indicating significant change relative to a: WS ($P<0.05$), b: WE ($p<0.05$), c: MS ($p<0.05$), d: ME ($p<0.05$).

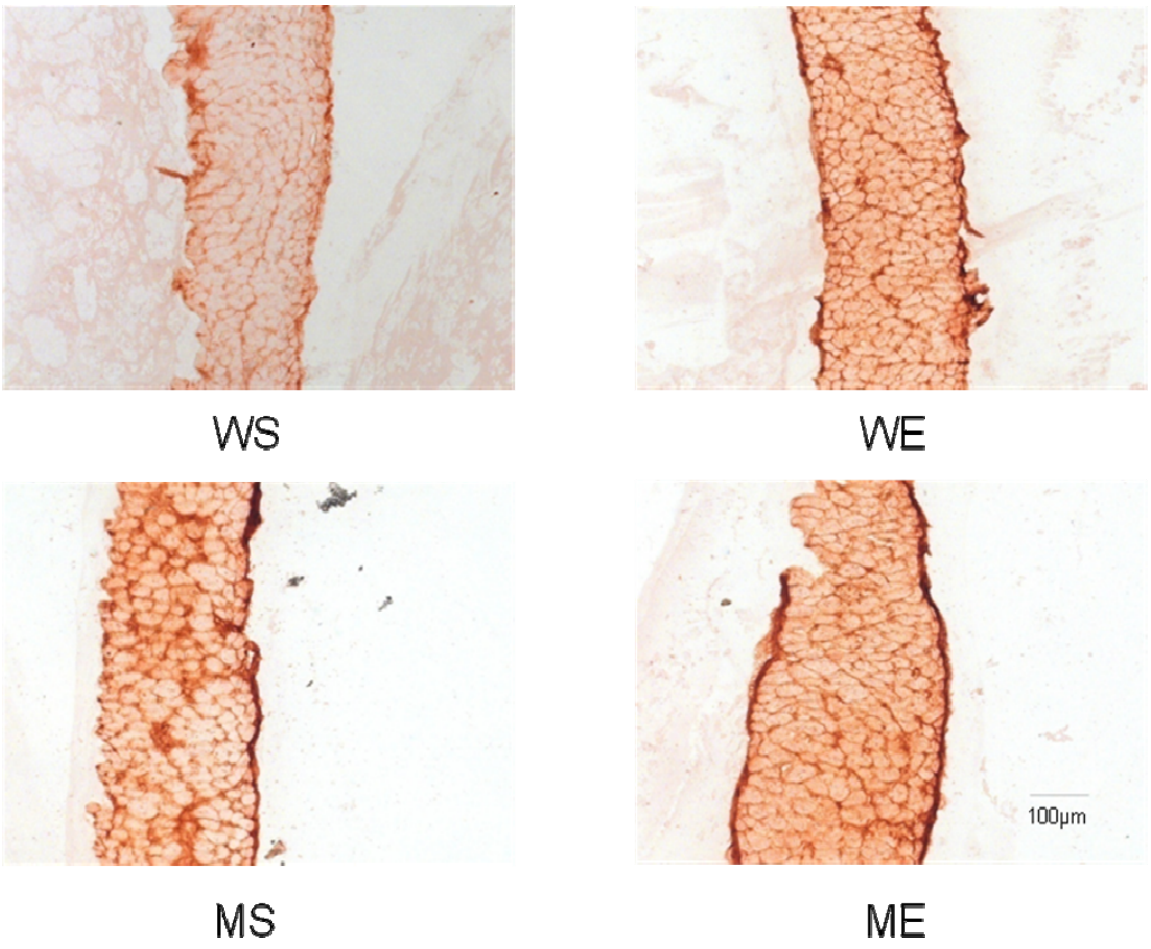

Figure 16. Effect of EUK-134 treatment on localization of macrophages in wild type and *mdx* mice. Data are expressed as mean ± SEM. Indicating significant change relative to a: WS ($P<0.05$), b: WE ($p<0.05$), c: MS ($p<0.05$), d: ME ($p<0.05$).

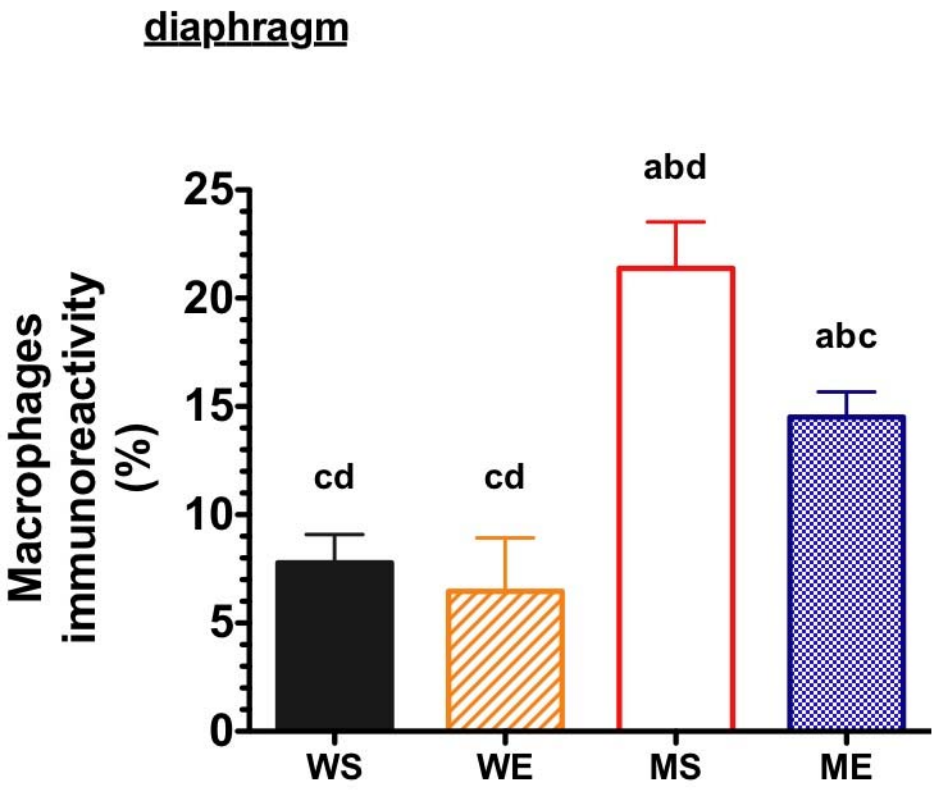

Figure 17. Effect of EUK-134 treatment on macrophages immunoreactivity in wild type and *mdx* mice. Data are expressed as mean ± SEM. Indicating significant change relative to a: WS ($P<0.05$), b: WE ($p<0.05$), c: MS ($p<0.05$), d: ME ($p<0.05$).

Effect of EUK-134 treatment on NF-kB p65 subunit DNA binding activity and protein levels in wild type and *mdx* mice

NF-κB p65 subunit DNA binding activity was significantly higher in *mdx* mice compared with wild type mice (+14.6%) (Figure 18). EUK-134 treatment resulted in a significant decrease of NF-κB p65 subunit DNA binding activity in *mdx* mice (-7.6%) (Figure 18). To verify if NF-κB DNA binding activity is directly related to NF-κB p65 subunit translocation, we measured the NF-κB p65 protein levels. The NF-κB p65 protein levels in the nucleosome fraction were higher in *mdx* mice compared with wild type mice (+60.2%) (Figure 19). 8 days of EUK-134 treatment resulted in a significant reduction in NF-κB nucleosome protein levels in *mdx* (-47.1%), but not in wild type mice (Figure 19).

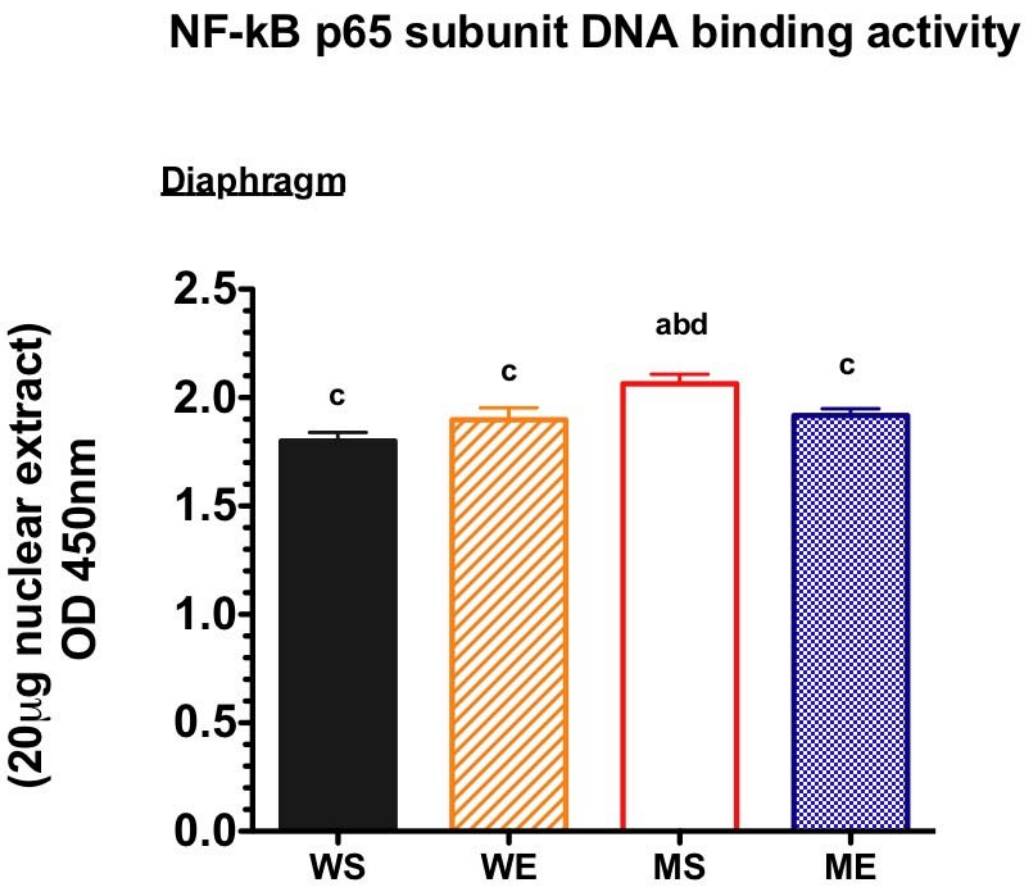

Figure 18. Effect of EUK-134 treatment on NF-kB p65 subunit DNA binding activity in nucleosome fraction of wild type and *mdx* mice. Data are expressed as mean ± SEM. Indicating significant change relative to a: WS ($P<0.05$), b: WE ($p<0.05$), c: MS ($p<0.05$), d: ME ($p<0.05$).

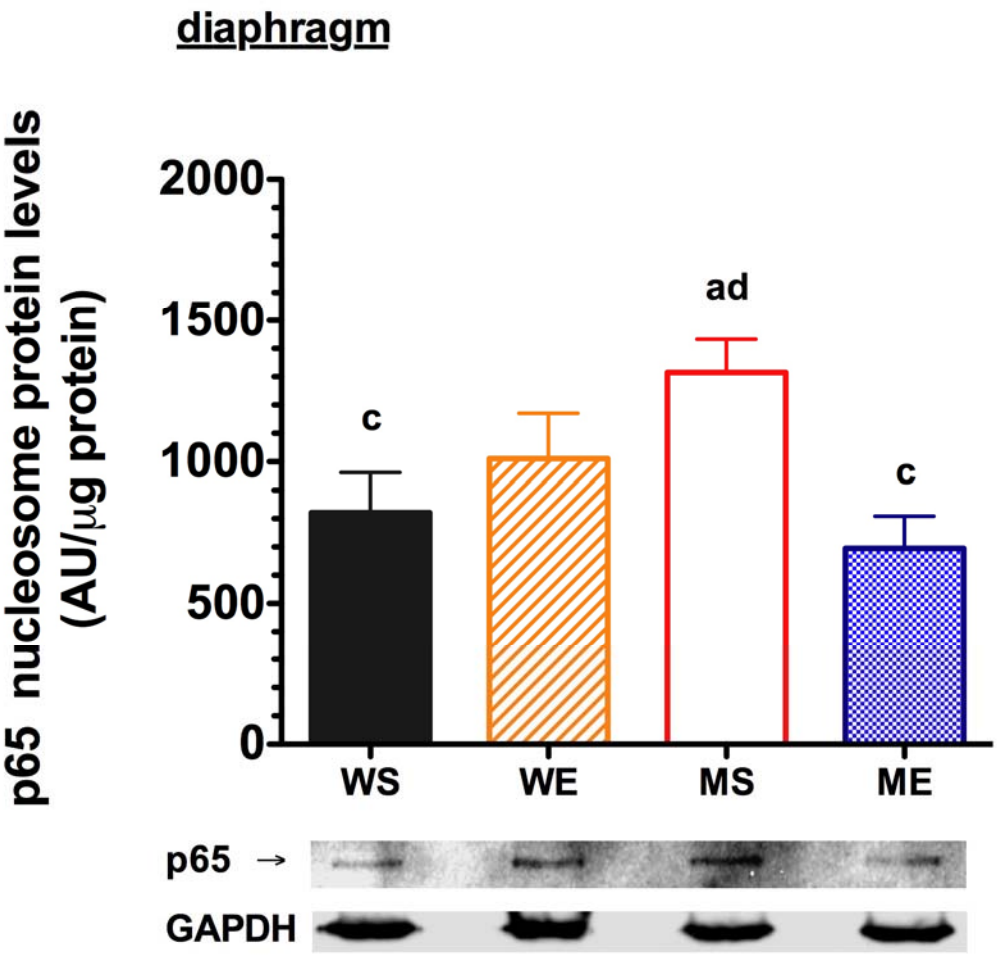

Figure 19. Effect of EUK-134 treatment on NF-kB p65 nucleosome protein levels in wild type and *mdx* mice. Data are expressed as mean ± SEM. Indicating significant change relative to a: WS ($P<0.05$), b: WE ($p<0.05$), c: MS ($p<0.05$), d: ME ($p<0.05$).

Effect of EUK-134 treatment on localization of dystrophin, nNOS and other cytoskeleal proteins in wild type and *mdx* mice

The expression of dystrophin was detected at the sarcolemma in wild type mice, but completely absent in *mdx* mice (Figure 20). In *mdx* mice, nNOS was absent from the sarcolemma but expressed in the cytosol although in small amounts (Figure 21). Remarkably, EUK-134 partially restored nNOS back to the sarcolemmal cytoskeleton in *mdx* mice (Figure 21). The α1-syntrophin which anchors nNOS to sarcolemma was absent in *mdx* mice (Figure 22). However, EUK-134 partly relocated α1-syntrophin back to the sarcolemmal region in *mdx* mice (Figure 22). The α-dystrobrevin and β-sarcoglycan were expressed sarcolemmal cytoskeleton in both wild type mice and *mdx* mice (Figures 23 & 24). There was no localization effect of EUK-134 on α-dystrobrevin and β-sarcoglycan in wild type and *mdx* mice (Figures 23 & 24).

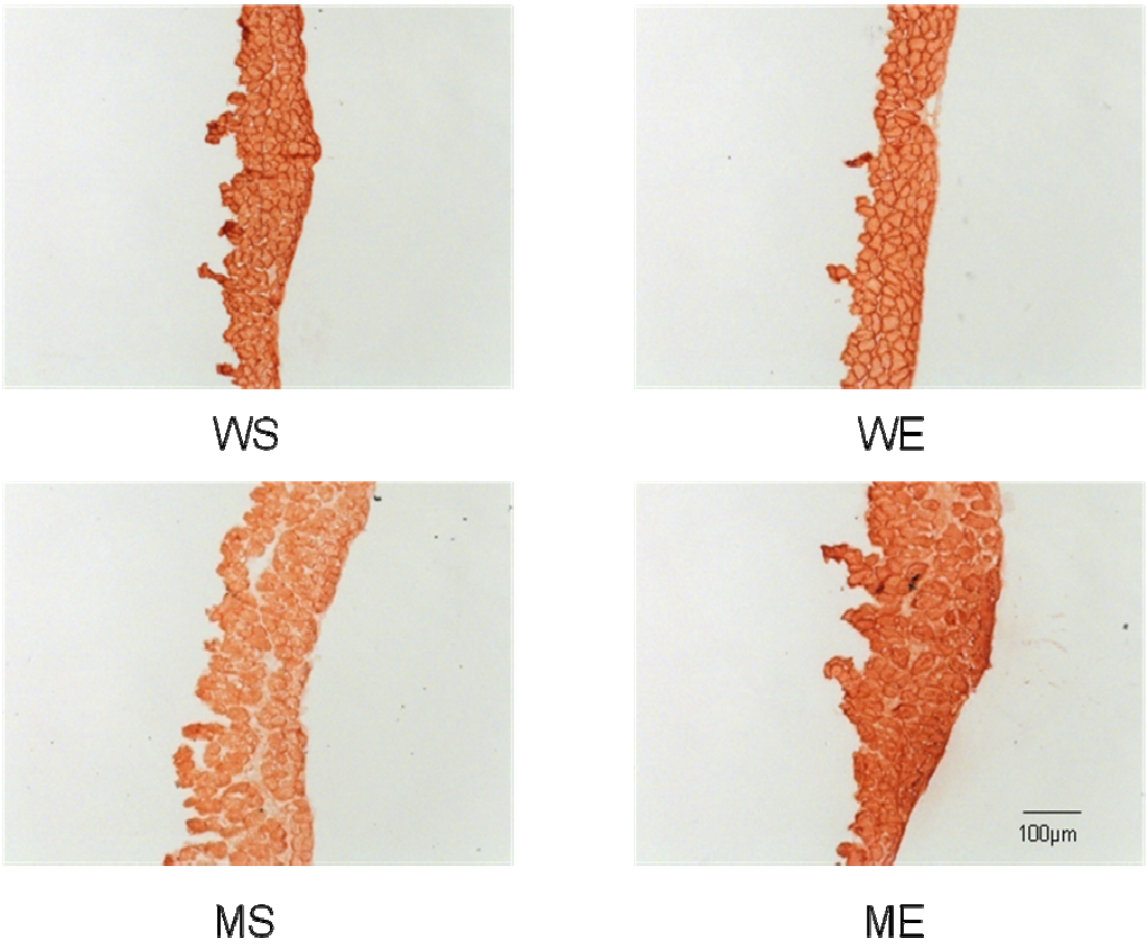

Figure 20. Effect of EUK-134 treatment on localization of dystrophin in wild type and *mdx* mice.

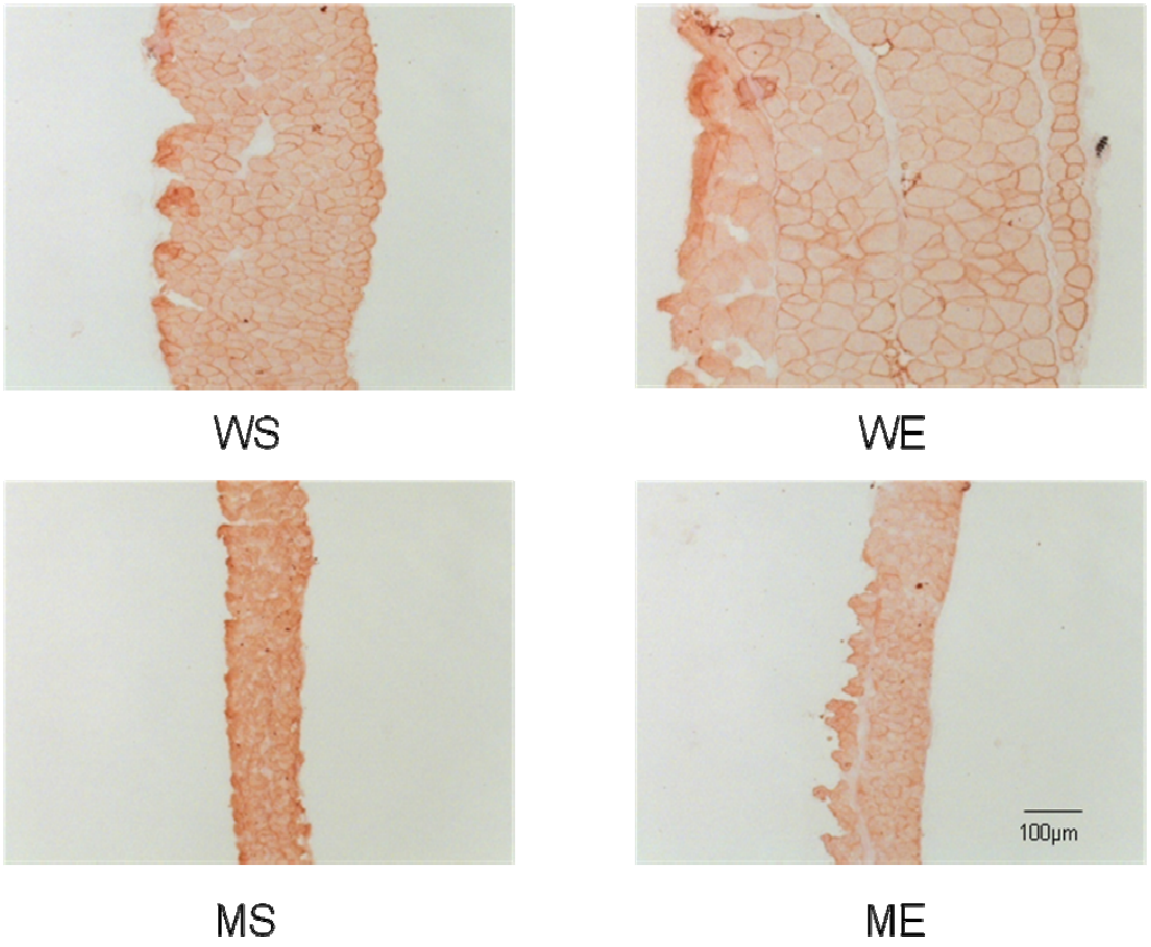

Figure 21. Effect of EUK-134 treatment on localization of nNOS in wild type and *mdx* mice.

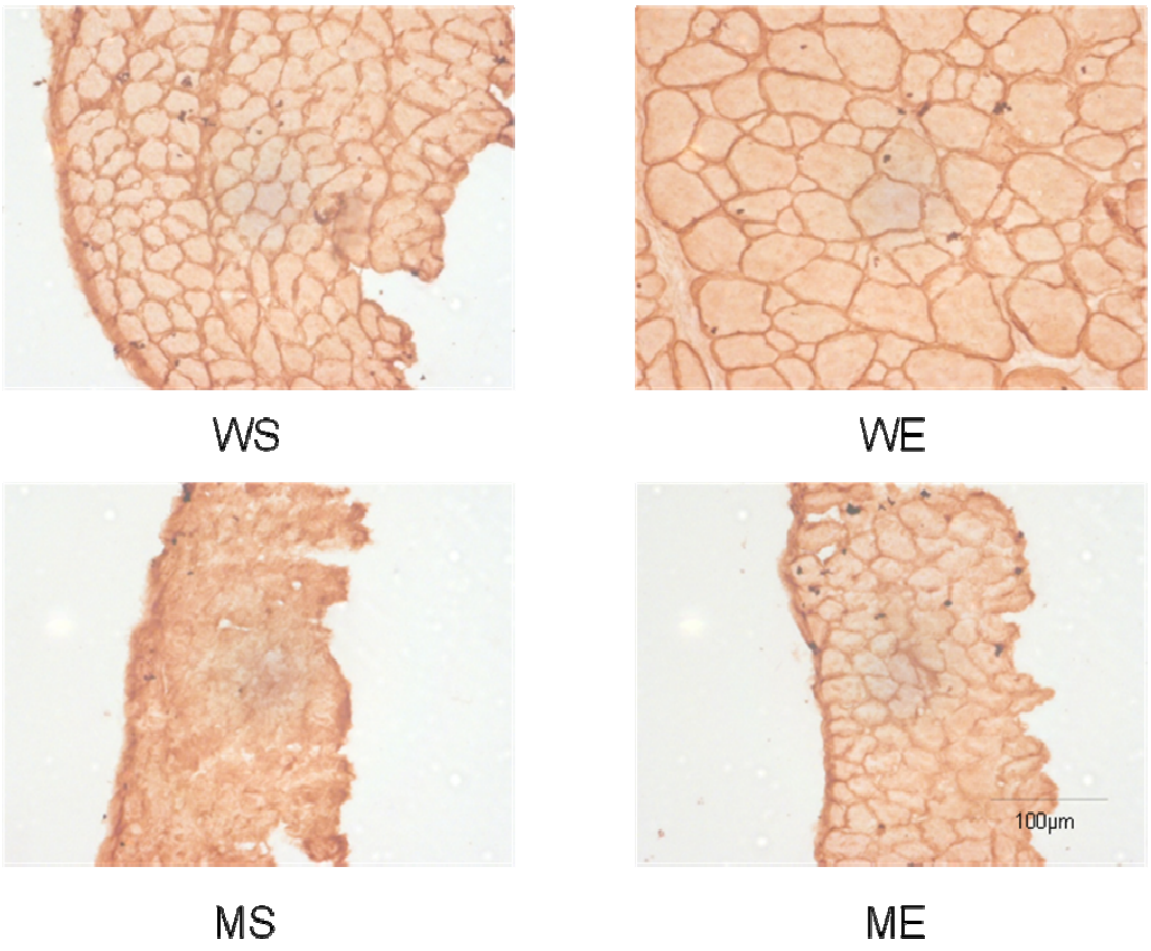

Figure 22. Effect of EUK-134 treatment on localization of α1-syntrophin in wild type and *mdx* mice.

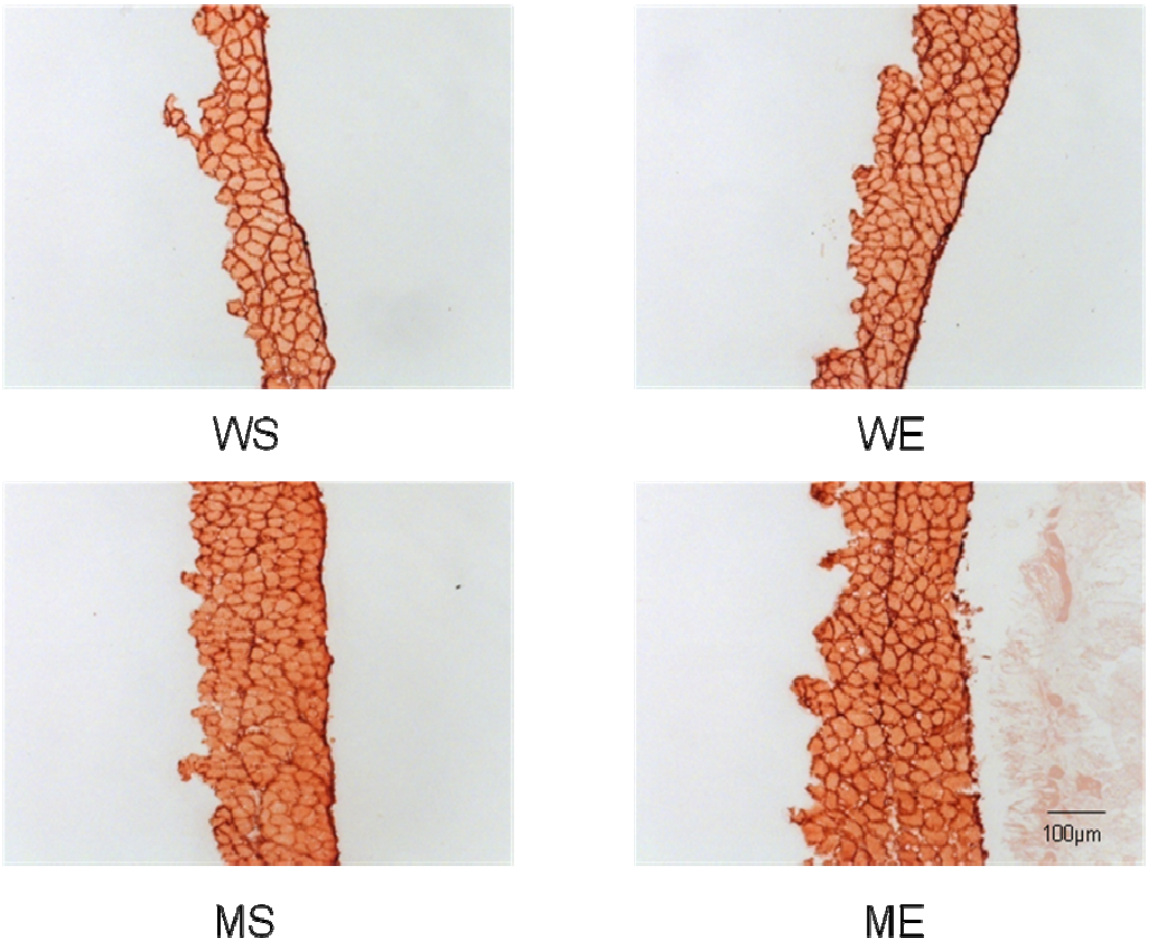

Figure 23. Effect of EUK-134 treatment on localization of α-dystrobrevin in wild type and *mdx* mice.

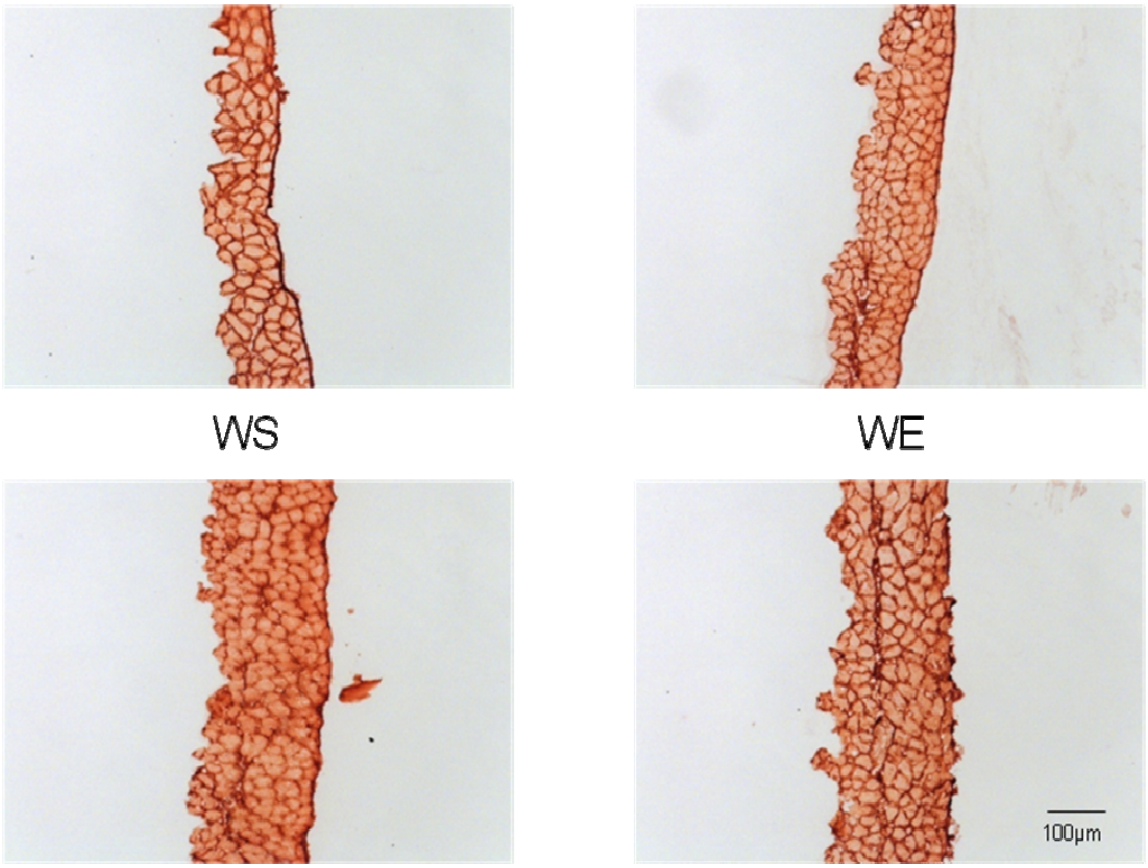

Figure 24. Effect of EUK-134 treatment on localization of β-sarcoglycan in wild type and *mdx* mice.

Effect of EUK-134 treatment on diaphragm muscle contractile function in wild type and *mdx* mice

Diaphragm muscle twitch (Lo), low frequency tension (20Hz) and maximal isometric tension (150Hz; Po) were higher in saline-treated wild type mice compared with saline-treated *mdx* mice (Figures 25-27). However, 8 days of EUK-134 treatment in *mdx* mice resulted in a significant increase in twitch, low frequency tension, and Po compared with saline-treated *mdx* mice (Figures 25-27).

Remarkably, even a single exposure of EUK-134 (50mM) in vitro resulted in a significant increase in twitch (+71.2%) and low frequency tension (+58.2%), but without affecting Po (+2.4%) in saline-treated *mdx* diaphragm compared with each initial tension value (Figures 28-30). There were no significant effects of a single exposure of EUK-134 on twitch (+6.6%, -16.9% and +5.4%, respectively), low frequency tension (+9.0%, -8.7% and +12.7%, respectively), and Po (+8.3%, +3.5% and +4.2%, respectively) in saline-treated wild type, EUK-134 treated wild type group and EUK-134 treated *mdx* group compared with each initial tension value (Figures 28-30).

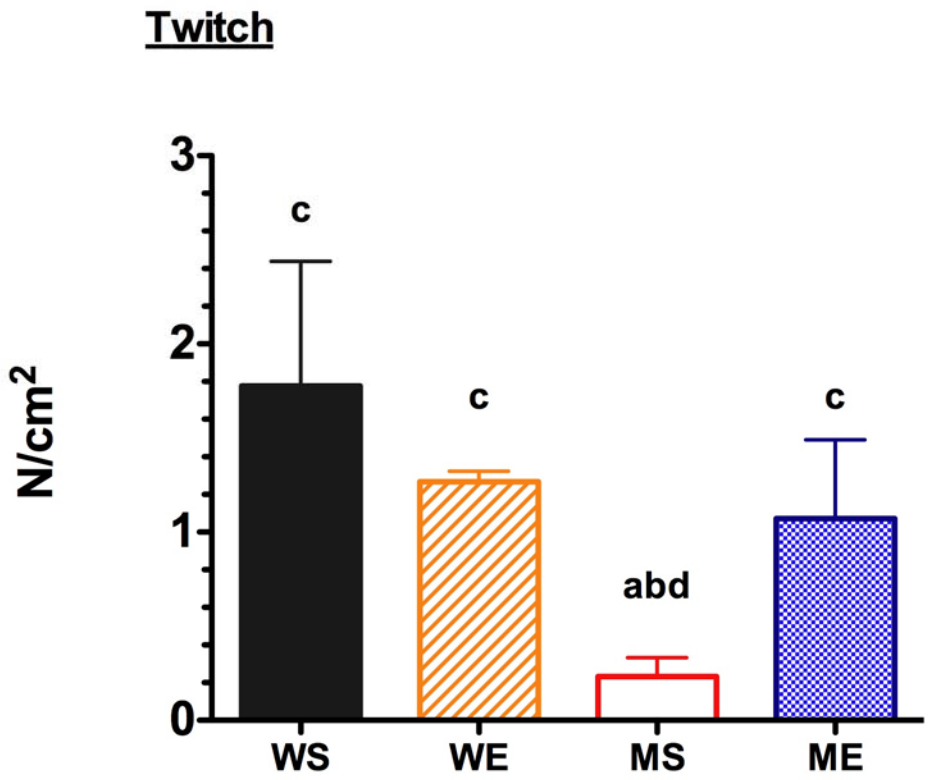

Figure 25. Effect of EUK-134 treatment on twitch tension in wild type and *mdx* mice. Data are expressed as mean ± SEM. Indicating significant change relative to a: WS ($P<0.05$), b: MS ($p<0.05$), c: ME ($p<0.05$).

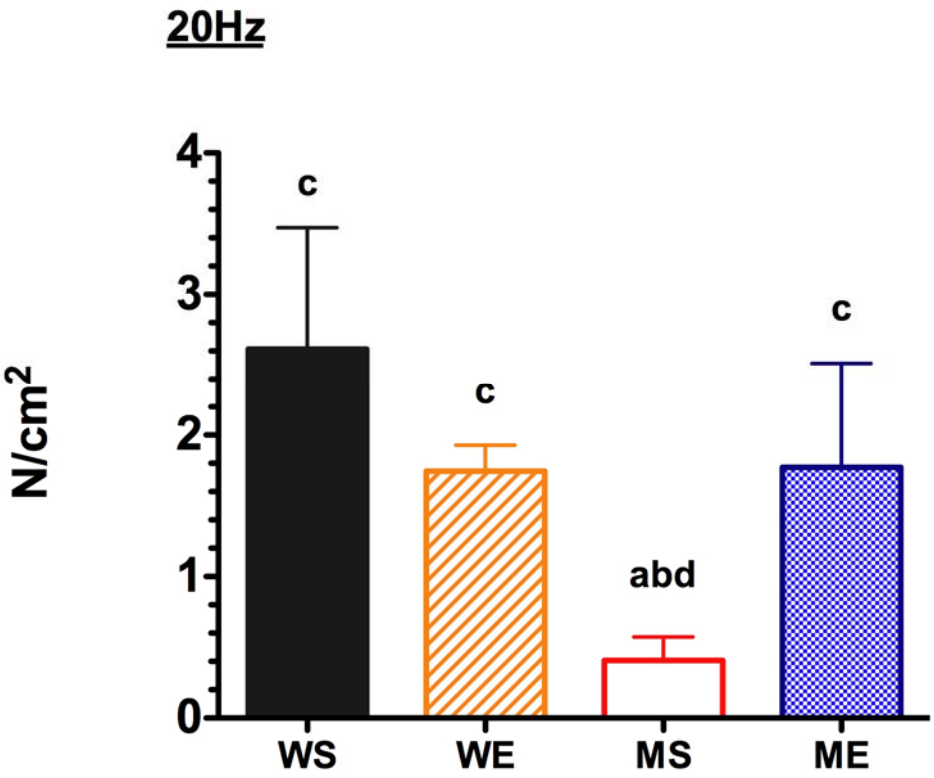

Figure 26. Effect of EUK-134 treatment on low-frequency tension (20Hz) in wild type and *mdx* mice. Data are expressed as mean ± SEM. Indicating significant change relative to a: WS ($P<0.05$), b: MS ($p<0.05$), c: ME ($p<0.05$).

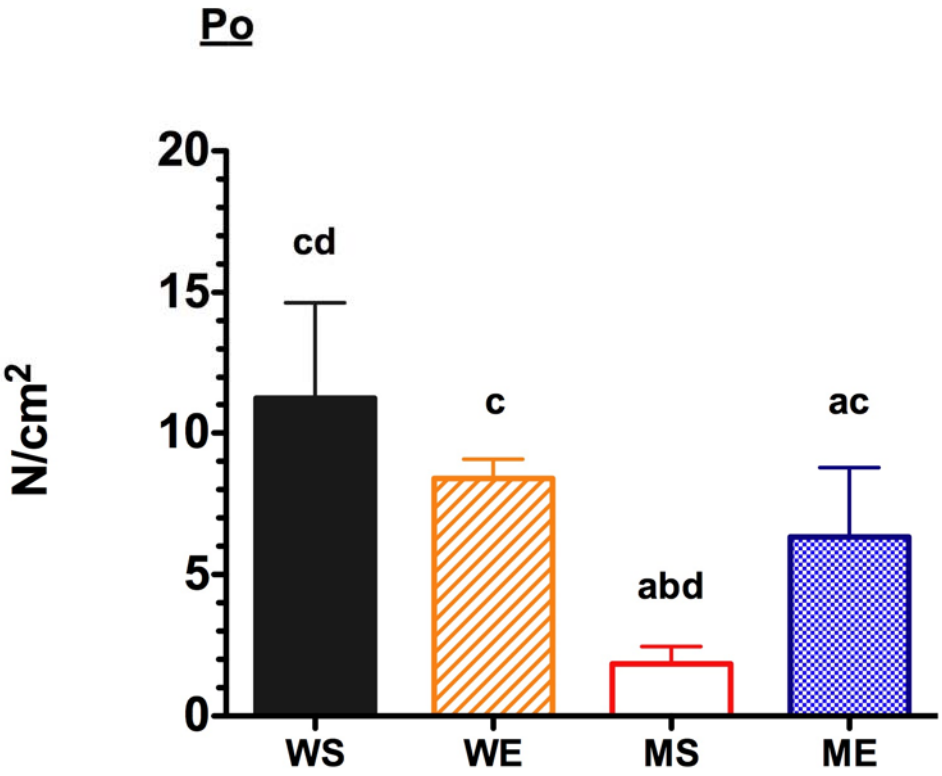

Figure 27. Effect of EUK-134 treatment on maximal isometric tension (Po) in wild type and *mdx* mice. Data are expressed as mean ± SEM. Indicating significant change relative to a: WS ($P<0.05$), b: MS ($p<0.05$), c: ME ($p<0.05$).

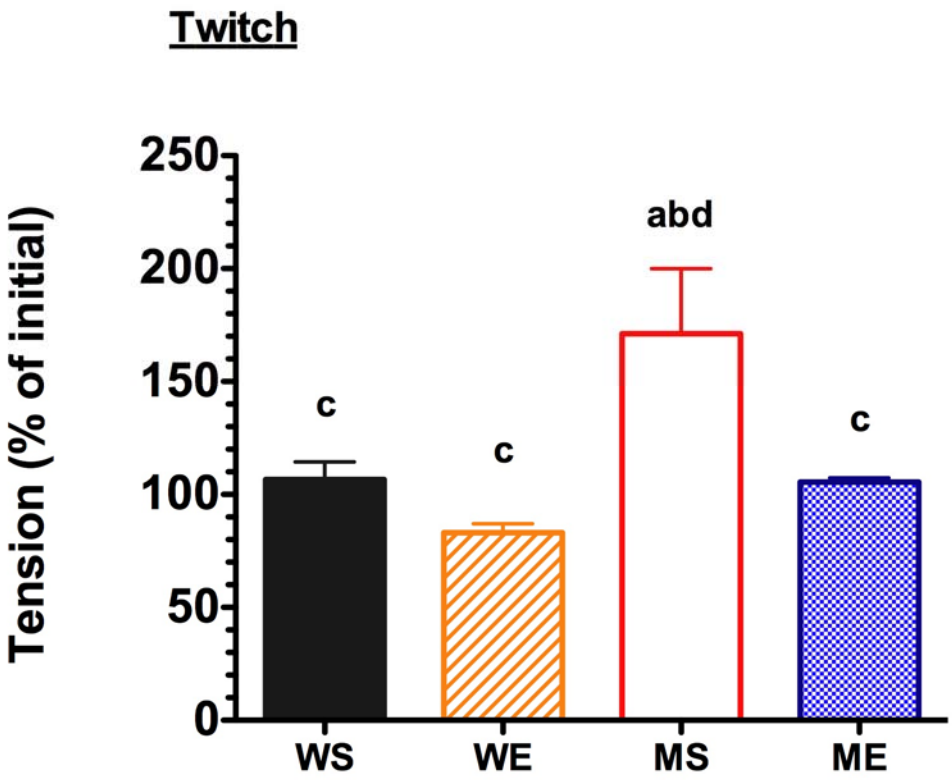

Figure 28. Effect of a single exposure of EUK-134 (50mM) on twitch tension in wild type and *mdx* mice. Data are expressed as mean ± SEM. Indicating significant change relative to a: WS ($P<0.05$), b: MS ($p<0.05$), c: ME ($p<0.05$).

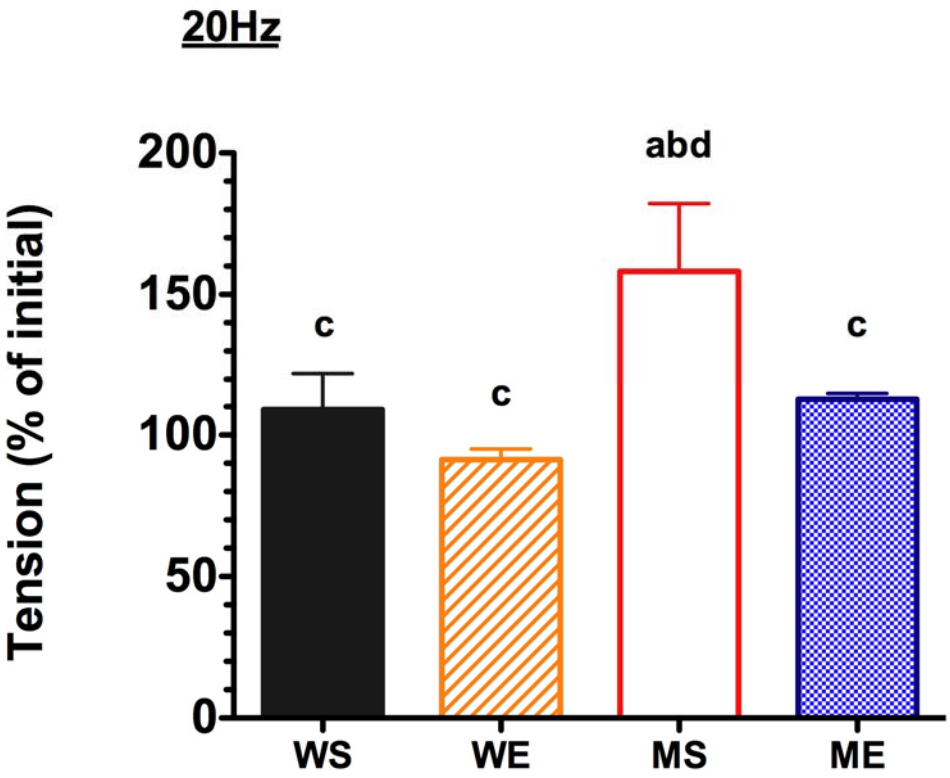

Figure 29. Effect of of a single exposure of EUK-134 (50mM) on low-frequency tension (20Hz) in wild type and *mdx* mice. Data are expressed as mean ± SEM. Indicating significant change relative to a: WS ($P<0.05$), b: MS ($p<0.05$), c: ME ($p<0.05$).

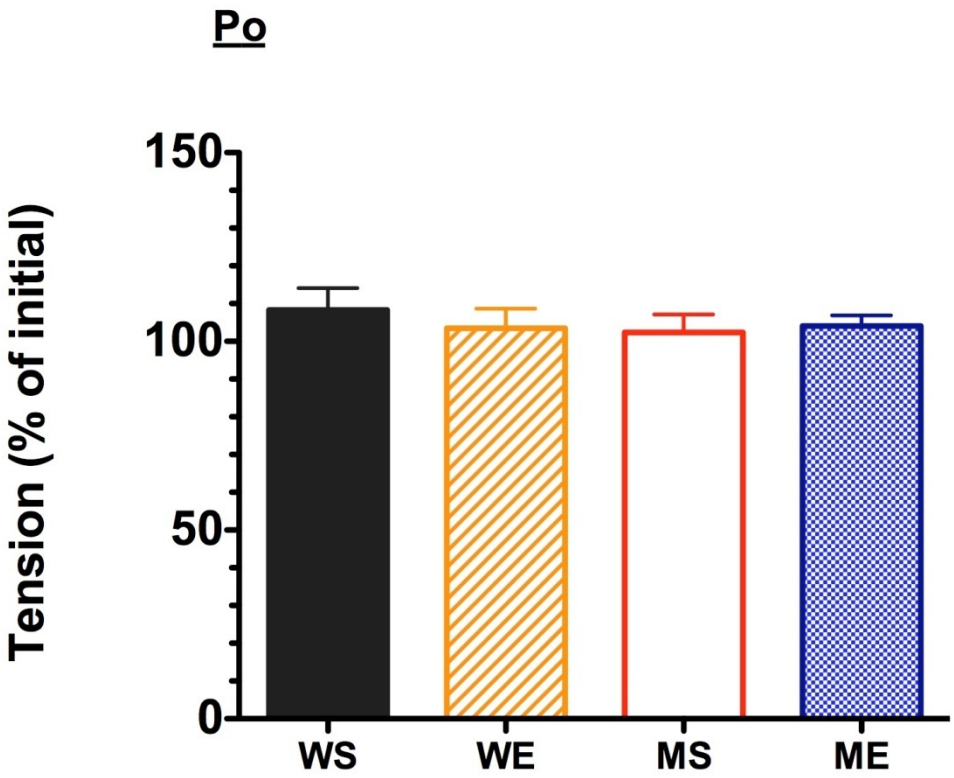

Figure 30. Effect of a single exposure of EUK-134 (50mM) on maximal isometric tension (Po) in wild type and *mdx* mice. Data are expressed as mean ± SEM. Indicating significant change relative to a: WS ($P<0.05$), b: MS ($p<0.05$), c: ME ($p<0.05$).

CHAPTER IV

DISCUSSION

In the present study we evaluated the potential direct benefit of EUK-134 treatment on diaphragm muscle morphology and function in dystrophin-deficient *mdx* mice and found the potential mechanisms involved in muscle damage and weakness. The rationale for this study was based on the proposed role of antioxidants [e.g., N-acetylcysteine (NAC), epigallocatechin-3-gallate (EGCG), and low-iron diet] which attenuate muscle damage and improve contractile function in the progression of muscle pathologies in muscular dystrophy (16, 22, 165). The novel findings of this study include that antioxidant EUK-134 protects muscle damage and weakness against oxidative stress and inflammation and enhances cellular and functional properties in *mdx* diaphragm.

We demonstrated that EUK-134 might protect against loss of body mass, diaphragm mass, diaphragm mass to body mass ratio in *mdx* mice. EUK-134 treatment in *mdx* mice resulted decreased internalized nuclei, cross-sectional area variability and type IIc fiber proportion, indicating that EUK-134 might ameliorate the dystrophic pathology by reducing muscle damage and degeneration in *mdx* mice. EUK-134, a specifically targeted antioxidant which can quench superoxide and hydrogen peroxide, also reduced some oxidative stress markers (e.g., total hydroperoxides and 4-HNE) in *mdx* diaphragm.

We demonstrated that EUK-134 might protect against inflammation by decreasing infiltration of T-cells (e.g., $CD4^+$ and $CD8^+$) and macrophages (e.g., CD11b).

NF-κB p65 subunit DNA binding activity and p65 protein levels in nucleosome fraction were ameliorated in EUK-134 treated *mdx* diaphragm.

EUK-134 also partially restored nNOS back to the sarcolemmal cytoskeleton, associated with relocation of α-1 syntrophin to myocyte periphery. In addition, specific force generation, particularly at twitch and low frequency tension (20Hz), was improved by 8 days of EUK-134 treatment as well as even a single exposure in vitro to EUK-134 in *mdx* diaphragm. These highly novel data indicate that muscle damage and weakness including compromised muscle contractility and DAPC disassembly with DMD are partially regulated by redox-dependant mechanisms.

To our knowledge, these are the first data to indicate that EUK-134 has a protective effect against muscle damage, inflammation, oxidative stress and contractile function in *mdx* diaphragm.

Effect of EUK-134 on muscle damage

In the present study we found that there is a significant reduction in body mass and diaphragm muscle mass of 20-28 day old *mdx* mice compared with age-matched wild type mice. Our findings are consistent with previous studies (38, 129), demonstrating that the reduction in body mass and muscle mass of *mdx* mice happens in early age (up to 2 months) mainly due to larger proportion of small muscle fibers. Compared with retardation in ontogenetic development of *mdx* mice at early age, several investigators have noted that body mass and muscle mass are either increased or not different with age in *mdx* mice compared with wild type mice (37, 53, 58, 129, 143).

We found that EUK-134 partially increased the body mass in *mdx* mice (+15.5%) and significantly increased diaphragm muscle mass both in *mdx* and wild type mice (Table 1). Interestingly, the degree of diaphragm muscle mass increase was greater than the degree of body mass increase, indicating that EUK-134 may protect against decrease in muscle mass to body mass ratio in *mdx* mice. However, increasing diaphragm muscle mass in EUK-134 treated wild type and *mdx* mice seem not occur as a result of muscle hypertrophy, as there was no EUK-134 treatment effect in diaphragm muscle cross-sectional area both *mdx* and wild type mice (Figure 3).

The ability of 8 days of EUK-134 treatment to improve the morphological characteristics and attenuate damage of diaphragm muscle in 4-week-old *mdx* mice are striking and novel finding. Based on the histological analysis in this study, EUK-134 treatment in *mdx* mice substantially reduced fiber cross-sectional area variability (Figure 4) and internalized nuclei (Figure 5), which are persistent indicators of fibers that have been damaged and experienced regeneration or repair.

Moreover, we noted widespread presence of immature, undifferentiated regenerating muscle fibers in *mdx* mice with intermediate ATPase activity that contribute to differences between the fiber type distributions compared with wild type mice. EUK-134 treatment may contribute to ameliorate muscle damage and regeneration and induce fiber type changes in *mdx* mice (Figure 25). In the present study, the reduction in regenerative type IIc fibers in EUK-134 treated *mdx* mice indicates that antioxidant EUK-134 can ameliorate the dystrophic pathology by reducing the initial damage to dystrophic muscle, rather than increasing regeneration.

It has been noted that extensive muscle damage is accompanied by the activation, proliferation, and fusion of resident myogenic precursor cells (satellite cells), which reside between the sarcolemma and basal lamina. The ability of the satellite cells to be reactivated however, is limited and progressive replacement of damaged cells lead to the senescence of satellite cells with DMD human (15, 162) and *mdx* mice (91).

Increased fatigue of respiratory muscles is a hallmark of human DMD as a result of disrupted mitochondrial metabolism and function with DMD (45, 48, 95). The current study showed that citrate synthase activity was decreased in *mdx* diaphragm (Figure 8), consistent with reduced oxidative capacity and mitochondrial density. Indeed, citrate synthase activity levels of diaphragm in EUK-134 treated *mdx* mice were similar to wild type controls (Figure 8).

Effect of EUK-134 treatment on oxidative stress

In the present study, we found that hydroperoxides and 4-HNE as lipid peroxidation endproduct markers were increased in 4-week-old *mdx* mice compared with wild type mice (Figures 9 & 10). Lipids are one of the most sensitive oxidation targets for reactive oxygen species (ROS) (81). Several reports have demonstrated that the amounts of lipid peroxidation are significantly increased in skeletal muscle and diaphragm of *mdx* mice and DMD patients compared with age-matched wild type controls (41, 69, 115).

Disatnik *et al* (41) found that lipid peroxidation increased in skeletal muscle of 15-20-day old *mdx* mice and demonstrated that oxidative stress levels rose in the

muscles at a pre-necrotic stage. Recently, Messina *et al* (99) established that lipid peroxidation inhibition attenuated tissue damage and enhanced muscle function in *mdx* mice. Nakae's group (105) have reported the enhanced lipofuscin formation in 2- to 7-year-old DMD muscle and 4-week-old *mdx* diaphragm, indicating that a product of oxidative injury of cellular macromolecules by oxygen-derived free radical and redox-active metal ion accumulates at an early age in both DMD humans and *mdx* mice.

In the present study, EUK-134 treatment decreased the lipid peroxidation in *mdx* diaphragm, indicating that the beneficial effects of EUK-134 on diaphragm function were a result of its properties as superoxide dismutase and catalase mimetic. It was demonstrated that muscles from *mdx* mice are more vulnerable to oxidative stress (40, 41, 119). Thus, diminishing oxidative stress via antioxidants might protect muscles from damage and weakness in *mdx* mice. EUK-134 has antioxidant properties and appears to be potent scavengers of superoxide and hydrogen peroxide known for their damaging effects on macromolecular cells.

In mormal muscles, neuronal nitric oxide (nNOS) also called muscle-specific isoform μNOS that catalyses nitric oxide ($NO^{\bullet}$) production is mostly present in the sarcolemma. However, nNOS is almost absent in dystrophin-deficient DMD and *mdx* muscles. In the present study, we showed that nNOS is not localized in sarcolemma in *mdx* diaphragm and antioxidant EUK-134 partially leads to restore nNOS back to the sarcolemma cytoskeleton, strongly indicating that cytoskeletal disruption with DMD is partially regulated in a redox-dependant manner.

Nitric oxide ($NO^{\bullet}$) has been shown to have both pro-oxidant and anti-oxidant properties (36, 101). $NO^{\bullet}$ reacts with superoxide ($O_2^{-\bullet}$) producing peroxynitrite ($ONOO^-$), which regulates a number of pro-oxidant reactions including protein nitration. It has been demonstrated that the altered regulation of nNOS in dystrophic muscle can induce the toxic interaction of nitric oxide ($NO^{\bullet}$) and superoxide ($O_2^{-\bullet}$) with the cell and contribute to necrotic degeneration (61). The antioxidant properties of $NO^{\bullet}$ is related with its ability to combine with more reactive species and convert them to less reactive species. The reaction of nitric oxide ($NO^{\bullet}$) with lipid peroxyl radicals which terminates lipid peroxidation is an example of nitric oxide ($NO^{\bullet}$) as a role of antioxidant (169).

Wehling *et al* (164) found that a muscle-specific nNOS transgene in *mdx* mice attenuates muscular dystrophy. They suggested that the loss of nNOS from sarcolemma in dystrophin-deficient muscles exacerbates membrane damage and inflammation. Although enhancing nitric oxide ($NO^{\bullet}$) production in dystrophin-deficient muscle can ameliorate muscle pathology (164) and nNOS deficiency can lead to recurrent ischemia-reperfusion injury (118), the relationship between nitric oxide ($NO^{\bullet}$) and dystrophic pathology is not simple. Several previous observations have suggested that the possibility that lacking either NO production (29, 35) or α-1 syntrophin (73) do not develop a muscular dystrophy. However, these findings are consistent with a "two-hit hypothesis", demonstrating that lack of nNOS exacerbates dystrophic pathology only in the presence of other defects associated with dystrophin-deficiency (118).

Effect of EUK-134 treatment on inflammation

In the current study, diaphragm muscle from *mdx* mice exhibited elevated inflammatory cells including T-cells ($CD4^+$ and $CD8^+$) and macrophages. EUK-134 significantly attenuated alterations in inflammatory cells (Figures 13-18). Interestingly, EUK-134 had no effect on infiltration of inflammatory cells in the diaphragm from wild-type. These data indicate that EUK-134 functions as anti-inflammatory agent specifically in *mdx* mice, but not in wild-type mice. Our findings are consistent with those to Monici *et al* (103) and Spencer *et al* (135) who reported elevated inflammatory response of muscle in DMD human and *mdx* mice.

In this study, we demonstrated the effects of antioxidant EUK-134 on NF-κB activation in *mdx* diaphragm (Figures 11 & 12). NF-κB activity of diaphragm muscle was upregulated in *mdx* mice compared with wild type mice, possibly through the generation of oxidative stress. NF-κB activation in dystrophin-deficient diaphragm muscle is associated with an increase of NF-κB p65 subunit DNA binding activity and p65 protein levels. This finding is consistent with previous studies (1, 82, 103), demonstrating the predominant role of NF-κB activation in dystrophin-deficient muscle pathology.

The novel findings in this study that antioxidant EUK-134 downregulates NF-κB activation and protein levels in nucleosome show that ameliorated pathology in EUK-134 treated *mdx* mice is highly regulated by redox dependant mechanism (Figures 11 & 12). It is well documented that NF-κB as a potential biomarker of oxidative stress is activated by low levels of reactive oxygen species (ROS) and inhibited by antioxidants (130, 157). As reactive oxygen species (ROS) are generated under numerous

pathological conditions including muscular dystrophy, NF-κB activation may provide important insight into etiology of dystrophin-deficient muscle pathology.

Indeed, antioxidant EUK-134 attenuated inflammatory responses in *mdx* mice. It has been demonstrated that inflammatory cells such as neutrophils and macrophages can produce reactive oxygen species (ROS) such as superoxide anion and hydrogen peroxide and it is thought that muscle-derived nitric oxide (NO) and antioxidants can scavenge reactive oxygen species (ROS) produced by inflammatory cells (106, 149). Wehling and colleagues (164) have proposed that NOS transgene ameliorated muscle damage and inflammatory cells in *mdx* mice. Our results, indicating that the inflammatory response was reduced in EUK-134 treated *mdx* mice, can be attributed to the reduced oxidative stress and partially relocated nNOS in sarcolemma.

Effect of EUK-134 treatment on muscle contractility

There is growing evidence that reactive oxygen species (ROS) and reactive nitrogen species (RNS) play a role in modulating contractile function in skeletal muscle (4, 77, 120). Reid (120) demonstrated that low levels of reactive oxygen species (ROS) are essential for optimal contractile function and the relationship between oxidative stress and contractile response in muscle is biphasic or reversed U shaped, indicating that low levels of oxidative stress enhances muscle contractility, while high levels do not they are above optimal levels of oxidative stress.

The main finding of the present study that contractile dysfunction occurred in *mdx* diaphragm was shown by a significant decrease in twitch, low-frequency (20Hz),

maximal isometric tension (Po) (Figures 19-21). Our findings are consistent with previous studies (53, 57, 90, 92, 140), indicating that dystrophin-deficient muscles are susceptible to force generating failure and contractile deficit. Moreover, Dupont-Versteegden *et al* (44) demonstrated that the degree of contractile impairment in *mdx* mice is greater in diaphragm muscle than in skeletal muscle. The impairment of contractile function in dystrophin-deficient muscles could have resulted from alteration in the step of excitation-contraction coupling to impaired interactions between contractile apparatus, actin and myosin as well as calcium related channels (90, 165).

The present findings show that antioxidant EUK-134 treatment in *mdx* mice resulted in improved muscle contractile function as demonstrated by significantly increased twitch, low-frequency (20Hz), maximal isometric tension (Po) (Figures 19-21). Several reports have demonstrated that exogenous antioxidants such as DMSO, N-acetylcysteine, superoxide dismutase, and catalse decreased force production in unfatigued muscle (121, 123, 124), but antioxidants also improved muscle contractility in fatigued or pathological status (122, 165).

Recently, Whitehead *et al* (165) demonstrated that antioxidant N-acetylcysteine (NAC) reduced oxidative stress and inflammation and provided protection against stretched-induced force reduction in *mdx* diaphragm. It is thus plausible to speculate that the improvement of diaphragm muscle contractile function in EUK-134 treated *mdx* mice most likely resulted from the decrease in muscle damage, oxidative stress, and inflammation. Our data show that even a single exposure in vitro of EUK-134 (50mM) for 5 minutes elevated twitch and low-frequency contractility in *mdx* mice, which

strongly suggests that antioxidant EUK-134 can even acutely compensate the compromised muscle contractility and excitation-contraction coupling in *mdx* diaphragm (Figures 22-24).

CHAPTER V

SUMMARY AND CONCLUSIONS

This studies outlined in this dissertation provide new evidence of the effects of EUK-134 on muscle damage, inflammation, and contractile function in *mdx* diaphragm. The specific aims of this study were to i) identify the role of oxidative stress on functional and morphological properties in *mdx* diaphragm (ii) identify the role of oxidative stress on inflammatory signaling pathways in *md*x diaphragm (iii) identify the role of oxidative stress on dislocation of nNOS, dystrophin-associated scaffolding proteins and contractile properties in *mdx* diaphragm.

The results of this study demonstrated that dystropin-deficient diaphragm muscle was associated with muscle damage, weakness and degeneration/regeneration, and was also susceptible to oxidative stress. However, EUK-134 treatment provided the diaphragm muscle significant protection against muscle damage and weakness via maintaining muscle mass, oxidative capacity, muscle contractility and decreasing oxidative stress and inflammation in 28-day-old *mdx* mice. These finding suggest that oxidative stress may contribute to tissue damage and weakness and antioxidanat treatment in early stage of pathology may have important therapeutic value against respiratory muscle failure in patients suffering from DMD.

REFERENCES

1. **Acharyya S, Villalta SA, Bakkar N, Bupha-Intr T, Janssen PM, Carathers M, Li ZW, Beg AA, Ghosh S, Sahenk Z, Weinstein M, Gardner KL, Rafael-Fortney JA, Karin M, Tidball JG, Baldwin AS, and Guttridge DC**. Interplay of IKK/NF-kappaB signaling in macrophages and myofibers promotes muscle degeneration in Duchenne muscular dystrophy. *J Clin Invest* 117: 889-901, 2007.

2. **Adams ME, Kramarcy N, Krall SP, Rossi SG, Rotundo RL, Sealock R, and Froehner SC**. Absence of alpha-syntrophin leads to structurally aberrant neuromuscular synapses deficient in utrophin. *J Cell Biol* 150: 1385-1398, 2000.

3. **Adams V, Jiang H, Yu J, Mobius-Winkler S, Fiehn E, Linke A, Weigl C, Schuler G, and Hambrecht R**. Apoptosis in skeletal myocytes of patients with chronic heart failure is associated with exercise intolerance. *J Am Coll Cardiol* 33: 959-965, 1999.

4. **Andrade FH, Reid MB, Allen DG, and Westerblad H**. Effect of hydrogen peroxide and dithiothreitol on contractile function of single skeletal muscle fibres from the mouse. *J Physiol* 509 (Pt 2): 565-575, 1998.

5. **Arbogast S, Smith J, Matuszczak Y, Hardin BJ, Moylan JS, Smith JD, Ware J, Kennedy AR, and Reid MB**. Bowman-Birk inhibitor concentrate prevents atrophy, weakness, and oxidative stress in soleus muscle of hindlimb-unloaded mice. *J Appl Physiol* 102: 956-964, 2007.

6. **Arnold L, Henry A, Poron F, Baba-Amer Y, van Rooijen N, Plonquet A, Gherardi RK, and Chazaud B**. Inflammatory monocytes recruited after skeletal

muscle injury switch into antiinflammatory macrophages to support myogenesis. *J Exp Med* 204: 1057-1069, 2007.

7. **Backman E, Nylander E, Johansson I, Henriksson KG, and Tagesson C**. Selenium and vitamin E treatment of Duchenne muscular dystrophy: no effect on muscle function. *Acta Neurol Scand* 78: 429-435, 1988.

8. **Badalamente MA, and Stracher A**. Delay of muscle degeneration and necrosis in mdx mice by calpain inhibition. *Muscle Nerve* 23: 106-111, 2000.

9. **Baker K, Marcus CB, Huffman K, Kruk H, Malfroy B, and Doctrow SR**. Synthetic combined superoxide dismutase/catalase mimetics are protective as a delayed treatment in a rat stroke model: a key role for reactive oxygen species in ischemic brain injury. *J Pharmacol Exp Ther* 284: 215-221, 1998.

10. **Baker MS, and Austin L**. The pathological damage in Duchenne muscular dystrophy may be due to increased intracellular OXY-radical generation caused by the absence of dystrophin and subsequent alterations in Ca2+ metabolism. *Med Hypotheses* 29: 187-193, 1989.

11. **Beller DI, and Unanue ER**. Regulation of macrophage populations. II. Synthesis and expression of Ia antigens by peritoneal exudate macrophages is a transient event. *J Immunol* 126: 263-269, 1981.

12. **Bernardi P**. Mitochondria in muscle cell death. *Ital J Neurol Sci* 20: 395-400, 1999.

13. **Betters JL, Criswell DS, Shanely RA, Van Gammeren D, Falk D, Deruisseau KC, Deering M, Yimlamai T, and Powers SK**. Trolox attenuates mechanical

ventilation-induced diaphragmatic dysfunction and proteolysis. *Am J Respir Crit Care Med* 170: 1179-1184, 2004.

14. **Binder HJ, Herting DC, Hurst V, Finch SC, and Spiro HM**. Tocopherol deficiency in man. *N Engl J Med* 273: 1289-1297, 1965.

15. **Blau HM, Webster C, and Pavlath GK**. Defective myoblasts identified in Duchenne muscular dystrophy. *Proc Natl Acad Sci U S A* 80: 4856-4860, 1983.

16. **Bornman L, Rossouw H, Gericke GS, and Polla BS**. Effects of iron deprivation on the pathology and stress protein expression in murine X-linked muscular dystrophy. *Biochem Pharmacol* 56: 751-757, 1998.

17. **Bouchentouf M, Benabdallah BF, and Tremblay JP**. Myoblast survival enhancement and transplantation success improvement by heat-shock treatment in mdx mice. *Transplantation* 77: 1349-1356, 2004.

18. **Brazier MW, Doctrow SR, Masters CL, and Collins SJ**. A manganese-superoxide dismutase/catalase mimetic extends survival in a mouse model of human prion disease. *Free Radic Biol Med* 45: 184-192, 2008.

19. **Brenman JE, Chao DS, Gee SH, McGee AW, Craven SE, Santillano DR, Wu Z, Huang F, Xia H, Peters MF, Froehner SC, and Bredt DS**. Interaction of nitric oxide synthase with the postsynaptic density protein PSD-95 and alpha1-syntrophin mediated by PDZ domains. *Cell* 84: 757-767, 1996.

20. **Brenman JE, Chao DS, Xia H, Aldape K, and Bredt DS**. Nitric oxide synthase complexed with dystrophin and absent from skeletal muscle sarcolemma in Duchenne muscular dystrophy. *Cell* 82: 743-752, 1995.

21. **Brunelli S, and Rovere-Querini P**. The immune system and the repair of skeletal muscle. *Pharmacol Res* 58: 117-121, 2008.

22. **Buetler TM, Renard M, Offord EA, Schneider H, and Ruegg UT**. Green tea extract decreases muscle necrosis in mdx mice and protects against reactive oxygen species. *Am J Clin Nutr* 75: 749-753, 2002.

23. **Bushby KM**. Making sense of the limb-girdle muscular dystrophies. *Brain* 122 (Pt 8): 1403-1420, 1999.

24. **Cai B, Spencer MJ, Nakamura G, Tseng-Ong L, and Tidball JG**. Eosinophilia of dystrophin-deficient muscle is promoted by perforin-mediated cytotoxicity by T cell effectors. *Am J Pathol* 156: 1789-1796, 2000.

25. **Carlson CG, Samadi A, and Siegel A**. Chronic treatment with agents that stabilize cytosolic IkappaB-alpha enhances survival and improves resting membrane potential in MDX muscle fibers subjected to chronic passive stretch. *Neurobiol Dis* 20: 719-730, 2005.

26. **Carter GT, and McDonald CM**. Preserving function in Duchenne dystrophy with long-term pulse prednisone therapy. *Am J Phys Med Rehabil* 79: 455-458, 2000.

27. **Chamberlain JS, Metzger J, Reyes M, Townsend D, and Faulkner JA**. Dystrophin-deficient mdx mice display a reduced life span and are susceptible to spontaneous rhabdomyosarcoma. *FASEB J* 21: 2195-2204, 2007.

28. **Chang WJ, Iannaccone ST, Lau KS, Masters BS, McCabe TJ, McMillan K, Padre RC, Spencer MJ, Tidball JG, and Stull JT**. Neuronal nitric oxide synthase and

dystrophin-deficient muscular dystrophy. *Proc Natl Acad Sci U S A* 93: 9142-9147, 1996.

29. **Chao DS, Silvagno F, and Bredt DS**. Muscular dystrophy in mdx mice despite lack of neuronal nitric oxide synthase. *J Neurochem* 71: 784-789, 1998.

30. **Chaturvedi LS, Mukherjee M, Srivastava S, Mittal RD, and Mittal B**. Point mutation and polymorphism in Duchenne/Becker muscular dystrophy (D/BMD) patients. *Exp Mol Med* 33: 251-256, 2001.

31. **Chen M, Cheng C, Yan M, Niu S, Gao S, Shi S, Liu H, Qin Y, and Shen A**. Involvement of CAPON and nitric oxide synthases in rat muscle regeneration after peripheral nerve injury. *J Mol Neurosci* 34: 89-100, 2008.

32. **Childers MK, Okamura CS, Bogan DJ, Bogan JR, Petroski GF, McDonald K, and Kornegay JN**. Eccentric contraction injury in dystrophic canine muscle. *Arch Phys Med Rehabil* 83: 1572-1578, 2002.

33. **Coral-Vazquez R, Cohn RD, Moore SA, Hill JA, Weiss RM, Davisson RL, Straub V, Barresi R, Bansal D, Hrstka RF, Williamson R, and Campbell KP**. Disruption of the sarcoglycan-sarcospan complex in vascular smooth muscle: a novel mechanism for cardiomyopathy and muscular dystrophy. *Cell* 98: 465-474, 1999.

34. **Cote PD, Moukhles H, and Carbonetto S**. Dystroglycan is not required for localization of dystrophin, syntrophin, and neuronal nitric-oxide synthase at the sarcolemma but regulates integrin alpha 7B expression and caveolin-3 distribution. *J Biol Chem* 277: 4672-4679, 2002.

35. **Crosbie RH, Straub V, Yun HY, Lee JC, Rafael JA, Chamberlain JS, Dawson VL, Dawson TM, and Campbell KP**. Mdx muscle pathology is independent of nNOS perturbation. *Hum Mol Genet* 7: 823-829, 1998.

36. **Darley-Usmar V, Wiseman H, and Halliwell B**. Nitric oxide and oxygen radicals: a question of balance. *FEBS Lett* 369: 131-135, 1995.

37. **De Luca A, Nico B, Liantonio A, Didonna MP, Fraysse B, Pierno S, Burdi R, Mangieri D, Rolland JF, Camerino C, Zallone A, Confalonieri P, Andreetta F, Arnoldi E, Courdier-Fruh I, Magyar JP, Frigeri A, Pisoni M, Svelto M, and Conte Camerino D**. A multidisciplinary evaluation of the effectiveness of cyclosporine a in dystrophic mdx mice. *Am J Pathol* 166: 477-489, 2005.

38. **De Luca A, Pierno S, Liantonio A, Cetrone M, Camerino C, Fraysse B, Mirabella M, Servidei S, Ruegg UT, and Conte Camerino D**. Enhanced dystrophic progression in mdx mice by exercise and beneficial effects of taurine and insulin-like growth factor-1. *J Pharmacol Exp Ther* 304: 453-463, 2003.

39. **Decraene D, Smaers K, Gan D, Mammone T, Matsui M, Maes D, Declercq L, and Garmyn M**. A synthetic superoxide dismutase/catalase mimetic (EUK-134) inhibits membrane-damage-induced activation of mitogen-activated protein kinase pathways and reduces p53 accumulation in ultraviolet B-exposed primary human keratinocytes. *J Invest Dermatol* 122: 484-491, 2004.

40. **Disatnik MH, Chamberlain JS, and Rando TA**. Dystrophin mutations predict cellular susceptibility to oxidative stress. *Muscle Nerve* 23: 784-792, 2000.

41. **Disatnik MH, Dhawan J, Yu Y, Beal MF, Whirl MM, Franco AA, and Rando TA**. Evidence of oxidative stress in mdx mouse muscle: studies of the pre-necrotic state. *J Neurol Sci* 161: 77-84, 1998.

42. **Disatnik MH, and Rando TA**. Integrin-mediated muscle cell spreading. The role of protein kinase c in outside-in and inside-out signaling and evidence of integrin cross-talk. *J Biol Chem* 274: 32486-32492, 1999.

43. **Duclos F, Straub V, Moore SA, Venzke DP, Hrstka RF, Crosbie RH, Durbeej M, Lebakken CS, Ettinger AJ, van der Meulen J, Holt KH, Lim LE, Sanes JR, Davidson BL, Faulkner JA, Williamson R, and Campbell KP**. Progressive muscular dystrophy in alpha-sarcoglycan-deficient mice. *J Cell Biol* 142: 1461-1471, 1998.

44. **Dupont-Versteegden EE, and McCarter RJ**. Differential expression of muscular dystrophy in diaphragm versus hindlimb muscles of mdx mice. *Muscle Nerve* 15: 1105-1110, 1992.

45. **Dupont-Versteegden EE, McCarter RJ, and Katz MS**. Voluntary exercise decreases progression of muscular dystrophy in diaphragm of mdx mice. *J Appl Physiol* 77: 1736-1741, 1994.

46. **Durham WJ, Arbogast S, Gerken E, Li YP, and Reid MB**. Progressive nuclear factor-kappaB activation resistant to inhibition by contraction and curcumin in mdx mice. *Muscle Nerve* 34: 298-303, 2006.

47. **Ehmsen J, Poon E, and Davies K**. The dystrophin-associated protein complex. *J Cell Sci* 115: 2801-2803, 2002.

48. **Escolar DM, and Scacheri CG**. Pharmacologic and genetic therapy for childhood muscular dystrophies. *Curr Neurol Neurosci Rep* 1: 168-174, 2001.

49. **Faist V, Koenig J, Hoeger H, and Elmadfa I**. Mitochondrial oxygen consumption, lipid peroxidation and antioxidant enzyme systems in skeletal muscle of senile dystrophic mice. *Pflugers Arch* 437: 168-171, 1998.

50. **Feghali CA, and Wright TM**. Cytokines in acute and chronic inflammation. *Front Biosci* 2: d12-26, 1997.

51. **Fenichel GM, Brooke MH, Griggs RC, Mendell JR, Miller JP, Moxley RT, 3rd, Park JH, Provine MA, Florence J, Kaiser KK, and et al.** Clinical investigation in Duchenne muscular dystrophy: penicillamine and vitamin E. *Muscle Nerve* 11: 1164-1168, 1988.

52. **Grady RM, Grange RW, Lau KS, Maimone MM, Nichol MC, Stull JT, and Sanes JR**. Role for alpha-dystrobrevin in the pathogenesis of dystrophin-dependent muscular dystrophies. *Nat Cell Biol* 1: 215-220, 1999.

53. **Gregorevic P, Plant DR, Leeding KS, Bach LA, and Lynch GS**. Improved contractile function of the mdx dystrophic mouse diaphragm muscle after insulin-like growth factor-I administration. *Am J Pathol* 161: 2263-2272, 2002.

54. **Grounds MD, and Torrisi J**. Anti-TNFalpha (Remicade) therapy protects dystrophic skeletal muscle from necrosis. *FASEB J* 18: 676-682, 2004.

55. **Hack AA, Ly CT, Jiang F, Clendenin CJ, Sigrist KS, Wollmann RL, and McNally EM**. Gamma-sarcoglycan deficiency leads to muscle membrane defects and apoptosis independent of dystrophin. *J Cell Biol* 142: 1279-1287, 1998.

56. **Haddad JJ**. Redox regulation of pro-inflammatory cytokines and IkappaB-alpha/NF-kappaB nuclear translocation and activation. *Biochem Biophys Res Commun* 296: 847-856, 2002.

57. **Harcourt LJ, Holmes AG, Gregorevic P, Schertzer JD, Stupka N, Plant DR, and Lynch GS**. Interleukin-15 administration improves diaphragm muscle pathology and function in dystrophic mdx mice. *Am J Pathol* 166: 1131-1141, 2005.

58. **Harcourt LJ, Schertzer JD, Ryall JG, and Lynch GS**. Low dose formoterol administration improves muscle function in dystrophic mdx mice without increasing fatigue. *Neuromuscul Disord* 17: 47-55, 2007.

59. **Hartel JV, Granchelli JA, Hudecki MS, Pollina CM, and Gosselin LE**. Impact of prednisone on TGF-beta1 and collagen in diaphragm muscle from mdx mice. *Muscle Nerve* 24: 428-432, 2001.

60. **Hauser E, Hoger H, Bittner R, Widhalm K, Herkner K, and Lubec G**. Oxyradical damage and mitochondrial enzyme activities in the mdx mouse. *Neuropediatrics* 26: 260-262, 1995.

61. **Haycock JW, MacNeil S, Jones P, Harris JB, and Mantle D**. Oxidative damage to muscle protein in Duchenne muscular dystrophy. *Neuroreport* 8: 357-361, 1996.

62. **Hayden MS, and Ghosh S**. Shared principles in NF-kappaB signaling. *Cell* 132: 344-362, 2008.

63. **Hnia K, Gayraud J, Hugon G, Ramonatxo M, De La Porte S, Matecki S, and Mornet D**. L-arginine decreases inflammation and modulates the nuclear factor-

kappaB/matrix metalloproteinase cascade in mdx muscle fibers. *Am J Pathol* 172: 1509-1519, 2008.

64. **Hodgetts S, Radley H, Davies M, and Grounds MD**. Reduced necrosis of dystrophic muscle by depletion of host neutrophils, or blocking TNFalpha function with Etanercept in mdx mice. *Neuromuscul Disord* 16: 591-602, 2006.

65. **Honda H, Kimura H, and Rostami A**. Demonstration and phenotypic characterization of resident macrophages in rat skeletal muscle. *Immunology* 70: 272-277, 1990.

66. **Hoshino S, Ohkoshi N, Ishii A, and Shoji S**. The expression of alpha-dystrobrevin and dystrophin during skeletal muscle regeneration. *J Muscle Res Cell Motil* 23: 131-138, 2002.

67. **Huang P, Zhao XS, Fields M, Ransohoff RM, and Zhou L**. Imatinib attenuates skeletal muscle dystrophy in mdx mice. *FASEB J* 2009.

68. **Huard J, Li Y, and Fu FH**. Muscle injuries and repair: current trends in research. *J Bone Joint Surg Am* 84-A: 822-832, 2002.

69. **Hunter MI, and Mohamed JB**. Plasma antioxidants and lipid peroxidation products in Duchenne muscular dystrophy. *Clin Chim Acta* 155: 123-131, 1986.

70. **Jarvinen TA, Jarvinen TL, Kaariainen M, Kalimo H, and Jarvinen M**. Muscle injuries: biology and treatment. *Am J Sports Med* 33: 745-764, 2005.

71. **Jones KJ, Compton AG, Yang N, Mills MA, Peters MF, Mowat D, Kunkel LM, Froehner SC, and North KN**. Deficiency of the syntrophins and alpha-dystrobrevin in patients with inherited myopathy. *Neuromuscul Disord* 13: 456-467, 2003.

72. **Kaczor JJ, Hall JE, Payne E, and Tarnopolsky MA**. Low intensity training decreases markers of oxidative stress in skeletal muscle of mdx mice. *Free Radic Biol Med* 43: 145-154, 2007.

73. **Kameya S, Miyagoe Y, Nonaka I, Ikemoto T, Endo M, Hanaoka K, Nabeshima Y, and Takeda S**. alpha1-syntrophin gene disruption results in the absence of neuronal-type nitric-oxide synthase at the sarcolemma but does not induce muscle degeneration. *J Biol Chem* 274: 2193-2200, 1999.

74. **Kaminski HJ, and Andrade FH**. Nitric oxide: biologic effects on muscle and role in muscle diseases. *Neuromuscul Disord* 11: 517-524, 2001.

75. **Kanatous SB, Davis RW, Watson R, Polasek L, Williams TM, and Mathieu-Costello O**. Aerobic capacities in the skeletal muscles of Weddell seals: key to longer dive durations? *J Exp Biol* 205: 3601-3608, 2002.

76. **Karin M, and Delhase M**. The I kappa B kinase (IKK) and NF-kappa B: key elements of proinflammatory signalling. *Semin Immunol* 12: 85-98, 2000.

77. **Khawli FA, and Reid MB**. N-acetylcysteine depresses contractile function and inhibits fatigue of diaphragm in vitro. *J Appl Physiol* 77: 317-324, 1994.

78. **Kim JH, Kwak HB, Leeuwenburgh C, and Lawler JM**. Lifelong exercise and mild (8%) caloric restriction attenuate age-induced alterations in plantaris muscle morphology, oxidative stress and IGF-1 in the Fischer-344 rat. *Exp Gerontol* 43: 317-329, 2008.

79. **Kosek DJ, and Bamman MM**. Modulation of the dystrophin-associated protein complex in response to resistance training in young and older men. *J Appl Physiol* 104: 1476-1484, 2008.

80. **Kramarcy NR, and Sealock R**. Syntrophin isoforms at the neuromuscular junction: developmental time course and differential localization. *Mol Cell Neurosci* 15: 262-274, 2000.

81. **Kregel KC, and Zhang HJ**. An integrated view of oxidative stress in aging: basic mechanisms, functional effects, and pathological considerations. *Am J Physiol Regul Integr Comp Physiol* 292: R18-36, 2007.

82. **Kumar A, and Boriek AM**. Mechanical stress activates the nuclear factor-kappaB pathway in skeletal muscle fibers: a possible role in Duchenne muscular dystrophy. *FASEB J* 17: 386-396, 2003.

83. **Kumar A, Takada Y, Boriek AM, and Aggarwal BB**. Nuclear factor-kappaB: its role in health and disease. *J Mol Med* 82: 434-448, 2004.

84. **Lagrota-Candido J, Vasconcellos R, Cavalcanti M, Bozza M, Savino W, and Quirico-Santos T**. Resolution of skeletal muscle inflammation in mdx dystrophic mouse is accompanied by increased immunoglobulin and interferon-gamma production. *Int J Exp Pathol* 83: 121-132, 2002.

85. **Lawler JM, Cline CC, Hu Z, and Coast JR**. Effect of oxidant challenge on contractile function of the aging rat diaphragm. *Am J Physiol* 272: E201-207, 1997.

86. **Lawler JM, Cline CC, Hu Z, and Coast JR**. Effect of oxidative stress and acidosis on diaphragm contractile function. *Am J Physiol* 273: R630-636, 1997.

87. **Lawler JM, Song W, and Demaree SR**. Hindlimb unloading increases oxidative stress and disrupts antioxidant capacity in skeletal muscle. *Free Radic Biol Med* 35: 9-16, 2003.

88. **Limoli CL, Giedzinski E, Baure J, Doctrow SR, Rola R, and Fike JR**. Using superoxide dismutase/catalase mimetics to manipulate the redox environment of neural precursor cells. *Radiat Prot Dosimetry* 122: 228-236, 2006.

89. **Lovering RM, Porter NC, and Bloch RJ**. The muscular dystrophies: from genes to therapies. *Phys Ther* 85: 1372-1388, 2005.

90. **Lowe DA, Williams BO, Thomas DD, and Grange RW**. Molecular and cellular contractile dysfunction of dystrophic muscle from young mice. *Muscle Nerve* 34: 92-100, 2006.

91. **Luz MA, Marques MJ, and Santo Neto H**. Impaired regeneration of dystrophin-deficient muscle fibers is caused by exhaustion of myogenic cells. *Braz J Med Biol Res* 35: 691-695, 2002.

92. **Lynch GS, Rafael JA, Hinkle RT, Cole NM, Chamberlain JS, and Faulkner JA**. Contractile properties of diaphragm muscle segments from old mdx and old transgenic mdx mice. *Am J Physiol* 272: C2063-2068, 1997.

93. **Macaione V, Aguennouz M, Rodolico C, Mazzeo A, Patti A, Cannistraci E, Colantone L, Di Giorgio RM, De Luca G, and Vita G**. RAGE-NF-kappaB pathway activation in response to oxidative stress in facioscapulohumeral muscular dystrophy. *Acta Neurol Scand* 115: 115-121, 2007.

94. **Macarthur M, Hold GL, and El-Omar EM**. Inflammation and Cancer II. Role of chronic inflammation and cytokine gene polymorphisms in the pathogenesis of gastrointestinal malignancy. *Am J Physiol Gastrointest Liver Physiol* 286: G515-520, 2004.

95. **Matecki S, Rivier F, Hugon G, Koechlin C, Michel A, Prefaut C, Mornet D, and Ramonatxo M**. The effect of respiratory muscle training with CO2 breathing on cellular adaptation of mdx mouse diaphragm. *Neuromuscul Disord* 15: 427-436, 2005.

96. **Matsumura K, and Campbell KP**. Dystrophin-glycoprotein complex: its role in the molecular pathogenesis of muscular dystrophies. *Muscle Nerve* 17: 2-15, 1994.

97. **McNally EM, and Pytel P**. Muscle diseases: the muscular dystrophies. *Annu Rev Pathol* 2: 87-109, 2007.

98. **Mendell JR, Engel WK, and Derrer EC**. Duchenne muscular dystrophy: functional ischemia reproduces its characteristic lesions. *Science* 172: 1143-1145, 1971.

99. **Messina S, Altavilla D, Aguennouz M, Seminara P, Minutoli L, Monici MC, Bitto A, Mazzeo A, Marini H, Squadrito F, and Vita G**. Lipid peroxidation inhibition blunts nuclear factor-kappaB activation, reduces skeletal muscle degeneration, and enhances muscle function in mdx mice. *Am J Pathol* 168: 918-926, 2006.

100. **Messina S, Bitto A, Aguennouz M, Minutoli L, Monici MC, Altavilla D, Squadrito F, and Vita G**. Nuclear factor kappa-B blockade reduces skeletal muscle degeneration and enhances muscle function in Mdx mice. *Exp Neurol* 198: 234-241, 2006.

101. **Miles AM, Bohle DS, Glassbrenner PA, Hansert B, Wink DA, and Grisham MB**. Modulation of superoxide-dependent oxidation and hydroxylation reactions by nitric oxide. *J Biol Chem* 271: 40-47, 1996.

102. **Miyagoe-Suzuki Y, and Takeda SI**. Association of neuronal nitric oxide synthase (nNOS) with alpha1-syntrophin at the sarcolemma. *Microsc Res Tech* 55: 164-170, 2001.

103. **Monici MC, Aguennouz M, Mazzeo A, Messina C, and Vita G**. Activation of nuclear factor-kappaB in inflammatory myopathies and Duchenne muscular dystrophy. *Neurology* 60: 993-997, 2003.

104. **Morrison J, Lu QL, Pastoret C, Partridge T, and Bou-Gharios G**. T-cell-dependent fibrosis in the mdx dystrophic mouse. *Lab Invest* 80: 881-891, 2000.

105. **Nakae Y, Stoward PJ, Kashiyama T, Shono M, Akagi A, Matsuzaki T, and Nonaka I**. Early onset of lipofuscin accumulation in dystrophin-deficient skeletal muscles of DMD patients and mdx mice. *J Mol Histol* 35: 489-499, 2004.

106. **Nguyen HX, and Tidball JG**. Interactions between neutrophils and macrophages promote macrophage killing of rat muscle cells in vitro. *J Physiol* 547: 125-132, 2003.

107. **Nguyen HX, and Tidball JG**. Null mutation of gp91phox reduces muscle membrane lysis during muscle inflammation in mice. *J Physiol* 553: 833-841, 2003.

108. **Ogilvie RW, and Feeback DL**. A metachromatic dye-ATPase method for the simultaneous identification of skeletal muscle fiber types I, IIA, IIB and IIC. *Stain Technol* 65: 231-241, 1990.

109. **Pan Y, Chen C, Shen Y, Zhu CH, Wang G, Wang XC, Chen HQ, and Zhu MS**. Curcumin alleviates dystrophic muscle pathology in mdx mice. *Mol Cells* 25: 531-537, 2008.

110. **Partridge T**. Animal models of muscular dystrophy--what can they teach us? *Neuropathol Appl Neurobiol* 17: 353-363, 1991.

111. **Pastoret C, and Sebille A**. Age-related differences in regeneration of dystrophic (mdx) and normal muscle in the mouse. *Muscle Nerve* 18: 1147-1154, 1995.

112. **Peters MF, Adams ME, and Froehner SC**. Differential association of syntrophin pairs with the dystrophin complex. *J Cell Biol* 138: 81-93, 1997.

113. **Peterson JM, and Guttridge DC**. Skeletal muscle diseases, inflammation, and NF-kappaB signaling: insights and opportunities for therapeutic intervention. *Int Rev Immunol* 27: 375-387, 2008.

114. **Petrucci TC, Macchia G, Macioce P, Brancaccio A, Paggi P, and Ceccarini M**. Functional flexibility of dystroglycan, a transmembrane linker between the extracellular matrix and the cytoskeleton. *Cell Mol Biol Lett* 6: 226, 2001.

115. **Ragusa RJ, Chow CK, and Porter JD**. Oxidative stress as a potential pathogenic mechanism in an animal model of Duchenne muscular dystrophy. *Neuromuscul Disord* 7: 379-386, 1997.

116. **Rando TA**. The dystrophin-glycoprotein complex, cellular signaling, and the regulation of cell survival in the muscular dystrophies. *Muscle Nerve* 24: 1575-1594, 2001.

117. **Rando TA**. Oxidative stress and the pathogenesis of muscular dystrophies. *Am J Phys Med Rehabil* 81: S175-186, 2002.

118. **Rando TA**. Role of nitric oxide in the pathogenesis of muscular dystrophies: a "two hit" hypothesis of the cause of muscle necrosis. *Microsc Res Tech* 55: 223-235, 2001.

119. **Rando TA, Disatnik MH, Yu Y, and Franco A**. Muscle cells from mdx mice have an increased susceptibility to oxidative stress. *Neuromuscul Disord* 8: 14-21, 1998.

120. **Reid MB**. Invited review: redox modulation of skeletal muscle contraction: what we know and what we don't. *J Appl Physiol* 90: 724-731, 2001.

121. **Reid MB**. Role of nitric oxide in skeletal muscle: synthesis, distribution and functional importance. *Acta Physiol Scand* 162: 401-409, 1998.

122. **Reid MB, Haack KE, Franchek KM, Valberg PA, Kobzik L, and West MS**. Reactive oxygen in skeletal muscle. I. Intracellular oxidant kinetics and fatigue in vitro. *J Appl Physiol* 73: 1797-1804, 1992.

123. **Reid MB, Khawli FA, and Moody MR**. Reactive oxygen in skeletal muscle. III. Contractility of unfatigued muscle. *J Appl Physiol* 75: 1081-1087, 1993.

124. **Reid MB, and Moody MR**. Dimethyl sulfoxide depresses skeletal muscle contractility. *J Appl Physiol* 76: 2186-2190, 1994.

125. **Rodriguez MC, and Tarnopolsky MA**. Patients with dystrophinopathy show evidence of increased oxidative stress. *Free Radic Biol Med* 34: 1217-1220, 2003.

126. **Roelofs RI, de Arango GS, Law PK, Kinsman D, Buchanan DC, and Park JH**. Treatment of Duchenne's muscular dystrophy with penicillamine. Results of a double-blind trial. *Arch Neurol* 36: 266-268, 1979.

127. **Rong Y, Doctrow SR, Tocco G, and Baudry M**. EUK-134, a synthetic superoxide dismutase and catalase mimetic, prevents oxidative stress and attenuates kainate-induced neuropathology. *Proc Natl Acad Sci U S A* 96: 9897-9902, 1999.

128. **Sandri M, and Carraro U**. Apoptosis of skeletal muscles during development and disease. *Int J Biochem Cell Biol* 31: 1373-1390, 1999.

129. **Schafer R, Zweyer M, Knauf U, Mundegar RR, and Wernig A**. The ontogeny of soleus muscles in mdx and wild type mice. *Neuromuscul Disord* 15: 57-64, 2005.

130. **Schreck R, Albermann K, and Baeuerle PA**. Nuclear factor kappa B: an oxidative stress-responsive transcription factor of eukaryotic cells (a review). *Free Radic Res Commun* 17: 221-237, 1992.

131. **Shiao T, Fond A, Deng B, Wehling-Henricks M, Adams ME, Froehner SC, and Tidball JG**. Defects in neuromuscular junction structure in dystrophic muscle are corrected by expression of a NOS transgene in dystrophin-deficient muscles, but not in muscles lacking alpha- and beta1-syntrophins. *Hum Mol Genet* 13: 1873-1884, 2004.

132. **Sicinski P, Geng Y, Ryder-Cook AS, Barnard EA, Darlison MG, and Barnard PJ**. The molecular basis of muscular dystrophy in the mdx mouse: a point mutation. *Science* 244: 1578-1580, 1989.

133. **Skrabek RQ, and Anderson JE**. Metabolic shifts and myocyte hypertrophy in deflazacort treatment of mdx mouse cardiomyopathy. *Muscle Nerve* 24: 192-202, 2001.

134. **Smith JK, Grisham MB, Granger DN, and Korthuis RJ**. Free radical defense mechanisms and neutrophil infiltration in postischemic skeletal muscle. *Am J Physiol* 256: H789-793, 1989.

135. **Spencer MJ, Montecino-Rodriguez E, Dorshkind K, and Tidball JG**. Helper (CD4(+)) and cytotoxic (CD8(+)) T cells promote the pathology of dystrophin-deficient muscle. *Clin Immunol* 98: 235-243, 2001.

136. **Spencer MJ, and Tidball JG**. Do immune cells promote the pathology of dystrophin-deficient myopathies? *Neuromuscul Disord* 11: 556-564, 2001.

137. **Spencer MJ, Walsh CM, Dorshkind KA, Rodriguez EM, and Tidball JG**. Myonuclear apoptosis in dystrophic mdx muscle occurs by perforin-mediated cytotoxicity. *J Clin Invest* 99: 2745-2751, 1997.

138. **Spurney CF, Knoblach S, Pistilli EE, Nagaraju K, Martin GR, and Hoffman EP**. Dystrophin-deficient cardiomyopathy in mouse: expression of Nox4 and Lox are associated with fibrosis and altered functional parameters in the heart. *Neuromuscul Disord* 18: 371-381, 2008.

139. **St Pierre BA, and Tidball JG**. Differential response of macrophage subpopulations to soleus muscle reloading after rat hindlimb suspension. *J Appl Physiol* 77: 290-297, 1994.

140. **Stedman HH, Sweeney HL, Shrager JB, Maguire HC, Panettieri RA, Petrof B, Narusawa M, Leferovich JM, Sladky JT, and Kelly AM**. The mdx mouse diaphragm reproduces the degenerative changes of Duchenne muscular dystrophy. *Nature* 352: 536-539, 1991.

141. **Stern LZ, Ringel SP, Ziter FA, Menander-Huber KB, Ionasescu V, Pellegrino RJ, and Snyder RD**. Drug trial of superoxide dismutase in Duchenne's muscular dystrophy. *Arch Neurol* 39: 342-346, 1982.

142. **Stevens ED, and Faulkner JA**. The capacity of mdx mouse diaphragm muscle to do oscillatory work. *J Physiol* 522 Pt 3: 457-466, 2000.

143. **Stupka N, Gregorevic P, Plant DR, and Lynch GS**. The calcineurin signal transduction pathway is essential for successful muscle regeneration in mdx dystrophic mice. *Acta Neuropathol* 107: 299-310, 2004.

144. **Summan M, McKinstry M, Warren GL, Hulderman T, Mishra D, Brumbaugh K, Luster MI, and Simeonova PP**. Inflammatory mediators and skeletal muscle injury: a DNA microarray analysis. *J Interferon Cytokine Res* 23: 237-245, 2003.

145. **Sun Y, and Oberley LW**. Redox regulation of transcriptional activators. *Free Radic Biol Med* 21: 335-348, 1996.

146. **Sussman M**. Duchenne muscular dystrophy. *J Am Acad Orthop Surg* 10: 138-151, 2002.

147. **Suzuki A, Yoshida M, Hayashi K, Mizuno Y, Hagiwara Y, and Ozawa E**. Molecular organization at the glycoprotein-complex-binding site of dystrophin. Three dystrophin-associated proteins bind directly to the carboxy-terminal portion of dystrophin. *Eur J Biochem* 220: 283-292, 1994.

148. **Tidball JG**. Inflammatory cell response to acute muscle injury. *Med Sci Sports Exerc* 27: 1022-1032, 1995.

149. **Tidball JG**. Inflammatory processes in muscle injury and repair. *Am J Physiol Regul Integr Comp Physiol* 288: R345-353, 2005.

150. **Tidball JG, Berchenko E, and Frenette J**. Macrophage invasion does not contribute to muscle membrane injury during inflammation. *J Leukoc Biol* 65: 492-498, 1999.

151. **Tidball JG, and St Pierre BA**. Apoptosis of macrophages during the resulution of muscle inflammation. *J Leukoc Biol* 59: 380-388, 1996.

152. **Tidball JG, and Wehling-Henricks M**. Expression of a NOS transgene in dystrophin-deficient muscle reduces muscle membrane damage without increasing the expression of membrane-associated cytoskeletal proteins. *Mol Genet Metab* 82: 312-320, 2004.

153. **Tidball JG, and Wehling-Henricks M**. The role of free radicals in the pathophysiology of muscular dystrophy. *J Appl Physiol* 102: 1677-1686, 2007.

154. **Tkatchenko AV, Le Cam G, L?er JJ, and Dechesne CA**. Large-scale analysis of differential gene expression in the hindlimb muscles and diaphragm of mdx mouse. *Biochim Biophys Acta* 1500: 17-30, 2000.

155. **Tkatchenko AV, Le Cam G, Leger JJ, and Dechesne CA**. Large-scale analysis of differential gene expression in the hindlimb muscles and diaphragm of mdx mouse. *Biochim Biophys Acta* 1500: 17-30, 2000.

156. **Toumi H, F'Guyer S, and Best TM**. The role of neutrophils in injury and repair following muscle stretch. *J Anat* 208: 459-470, 2006.

157. **van den Berg R, Haenen GR, van den Berg H, and Bast A**. Transcription factor NF-kappaB as a potential biomarker for oxidative stress. *Br J Nutr* 86 Suppl 1: S121-127, 2001.

158. **Wakayama Y, Inoue M, Murahashi M, Shibuya S, Jimi T, Kojima H, and Oniki H**. Ultrastructural localization of alpha 1-syntrophin and neuronal nitric oxide synthase in normal skeletal myofiber, and their relation to each other and to dystrophin. *Acta Neuropathol* 94: 455-464, 1997.

159. **Walden DL, McCutchan HJ, Enquist EG, Schwappach JR, Shanley PF, Reiss OK, Terada LS, Leff JA, and Repine JE**. Neutrophils accumulate and contribute to skeletal muscle dysfunction after ischemia-reperfusion. *Am J Physiol* 259: H1809-1812, 1990.

160. **Wallace GQ, and McNally EM**. Mechanisms of muscle degeneration, regeneration, and repair in the muscular dystrophies. *Annu Rev Physiol* 2008.

161. **Warren GL, Hayes DA, Lowe DA, Prior BM, and Armstrong RB**. Materials fatigue initiates eccentric contraction-induced injury in rat soleus muscle. *J Physiol* 464: 477-489, 1993.

162. **Webster C, and Blau HM**. Accelerated age-related decline in replicative life-span of Duchenne muscular dystrophy myoblasts: implications for cell and gene therapy. *Somat Cell Mol Genet* 16: 557-565, 1990.

163. **Wehling-Henricks M, Sokolow S, Lee JJ, Myung KH, Villalta SA, and Tidball JG**. Major basic protein-1 promotes fibrosis of dystrophic muscle and attenuates the cellular immune response in muscular dystrophy. *Hum Mol Genet* 17: 2280-2292, 2008.

164. **Wehling M, Spencer MJ, and Tidball JG**. A nitric oxide synthase transgene ameliorates muscular dystrophy in mdx mice. *J Cell Biol* 155: 123-131, 2001.

165. **Whitehead NP, Pham C, Gervasio OL, and Allen DG**. N-Acetylcysteine ameliorates skeletal muscle pathophysiology in mdx mice. *J Physiol* 586: 2003-2014, 2008.

166. **Williams IA, and Allen DG**. The role of reactive oxygen species in the hearts of dystrophin-deficient mdx mice. *Am J Physiol Heart Circ Physiol* 293: H1969-1977, 2007.

167. **Williams JC, Armesilla AL, Mohamed TM, Hagarty CL, McIntyre FH, Schomburg S, Zaki AO, Oceandy D, Cartwright EJ, Buch MH, Emerson M, and Neyses L**. The sarcolemmal calcium pump, alpha-1 syntrophin, and neuronal nitric-oxide synthase are parts of a macromolecular protein complex. *J Biol Chem* 281: 23341-23348, 2006.

168. **Williamson RA, Henry MD, Daniels KJ, Hrstka RF, Lee JC, Sunada Y, Ibraghimov-Beskrovnaya O, and Campbell KP**. Dystroglycan is essential for early embryonic development: disruption of Reichert's membrane in Dag1-null mice. *Hum Mol Genet* 6: 831-841, 1997.

169. **Wink DA, and Mitchell JB**. Chemical biology of nitric oxide: insights into regulatory, cytotoxic, and cytoprotective mechanisms of nitric oxide. *Free Radic Biol Med* 25: 434-456, 1998.

170. **Yiu EM, and Kornberg AJ**. Duchenne muscular dystrophy. *Neurol India* 56: 236-247, 2008.

APPENDIX

1. A integrative model for DMD and *mdx* pathology

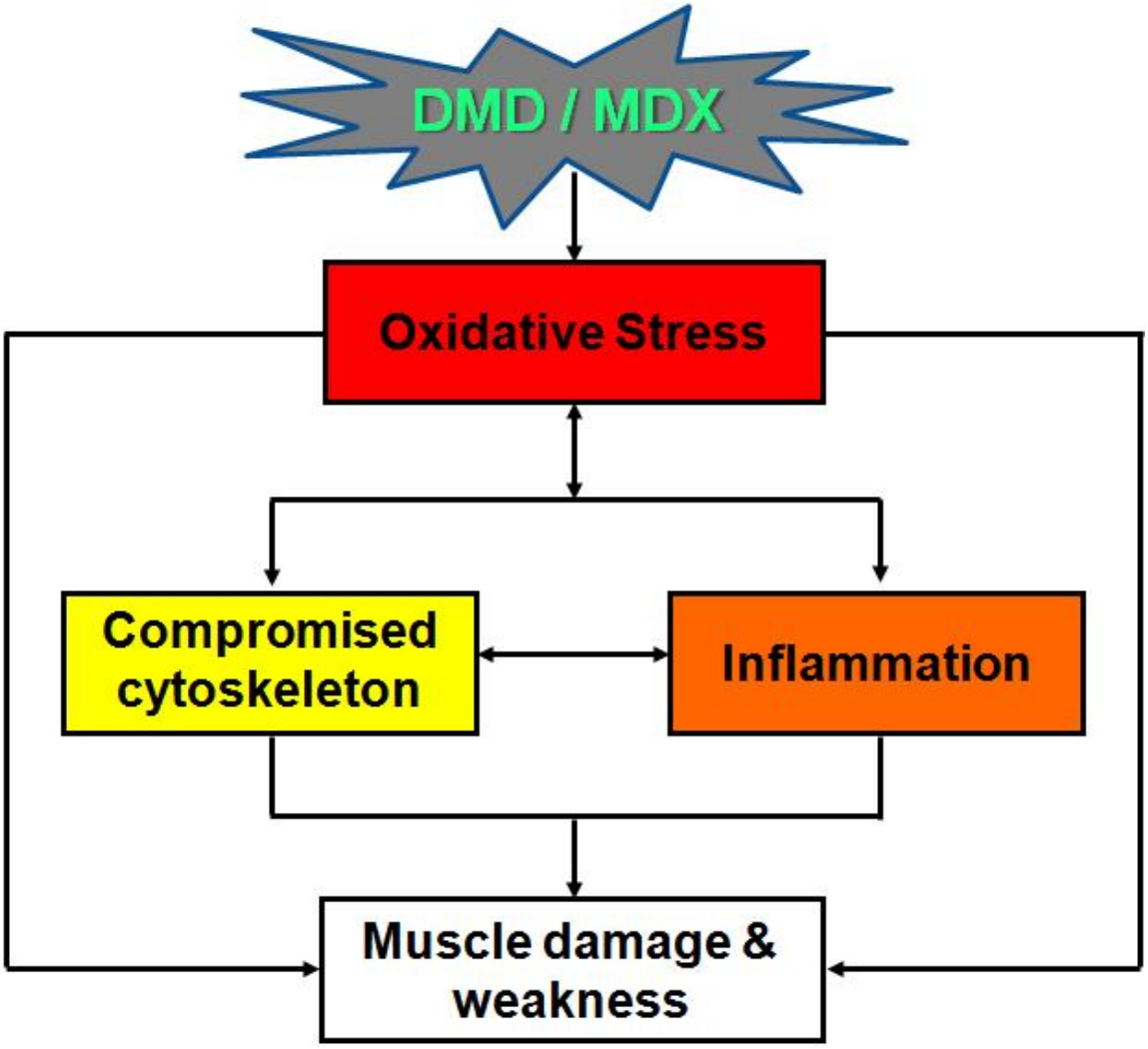

2. Potential targets of EUK-134 in the diaphragm muscle cell

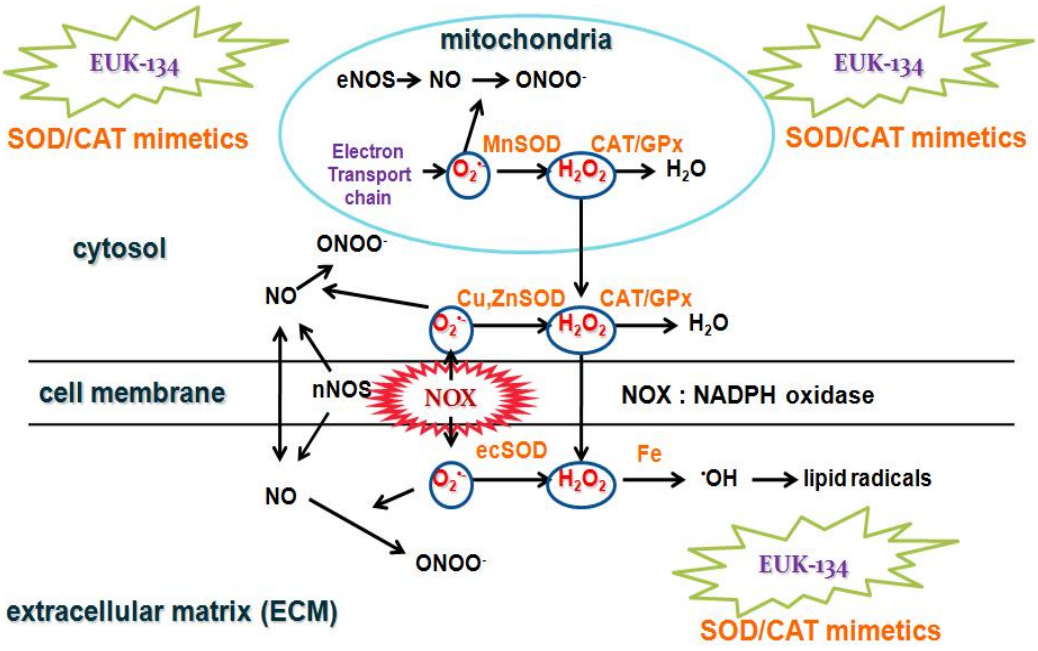

3. In vitro muscle preparation

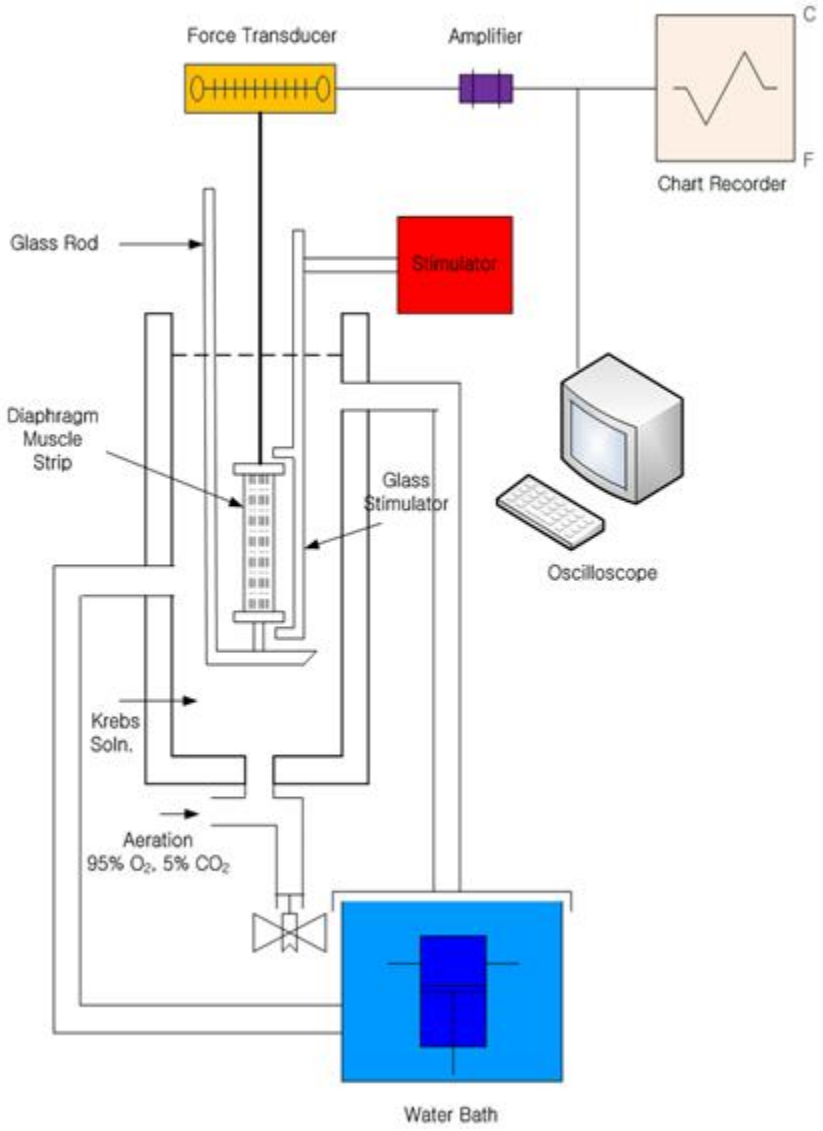

4. Statistics

Body mass changes

Repeated Measures Analysis of Variance (ANOVA)

The P value is < 0.0001, considered extremely significant.
Variation among column means is significantly greater than expected by chance.

Student-Newman-Keuls Multiple Comparisons Test

Comparison	Mean Difference		P value
MS vs WE	-4.6302	***	P<0.001
MS vs WS	-4.6873	***	P<0.001
MS vs ME	-1.2450	ns	P>0.05
ME vs WE	-3.3852	**	P<0.01
ME vs WS	-3.4423	**	P<0.01
WS vs WE	0.0571	ns	P>0.05

With Student-Newman-Keuls test, it is impossible to calculate confidence intervals.

Intermediate calculations. ANOVA table

Tests of Within-Subjects Effects

Source of variation	Degree of freedom	Sum of squares	Mean square	F
Treatment	8	925.975	115.747	547.009
Treatment*Group	24	20.895	0.871	4.115
Residuals	176	37.242	0.212	
Total	208	984.112		

Tests of Between-Subjects Effects

Source of variation	Degree of freedom	Sum of squares	Mean square	F
Intercept	1	24092.836	24092.836	1011.052
Group	3	1021.999	340.666	14.296
Residuals	22	524.248	23.829	
Total	26	25639.083		

Diaphragm mass

One-way Analysis of Variance (ANOVA)

The P value is < 0.0001, considered extremely significant.
Variation among column means is significantly greater than expected by chance.

Student-Newman-Keuls Multiple Comparisons Test

Comparison	Mean Difference	Q		P value
MS vs WE	-0.05557	13.167	***	P<0.001
MS vs WS	-0.02357	5.813	**	P<0.01
MS vs ME	-0.01974	4.677	**	P<0.01
ME vs WE	-0.03583	8.181	***	P<0.001
ME vs WS	-0.003833	0.9082	ns	P>0.05
WS vs WE	-0.03200	7.582	***	P<0.001

With Student-Newman-Keuls test, it is impossible to calculate confidence intervals.

Intermediate calculations. ANOVA table

Source of variation	Degree of freedom	Sum of squares	Mean square
Treatments (between columns)	3	0.01012	0.003374
Residuals (within columns)	22	0.002532	0.0001151
Total	25	0.01265	

F = 29.309 = (MStreatment/MSresidual)

Summary of Data

Group	Numbers of Points	Standard Mean	Standard Error of Deviation	Standard Error of Mean	Standard Error of Median
WS	7	0.05580	0.007778	0.002940	0.05780
WE	6	0.08780	0.01862	0.007601	0.08845
MS	7	0.03223	0.004647	0.001757	0.03220
ME	6	0.05197	0.007832	0.003197	0.05250

Diaphragm mass to body mass

One-way Analysis of Variance (ANOVA)

The P value is < 0.0001, considered extremely significant.
Variation among column means is significantly greater than expected by chance.

Student-Newman-Keuls Multiple Comparisons Test

Comparison	Mean Difference	q		P value
MS vs WE	-2.557	11.021	***	P<0.001
MS vs ME	-1.204	5.191	**	P<0.01
MS vs WS	-0.4321	1.939	ns	P>0.05
WS vs WE	-2.124	9.158	***	P<0.001
WS vs ME	-0.7719	3.328	*	P<0.05
ME vs WE	-1.353	5.618	***	P<0.001

With Student-Newman-Keuls test, it is impossible to calculate confidence intervals.

Intermediate calculations. ANOVA table

Source of variation	Degree of freedom	Sum of squares	Mean square
Treatments (between columns)	3	24.037	8.012
Residuals (within columns)	22	7.649	0.3477
Total	25	31.686	

F = 23.045 = (MStreatment/MSresidual)

Summary of Data

Group	Numbers of Points	Standard Mean	Standard Error of Deviation	Standard Error of Mean	Standard Error of Median
WS	7	3.544	0.3865	0.1461	3.729
WE	6	5.669	0.9575	0.3909	5.444
MS	7	3.112	0.4484	0.1695	2.969
ME	6	4.316	0.4386	0.1791	4.347

Diaphragm muscle cross-sectional area (CSA)

One-way Analysis of Variance (ANOVA)

The P value is < 0.0001, considered extremely significant.
Variation among column means is significantly greater than expected by chance.

Student-Newman-Keuls Multiple Comparisons Test

Comparison	Mean Difference	q		P value
ME vs WE	-180.00	11.261	***	P<0.001
ME vs WS	-163.68	9.674	***	P<0.001
ME vs MS	-1.611	0.1005	ns	P>0.05
MS vs WE	-178.39	10.176	***	P<0.001
MS vs WS	-162.06	8.814	***	P<0.001
WS vs WE	-16.325	0.8900	ns	P>0.05

With Student-Newman-Keuls test, it is impossible to calculate confidence intervals.

Intermediate calculations. ANOVA table

Source of variation	Degree of freedom	Sum of squares	Mean square
Treatments (between columns)	3	2.07307409e+7	6910247
Residuals (within columns)	2854	5.78443605e+8	202678
Total	2857	5.99174346e+8	

F = 34.095 = (MStreatment/MSresidual)

Summary of Data

Group	Numbers of Points	Standard Mean	Standard Error of Deviation	Standard Error of Mean	Standard Error of Median
WS	552	858.45	263.24	11.204	823.50
WE	663	874.78	447.31	17.372	758.00
MS	656	696.39	314.83	12.292	635.00
ME	987	694.78	589.70	18.770	569.00

CSA variability

One-way Analysis of Variance (ANOVA)

The P value is 0.0037, considered very significant.
Variation among column means is significantly greater than expected by chance.

Student-Newman-Keuls Multiple Comparisons Test

Comparison	Mean Difference	q		P value
WS vs MS	-72.257	4.187	*	P<0.05
WS vs ME	-6.589	0.3798	ns	P>0.05
WS vs WE	-0.7728	---	ns	P>0.05
WE vs MS	-71.4843	4.142	*	P<0.05
WE vs ME	-5.817	---	ns	P>0.05
ME vs MS	-65.668	4.243	**	P<0.01

With Student-Newman-Keuls test, it is impossible to calculate confidence intervals.

Intermediate calculations. ANOVA table

Source of variation	Degree of freedom	Sum of squares	Mean square
Treatments (between columns)	3	127595	42532
Residuals (within columns)	121	1086729	8981.2
Total	124	1214325	

F = 4.736 = (MStreatment/MSresidual)

Summary of Data

Group	Numbers of Points	Standard Mean	Standard Error of Deviation	Standard Error of Mean	Standard Error of Median
WS	25	193.75	40.811	8.162	188.73
WE	25	194.52	90.748	18.150	185.76
MS	38	266.00	126.43	20.509	222.15
ME	37	200.34	84.607	13.909	186.11

Internal nuclei

One-way Analysis of Variance (ANOVA)

The P value is < 0.0001, considered extremely significant.
Variation among column means is significantly greater than expected by chance.

Student-Newman-Keuls Multiple Comparisons Test

Comparison	Mean Difference	q		P value
WE vs MS	-7.893	15.959	***	P<0.001
WE vs ME	-4.064	8.367	***	P<0.001
WE vs WS	-0.3146	0.5732	ns	P>0.05
WS vs MS	-7.578	14.247	***	P<0.001
WS vs ME	-3.749	7.160	***	P<0.001
ME vs MS	-3.829	8.208	***	P<0.001

With Student-Newman-Keuls test, it is impossible to calculate confidence intervals.

Intermediate calculations. ANOVA table

Source of variation	Degree of freedom	Sum of squares	Mean square
Treatments (between columns)	3	1330.2	443.39
Residuals (within columns)	126	1026.6	8.148
Total	129	2356.8	

F = 54.417 = (MStreatment/MSresidual)

Summary of Data

Group	Numbers of Points	Standard Mean	Standard Error of Deviation	Standard Error of Mean	Standard Error of Median
WS	24	1.009	1.740	0.3552	0.000
WE	31	0.6942	1.197	0.2149	0.000
MS	36	8.587	4.396	0.7326	8.060
ME	39	4.758	2.501	0.4005	5.380

Type I fiber (%)

One-way Analysis of Variance (ANOVA)

The P value is 0.0359, considered significant.
Variation among column means is significantly greater than expected by chance.

Student-Newman-Keuls Multiple Comparisons Test

Comparison	Mean Difference	q		P value
MS vs WS	-1.576	4.270	*	P<0.05
MS vs WE	-0.8839	2.394	ns	P>0.05
MS vs ME	-0.6465	---	ns	P>0.05
ME vs WS	-0.9295	2.518	ns	P>0.05
ME vs WE	-0.2373	---	ns	P>0.05
WE vs WS	-0.6921	---	ns	P>0.05

With Student-Newman-Keuls test, it is impossible to calculate confidence intervals.

Intermediate calculations. ANOVA table

Source of variation	Degree of freedom	Sum of squares	Mean square
Treatments (between columns)	3	15.247	5.082
Residuals (within columns)	44	71.943	1.635
Total	47	87.191	

F = 3.108 = (MStreatment/MSresidual)

Summary of Data

Group	Numbers of Points	Standard Mean	Standard Error of Deviation	Standard Error of Mean	Standard Error of Median
WS	12	8.365	1.350	0.3898	7.836
WE	12	7.673	0.6937	0.2003	7.526
MS	12	6.789	1.521	0.4390	7.147
ME	12	7.435	1.387	0.4003	7.719

Type II fiber (%)

One-way Analysis of Variance (ANOVA)

The P value is 0.0042, considered very significant.
Variation among column means is significantly greater than expected by chance.

Student-Newman-Keuls Multiple Comparisons Test

Comparison	Mean Difference	Q		P value
MS vs WE	-5.859	6.298	**	P<0.01
MS vs WS	-4.824	5.186	**	P<0.01
MS vs ME	-3.190	3.429	*	P<0.05
ME vs WE	-2.669	2.869	ns	P>0.05
ME vs WS	-1.634	---	ns	P>0.05
WS vs WE	-1.035	---	ns	P>0.05

With Student-Newman-Keuls test, it is impossible to calculate confidence intervals.

Intermediate calculations. ANOVA table

Source of variation	Degree of freedom	Sum of squares	Mean square
Treatments (between columns)	3	78.640	26.213
Residuals (within columns)	12	41.543	3.462
Total	15	120.18	

F = 7.572 = (MStreatment/MSresidual)

Summary of Data

Group	Numbers of Points	Standard Mean	Standard Error of Deviation	Standard Error of Mean	Standard Error of Median
WS	4	89.598	0.4546	0.2273	89.481
WE	4	90.633	0.2810	0.1405	90.682
MS	4	84.774	2.945	1.473	85.134
ME	4	87.964	2.211	1.105	88.942

Type IIc fiber (%)

One-way Analysis of Variance (ANOVA)

The P value is 0.0001, considered extremely significant.
Variation among column means is significantly greater than expected by chance.

Student-Newman-Keuls Multiple Comparisons Test

Comparison	Mean Difference	Q		P value
WE vs MS	-6.743	6.907	***	P<0.001
WE vs ME	-2.906	2.977	ns	P>0.05
WE vs WS	-0.3424	---	ns	P>0.05
WS vs MS	-6.400	6.556	***	P<0.001
WS vs ME	-2.564	---	ns	P>0.05
ME vs MS	-3.836	3.930	**	P<0.01

With Student-Newman-Keuls test, it is impossible to calculate confidence intervals.

Intermediate calculations. ANOVA table

Source of variation	Degree of freedom	Sum of squares	Mean square
Treatments (between columns)	3	232.57	77.522
Residuals (within columns)	28	213.47	7.624
Total	31	446.04	

F = 10.168 = (MStreatment/MSresidual)

Summary of Data

Group	Numbers of Points	Standard Mean	Standard Error of Deviation	Standard Error of Mean	Standard Error of Median
WS	8	2.037	1.103	0.3901	2.512
WE	8	1.694	0.4658	0.1647	1.732
MS	8	8.437	4.262	1.507	7.719
ME	8	4.601	3.301	1.167	3.083

Soluble protein concentration

One-way Analysis of Variance (ANOVA)

The P value is 0.0071, considered very significant.
Variation among column means is significantly greater than expected by chance.

Student-Newman-Keuls Multiple Comparisons Test

Comparison	Mean Difference	Q		P value
MS vs WE	-4.817	4.536	*	P<0.05
MS vs WS	-4.490	4.402	**	P<0.01
MS vs ME	-2.942	2.884	*	P<0.05
ME vs WE	-1.874	1.765	ns	P>0.05
ME vs WS	-1.548	---	ns	P>0.05
WS vs WE	-0.3262	---	ns	P>0.05

With Student-Newman-Keuls test, it is impossible to calculate confidence intervals.

Intermediate calculations. ANOVA table

Source of variation	Degree of freedom	Sum of squares	Mean square
Treatments (between columns)	3	196.74	65.579
Residuals (within columns)	50	728.42	14.568
Total	53	925.15	

F = 4.501 = (MStreatment/MSresidual)

Summary of Data

Group	Numbers of Points	Standard Mean	Standard Error of Deviation	Standard Error of Mean	Standard Error of Median
WS	14	36.033	4.027	1.076	36.848
WE	12	36.360	3.184	0.9193	36.291
MS	14	31.543	4.622	1.235	31.708
ME	14	34.485	3.142	0.8398	35.498

Nucleosome protein concentration

One-way Analysis of Variance (ANOVA)

The P value is 0.0001, considered extremely significant.
Variation among column means is significantly greater than expected by chance.

Student-Newman-Keuls Multiple Comparisons Test

Comparison	Mean Difference	Q		P value
WS vs ME	-3.482	6.470	***	P<0.001
WS vs WE	-0.8743	1.561	ns	P>0.05
WS vs MS	-0.5165	---	ns	P>0.05
MS vs ME	-2.966	5.510	***	P<0.001
MS vs WE	-0.3578	---	ns	P>0.05
WE vs ME	-2.608	4.655	**	P<0.01

With Student-Newman-Keuls test, it is impossible to calculate confidence intervals.

Intermediate calculations. ANOVA table

Source of variation	Degree of freedom	Sum of squares	Mean square
Treatments (between columns)	3	100.84	33.615
Residuals (within columns)	50	202.79	4.056
Total	53	303.64	

F = 8.288 = (MStreatment/MSresidual)

Summary of Data

Group	Numbers of Points	Standard Mean	Standard Error of Deviation	Standard Error of Mean	Standard Error of Median
WS	14	15.609	1.768	0.4725	15.685
WE	12	16.483	2.087	0.6024	15.875
MS	14	16.126	2.158	0.5767	15.230
ME	14	19.091	2.033	0.5432	18.669

Citrate synthase activity

One-way Analysis of Variance (ANOVA)

The P value is 0.0076, considered very significant.
Variation among column means is significantly greater than expected by chance.

Student-Newman-Keuls Multiple Comparisons Test

Comparison	Mean Difference	Q		P value
MS vs ME	-4.379	5.055	**	P<0.01
MS vs WS	-3.809	4.397	*	P<0.05
MS vs WE	-3.142	3.485	*	P<0.05
WE vs ME	-1.237	1.372	ns	P>0.05
WE vs WS	-0.6667	---	ns	P>0.05
WS vs ME	-0.5700	---	ns	P>0.05

With Student-Newman-Keuls test, it is impossible to calculate confidence intervals.

Intermediate calculations. ANOVA table

Source of variation	Degree of freedom	Sum of squares	Mean square
Treatments (between columns)	3	80.133	26.711
Residuals (within columns)	23	120.82	5.253
Total	26	200.95	

F = 5.085 = (MStreatment/MSresidual)

Summary of Data

Group	Numbers of Points	Standard Mean	Standard Error of Deviation	Standard Error of Mean	Standard Error of Median
WS	7	14.050	2.098	0.7929	14.470
WE	6	13.383	2.928	1.196	14.260
MS	7	10.241	2.689	1.016	10.560
ME	7	14.620	1.165	0.4402	14.840

Total hydroperoxides

One-way Analysis of Variance (ANOVA)

The P value is 0.0075, considered very significant.
Variation among column means is significantly greater than expected by chance.

Student-Newman-Keuls Multiple Comparisons Test

Comparison	Mean Difference	Q		P value
WS vs MS	-79.044	5.089	**	P<0.01
WS vs ME	-28.005	1.803	ns	P>0.05
WS vs WE	-8.887	---	ns	P>0.05
WE vs MS	-70.157	4.340	*	P<0.05
WE vs ME	-19.117	---	ns	P>0.05
ME vs MS	-51.040	3.286	*	P<0.05

With Student-Newman-Keuls test, it is impossible to calculate confidence intervals.

Intermediate calculations. ANOVA table

Source of variation	Degree of freedom	Sum of squares	Mean square
Treatments (between columns)	3	25838	8612.6
Residuals (within columns)	23	38843	1688.8
Total	26	64681	

F = 5.100 = (MStreatment/MSresidual)

Summary of Data

Group	Numbers of Points	Standard Mean	Standard Error of Deviation	Standard Error of Mean	Standard Error of Median
WS	7	660.01	18.332	6.929	655.99
WE	6	668.90	13.468	5.498	667.71
MS	7	739.06	31.280	11.823	733.12
ME	7	688.02	70.768	26.748	678.30

$CD4^+$ immunoreactivity

One-way Analysis of Variance (ANOVA)

The P value is < 0.0001, considered extremely significant.
Variation among column means is significantly greater than expected by chance.

Student-Newman-Keuls Multiple Comparisons Test

Comparison	Mean Difference	Q		P value
WS vs MS	-12.936	7.689	***	P<0.001
WS vs ME	-6.636	3.803	*	P<0.05
WS vs WE	-0.2451	0.1499	ns	P>0.05
WE vs MS	-12.691	8.427	***	P<0.001
WE vs ME	-6.391	4.056	**	P<0.01
ME vs MS	-6.300	3.877	**	P<0.01

With Student-Newman-Keuls test, it is impossible to calculate confidence intervals.

Intermediate calculations. ANOVA table

Source of variation	Degree of freedom	Sum of squares	Mean square
Treatments (between columns)	3	2200.1	733.36
Residuals (within columns)	71	3445.3	48.526
Total	74	5645.4	

F = 15.113 = (MStreatment/MSresidual)

Summary of Data

Group	Numbers of Points	Standard Mean	Standard Error of Deviation	Standard Error of Mean	Standard Error of Median
WS	15	8.453	6.781	1.751	8.043
WE	23	8.698	7.187	1.499	9.966
MS	20	21.389	4.649	1.040	21.518
ME	17	15.089	8.854	2.148	13.568

$CD8^+$ immunoreactivity

One-way Analysis of Variance (ANOVA)

The P value is < 0.0001, considered extremely significant.
Variation among column means is significantly greater than expected by chance.

Student-Newman-Keuls Multiple Comparisons Test

Comparison	Mean Difference	Q		P value
WS vs MS	-14.961	10.417	***	P<0.001
WS vs ME	-1.863	1.133	ns	P>0.05
WS vs WE	-0.02179	---	ns	P>0.05
WE vs MS	-14.939	10.023	***	P<0.001
WE vs ME	-6.391	4.056	**	P<0.01
ME vs MS	-6.300	3.877	**	P<0.01

With Student-Newman-Keuls test, it is impossible to calculate confidence intervals.

Intermediate calculations. ANOVA table

Source of variation	Degree of freedom	Sum of squares	Mean square
Treatments (between columns)	3	3821.1	1273.7
Residuals (within columns)	75	3436.3	45.817
Total	78	7257.4	

F = 27.800 = (MStreatment/MSresidual)

Summary of Data

Group	Numbers of Points	Standard Mean	Standard Error of Deviation	Standard Error of Mean	Standard Error of Median
WS	18	4.530	4.577	1.079	1.555
WE	16	4.551	3.328	0.8321	2.581
MS	29	19.491	9.560	1.775	21.933
ME	16	6.393	4.865	1.216	6.671

Macrophages immunoreactivity

One-way Analysis of Variance (ANOVA)

The P value is < 0.0001, considered extremely significant.
Variation among column means is significantly greater than expected by chance.

Student-Newman-Keuls Multiple Comparisons Test

Comparison	Mean Difference	Q		P value
WE vs MS	-14.910	6.863	***	P<0.001
WE vs ME	-8.043	3.702	*	P<0.05
WE vs WS	-1.322	0.5625	ns	P>0.05
WS vs MS	-13.588	7.494	***	P<0.001
WS vs ME	-6.721	3.707	*	P<0.05
ME vs MS	-6.867	4.357	**	P<0.01

With Student-Newman-Keuls test, it is impossible to calculate confidence intervals.

Intermediate calculations. ANOVA table

Source of variation	Degree of freedom	Sum of squares	Mean square
Treatments (between columns)	3	2735.1	911.69
Residuals (within columns)	79	5494.0	69.544
Total	82	8229.1	

F = 13.109 = (MStreatment/MSresidual)

Summary of Data

Group	Numbers of Points	Standard Mean	Standard Error of Deviation	Standard Error of Mean	Standard Error of Median
WS	17	7.789	5.359	1.300	9.075
WE	10	6.467	7.773	2.458	1.391
MS	28	21.377	11.334	2.142	22.469
ME	28	14.510	6.153	1.163	14.933

NF-κB p65 DNA binding activity

One-way Analysis of Variance (ANOVA)

The P value is 0.0020, considered very significant.
Variation among column means is significantly greater than expected by chance.

Student-Newman-Keuls Multiple Comparisons Test

Comparison	Mean Difference	Q		P value
WS vs MS	-0.2629	6.303	***	P<0.001
WS vs ME	-0.1171	2.809	ns	P>0.05
WS vs WE	-0.09690	---	ns	P>0.05
WE vs MS	-0.1660	3.823	*	P<0.05
WE vs ME	-0.02024	---	ns	P>0.05
ME vs MS	-0.1457	3.494	*	P<0.05

With Student-Newman-Keuls test, it is impossible to calculate confidence intervals.

Intermediate calculations. ANOVA table

Source of variation	Degree of freedom	Sum of squares	Mean square
Treatments (between columns)	3	0.2469	0.08230
Residuals (within columns)	23	0.2800	0.01217
Total	26	0.5269	

F = 6.761 = (MStreatment/MSresidual)

Summary of Data

Group	Numbers of Points	Standard Mean	Standard Error of Deviation	Standard Error of Mean	Standard Error of Median
WS	7	1.800	0.1020	0.03856	1.798
WE	6	1.897	0.1364	0.05568	1.906
MS	7	2.063	0.1172	0.04430	2.051
ME	7	1.918	0.08374	0.03165	1.924

NF-κB p65 nucleosome protein levels

One-way Analysis of Variance (ANOVA)

The P value is 0.0216, considered significant.
Variation among column means is significantly greater than expected by chance.

Student-Newman-Keuls Multiple Comparisons Test

Comparison	Mean Difference	Q		P value
ME vs MS	-619.67	4.612	*	P<0.05
ME vs WE	-315.00	2.345	ns	P>0.05
ME vs WS	-125.17	---	ns	P>0.05
WS vs MS	-494.50	3.681	*	P<0.05
WS vs WE	-189.83	---	ns	P>0.05
WE vs MS	-304.67	2.268	ns	P>0.05

With Student-Newman-Keuls test, it is impossible to calculate confidence intervals.

Intermediate calculations. ANOVA table

Source of variation	Degree of freedom	Sum of squares	Mean square
Treatments (between columns)	3	1308401	436134
Residuals (within columns)	20	2165847	108292
Total	23	3474248	

F = 4.027 = (MStreatment/MSresidual)

Summary of Data

Group	Numbers of Points	Standard Mean	Standard Error of Deviation	Standard Error of Mean	Standard Error of Median
WS	6	820.83	344.40	140.60	717.00
WE	6	1010.7	392.70	160.32	1051.0
MS	6	1315.3	287.89	117.53	1227.5
ME	6	695.67	278.31	113.62	709.00

Twitch

One-way Analysis of Variance (ANOVA)

The P value is 0.0007, considered extremely significant.
Variation among column means is significantly greater than expected by chance.

Student-Newman-Keuls Multiple Comparisons Test

Comparison	Mean Difference	Q		P value
MS vs WS	-1.544	6.854	***	P<0.001
MS vs WE	-1.036	4.601	**	P<0.01
MS vs ME	-0.8393	3.726	*	P<0.05
ME vs WS	-0.7047	2.926	ns	P>0.05
ME vs WE	-0.1970	---	ns	P>0.05
WE vs WS	-0.5077	---	ns	P>0.05

With Student-Newman-Keuls test, it is impossible to calculate confidence intervals.

Intermediate calculations. ANOVA table

Source of variation	Degree of freedom	Sum of squares	Mean square
Treatments (between columns)	3	8.783	2.928
Residuals (within columns)	22	7.655	0.3480
Total	25	16.438	

F = 8.413 = (MStreatment/MSresidual)

Summary of Data

Group	Numbers of Points	Standard Mean	Standard Error of Deviation	Standard Error of Mean	Standard Error of Median
WS	6	1.776	1.026	0.4190	1.936
WE	6	1.268	0.08608	0.03514	1.242
MS	8	0.2320	0.1883	0.066581	0.1625
ME	6	1.071	0.6486	0.2648	0.9990

Low frequency tension (20Hz)

One-way Analysis of Variance (ANOVA)

The P value is 0.0009, considered extremely significant.
Variation among column means is significantly greater than expected by chance.

Student-Newman-Keuls Multiple Comparisons Test

Comparison	Mean Difference	Q		P value
MS vs WS	-2.208	6.678	***	P<0.001
MS vs ME	-1.365	4.129	*	P<0.05
MS vs WE	-1.339	4.050	**	P<0.01
WE vs WS	-0.8687	2.458	ns	P>0.05
WE vs ME	-0.02600	---	ns	P>0.05
ME vs WS	-0.8427	---	ns	P>0.05

With Student-Newman-Keuls test, it is impossible to calculate confidence intervals.

Intermediate calculations. ANOVA table

Source of variation	Degree of freedom	Sum of squares	Mean square
Treatments (between columns)	3	17.773	5.924
Residuals (within columns)	22	16.483	0.7492
Total	25	34.256	

F = 7.908 = (MStreatment/MSresidual)

Summary of Data

Group	Numbers of Points	Standard Mean	Standard Error of Deviation	Standard Error of Mean	Standard Error of Median
WS	6	2.614	1.329	0.5426	2.848
WE	6	1.745	0.2826	0.1154	1.829
MS	8	0.4065	0.3088	0.1092	0.3230
ME	6	1.771	1.148	0.4685	1.780

Maximal isometric tension (Po)

One-way Analysis of Variance (ANOVA)

The P value is 0.0002, considered extremely significant.
Variation among column means is significantly greater than expected by chance.

Student-Newman-Keuls Multiple Comparisons Test

Comparison	Mean Difference	Q		P value
MS vs WS	-9.385	7.653	***	P<0.001
MS vs WE	-6.557	5.347	**	P<0.01
MS vs ME	-4.482	3.654	*	P<0.05
ME vs WS	-4.903	3.740	*	P<0.05
ME vs WE	-2.075	1.583	ns	P>0.05
WE vs WS	-2.828	2.157	ns	P>0.05

With Student-Newman-Keuls test, it is impossible to calculate confidence intervals.

Intermediate calculations. ANOVA table

Source of variation	Degree of freedom	Sum of squares	Mean square
Treatments (between columns)	3	329.39	109.80
Residuals (within columns)	22	226.89	10.313
Total	25	556.28	

F = 10.646 = (MStreatment/MSresidual)

Summary of Data

Group	Numbers of Points	Standard Mean	Standard Error of Deviation	Standard Error of Mean	Standard Error of Median
WS	6	11.227	5.284	2.157	13.383
WE	6	8.399	1.044	0.4263	8.120
MS	8	1.842	1.147	0.4054	1.894
ME	6	6.324	3.812	1.556	7.221

Twitch in single exposure of EUK-134

One-way Analysis of Variance (ANOVA)

The P value is 0.0001, considered extremely significant.
Variation among column means is significantly greater than expected by chance.

Student-Newman-Keuls Multiple Comparisons Test

Comparison	Mean Difference	Q		P value
WE vs MS	-88.107	7.470	***	P<0.001
WE vs WS	-23.520	1.865	ns	P>0.05
WE vs ME	-22.383	---	ns	P>0.05
ME vs MS	-65.723	5.572	**	P<0.01
ME vs WS	-1.137	---	ns	P>0.05
WS vs MS	-64.587	5.476	***	P<0.001

With Student-Newman-Keuls test, it is impossible to calculate confidence intervals.

Intermediate calculations. ANOVA table

Source of variation	Degree of freedom	Sum of squares	Mean square
Treatments (between columns)	3	31468	10489
Residuals (within columns)	22	20987	953.97
Total	25	52456	

F = 10.996 = (MStreatment/MSresidual)

Summary of Data

Group	Numbers of Points	Standard Mean	Standard Error of Deviation	Standard Error of Mean	Standard Error of Median
WS	6	106.57	12.141	4.956	106.86
WE	6	83.053	6.282	2.565	86.250
MS	8	171.16	53.468	18.904	152.15
ME	6	105.44	2.873	1.173	106.00

Low frequency tension (20Hz) in single exposure of EUK-134

One-way Analysis of Variance (ANOVA)

The P value is 0.0008, considered extremely significant.
Variation among column means is significantly greater than expected by chance.

Student-Newman-Keuls Multiple Comparisons Test

Comparison	Mean Difference	Q		P value
WE vs MS	-66.859	6.483	***	P<0.001
WE vs ME	-21.363	1.938	ns	P>0.05
WE vs WS	-17.729	---	ns	P>0.05
WS vs MS	-49.130	4.764	**	P<0.01
WS vs ME	-3.634	---	ns	P>0.05
ME vs MS	-45.496	4.412	**	P<0.01

With Student-Newman-Keuls test, it is impossible to calculate confidence intervals.

Intermediate calculations. ANOVA table

Source of variation	Degree of freedom	Sum of squares	Mean square
Treatments (between columns)	3	17616	5871.8
Residuals (within columns)	22	16044	729.28
Total	25	33660	

F = 8.052 = (MStreatment/MSresidual)

Summary of Data

Group	Numbers of Points	Standard Mean	Standard Error of Deviation	Standard Error of Mean	Standard Error of Median
WS	6	109.04	20.228	8.258	100.00
WE	6	91.313	5.750	2.347	93.620
MS	8	158.17	44.374	15.689	144.92
ME	6	112.68	3.152	1.287	111.36

Maximal isometric tension (Po) in single exposure of EUK-134

One-way Analysis of Variance (ANOVA)

The P value is 0.5345, considered not significant.
Variation among column means is not significantly greater than expected by chance.

Post tests
Post tests were not calculated because the P value was greater than 0.05.

Intermediate calculations. ANOVA table

Source of variation	Degree of freedom	Sum of squares	Mean square
Treatments (between columns)	3	128.68	42.894
Residuals (within columns)	22	1259.7	57.259
Total	25	1388.4	

F = 0.7491 = (MStreatment/MSresidual)

Summary of Data

Group	Numbers of Points	Standard Mean	Standard Error of Deviation	Standard Error of Mean	Standard Error of Median
WS	6	108.30	8.956	3.656	103.55
WE	6	103.46	8.009	3.270	98.430
MS	8	102.40	8.763	3.098	102.22
ME	6	104.19	0.2890	0.1180	104.11

VITA

Jong Hee Kim

EDUCATION

Institution	Degree	Date	Field
Seoul National University	B.Ed.	1997	Physical Education
Seoul National University	M.Ed.	1999	Exercise Physiology
Texas A&M University	Ph.D.	2009	Exercise Physiology

HONORS and AWARDS

2009 Student Research Presentation Award, First Place (Doctoral Category) at Texas Regional Chapter of the American College of Sports Medicine

2008 International Education Fee Scholarship from International Student Services (ISS) at Texas A&M University

2007 Educational Research Exchange (ERE) Presentation Award, First Place in the College of Education and Human Development at Texas A&M University

2005 Doctoral Fellowship in College of Education and Human Development at Texas A&M University

2004 Doctoral Fellowship in College of Education and Human Development at Texas A&M University

PUBLICATIONS

1. Song, W., H.B. Kwak, **J.-H. Kim**, and Lawler, J.M. Exercise training modulates the nitric oxide synthase profile in skeletal muscle from old rats. *The Journals of Gerontology. Series A, Biological Sciences and Medical Sciences.* 64(5):540-549, 2009.
2. Lawler, J.M, H.B. Kwak, **J.-H. Kim,** and M.-H. Suk. Exercise training inducibility of MnSOD protein expression and activity is retained while reducing prooxidant signaling in the heart of senescent rats. *Am J Physiol Regul Integr Comp Physiol.* 296:1496-1502, 2009.
3. **Kim, J.-H**., H.B. Kwak, C. Leeuwenburgh, and J.M. Lawler. Lifelong exercise and mild (8%) caloric restriction attenuate age-induced alterations in plantaris muscle morphology, oxidative stress and IGF-1 in the Fischer-344 rat. *Experimental Gerontology.* 43(4):317-329, 2008.

CONTACT ADDRESS

158 Read Building, Department of Health and Kinesiology, Texas A&M University, College Station, TX 77843-4243